Synthesis of Model Compounds for a "Bottom-Up" Approach to the Eumelanin Challenge

Laura Jeliazkov, Department of Chemistry

McGill University, Montréal, QC

August 2024

A thesis submitted to McGill University in partial fulfillment of the requirements of the degree of Master of Science.

Dedicated to Ms. Jean Rosenberg.

Acknowledgements

There are many people who contributed immensely to the completion of this degree. I will cover as much ground as I can on this single page here, but please know that my gratitude extends beyond the following paragraphs.

Firstly, I must thank my supervisor Dr. Jean-Philip Lumb for welcoming me into the group. I am in awe of his endless knowledge and passion for chemistry, and grateful for the environment he provided in which to learn and grow not only as a scientist, but as a person during this academic pursuit. Next, I thank the entire McGill Chemistry Department for the assortment of support and encouragement that it provided me with. A million thank you's to: Ms. Chantal Marotte, for answering my myriad questions; Dr. Robin Stein, Dr. Tara Sprules, and Dr. Kirill Levin for incredible support down in the NMR room; Dr. Alex Wahba for HRMS services and for always taking the time to ask how I am; Mr. Jean-Marc Gauthier for the technical support; and Ms. Joyce Gyan & Mr. Quenton Danglade-Mills for their services down in the Chemistry Stores.

Thank you to the Gen Chem Lab staff that I worked with during my time working as teaching assistant – Mr. Badawy Sha'ath, Mr. Mitch Huot, Mr. Mathieu Bédard and Professor Pallavi Sirjoosingh – for being incredibly kind people and for creating such a fun work environment down in the Otto Maass basement. Also, very importantly, a huge thank you to my Gen Chem students ! for reminding me how to be excited about chemistry.

I will forever be indebted to my colleague Mr. Simon Edelmann for all his mentorship, advice, time, and patience. There is no form of 'thank you' that would suffice. Without him I would certainly not have made it this far.

I was lucky to walk into such a kind group of people in the Lumb Lab. An enormous thank you to all of my colleagues: Dr. Haiyan Huang for friendship and conversations of life; Ms. Xueqing Wang for showing me the ropes and helping me to build character; Mr. Derek Meng for being a source of inspiration, comfort and comic relief; Ms. Madison Carrol-Pöhls for teaching me to titrate *t*-BuLi and partaking in my puzzles; Mr. Carlos R.A. Nicolas for answering my redundant questions; Yiming Zhang for getting me through coursework; post-docs Dr. Burhan Hussein, Dr. Camilo J. Viasus Pérez and Dr. Eric Falk for all being wonderfully supportive mentors; and Mr. Darcy Burley for being a great coffee-break-mate and friend.

I am so happy to have the incredible GMH team of Bruno, Soledad, Matias, Pablo, Anel, Ivan, Cheyenne, Grace, Ivandro, Alex, Alma, Yan, James, and Lisanne to thank for company during this undertaking. I extend the gratitude also to any and all of the GMH visitors who sat with me in the coworking room.

Obrigada to my girls Émilie, Nicole and Tabea for helping me to mix in hysterical laughs and fantastic times.

Thank you to the wonderful Café Orr for housing, caffeinating and nourishing my writing days.

And, of course, thank you to my family for putting up with me. They pushed me to keep at it – and I suppose I must admit that I am grateful.

Laura Jeliazkov

Abstract

Eumelanin is a ubiquitous biopolymer found throughout the human body. It is the pigment responsible for coloration of the skin, hair and eyes. Its biosynthetic pathway begins with tyrosinase-catalyzed oxidation of L-tyrosine to either 5,6-dihydroxyindole (**DHI**) or 5,6-dihydroxyindole-2-carboxylic acid (**DHICA**). Interestingly, **DHI** and **DHICA** are the last-known intermediates in the pathway, as their spontaneous aerobic oxidation leads to complex and heterogeneous materials which are insoluble in organic solvent and thus not characterizable by many conventional characterization techniques.

Despite a recent surge in experimental and theoretical efforts, the structure of the eumelanin biopolymer has yet to be fully elucidated. The structural origins of its signature properties – such as broadband UV absorption, ultrafast non-radiative decay, radical character, and metal-chelation – therefore remain a mystery. Thus far, top-down biomimetic synthetic studies only yield similarly heterogeneous and undefined materials. Bottom-up studies aiming to access a discrete oxidized monomeric subunit are challenged by the rapid polymerization that occurs upon oxidation.

Recent work in the research group of Dr. Jean-Philip Lumb, however, has successfully developed a "blocking" strategy, whereby a stable **DHI** molecule with aryl functional groups installed at each of the C2, C4 and C7 positions can be oxidized to an isolable indole-5,6-quinone (**IQ**). These aryl groups effectively block covalent bond formation which would typically be occurring upon oxidation of the **DHI** unit *in vivo* – and therefore, prevent the spontaneous polymerization processes which would lead ultimately to the heterogenous eumelanin pigment. These blocked compounds, interestingly, emulate many of the signature properties of the biopolymer; their study has already contributed to the structure-function-property understanding of the eumelanin network.

Expanding this blocking strategy to **DHICA** is the next step in the project's investigation of the eumelanin mystery. This thesis details our synthetic progress towards obtaining blocked **DHICA** derivatives.

Abstrait

L'eumélanine est un biopolymère présent dans l'ensemble du corps humain. C'est le pigment responsable de la coloration de la peau, des cheveux et des yeux. Sa voie biosynthétique commence par l'oxydation de la L-tyrosine catalysée par la tyrosinase en passant par le 5,6-dihydroxyindole (**DHI**) ou l'acide 5,6-dihydroxyindole-2-carboxylique (**DHICA**). Il faut noter que le **DHI** et le **DHICA** sont les derniers intermédiaires recensés dans la voie biosynthétique, car leurs oxydation aérobie spontanée conduit à des matériaux complexes et hétérogènes insolubles dans les solvants organiques et donc non analysable par plusieurs techniques de caractérisation conventionnelles.

Malgré un redoublement récent des efforts expérimentaux et théoriques, la structure du biopolymère de l'eumélanine n'a pas encore été entièrement élucidée. De fait, l'origine structurelle des propriétés caractéristiques – telles que sa large bande d'absoption dans le domaine UV, sa désintégration non-radiative ultra-rapide, son caractère radicalaire, et sa chélation des métaux – reste un mystère. Jusqu'au présent, les études portant sur une synthese biomimétique (« top-down ») n'ont conduit qu'a des matériaux aussi hétérogènes et indéfinis que l'eumelanine. Les études visant à accéder à une sous-unité monomèrique oxydée (« bottom-up ») se heurtent à la polymérisation rapide qui se produit lors de l'oxydation.

Des travaux récents du groupe de recherche du professeur Jean-Philip Lumb ont conduit au developpement d'une stratégie de « blocage, » par laquelle une molecule **DHI**, portant des cycles aromatiques aux positions C2, C4 et C7, est stable et peut être oxydée en une indole-5,6-quinone (**IQ**) isolable. Ces cycles aromatiques bloquent efficacement la formation de liaisons covalentes qui se forment généralement lors de l'oxydation de l'unité **DHI** *in vivo* – et empêchent donc les processus de polymérisation spontanée conduisant au pigment hétérogène d'eumélanine. Il est essentiel de noter que ces sous-unités bloqués reproduisent certaines des propriétés caractéristiques du biopolymère; leurs étude a déjà contribué à la compréhension des relations structure-activité du réseau d'eumélanine.

L'extension de cette strategie de blocage au **DHICA** s'inscrit comme une suite logique dans notre enquête sur l'eumélanine mystèrieuse. La présente thèse de maîtrise détaille nos progrès dans la synthèse de tels dérivés bloqués du **DHICA**.

Table of Contents

Table of Tables

Table of Schemes

Chapter 1: Eumelanin and the DHICA Precursor

1. Introduction

Melanin is a category that encompasses a class of ubiquitous multi-functional biopolymers found within organisms of the kingdoms of bacteria, fungi, plants and animals. It is therefore an extremely complex and multi-faceted term; materials classified as 'melanin' comprise a very wide scope of chemical composition and biosynthetic precursors and pathways. The word 'melanin' itself originates from the Greek word *melanos*, meaning black, or dark; this is meant to reflect the range of black, brown, yellow and red varieties across the phylogenetic tree.

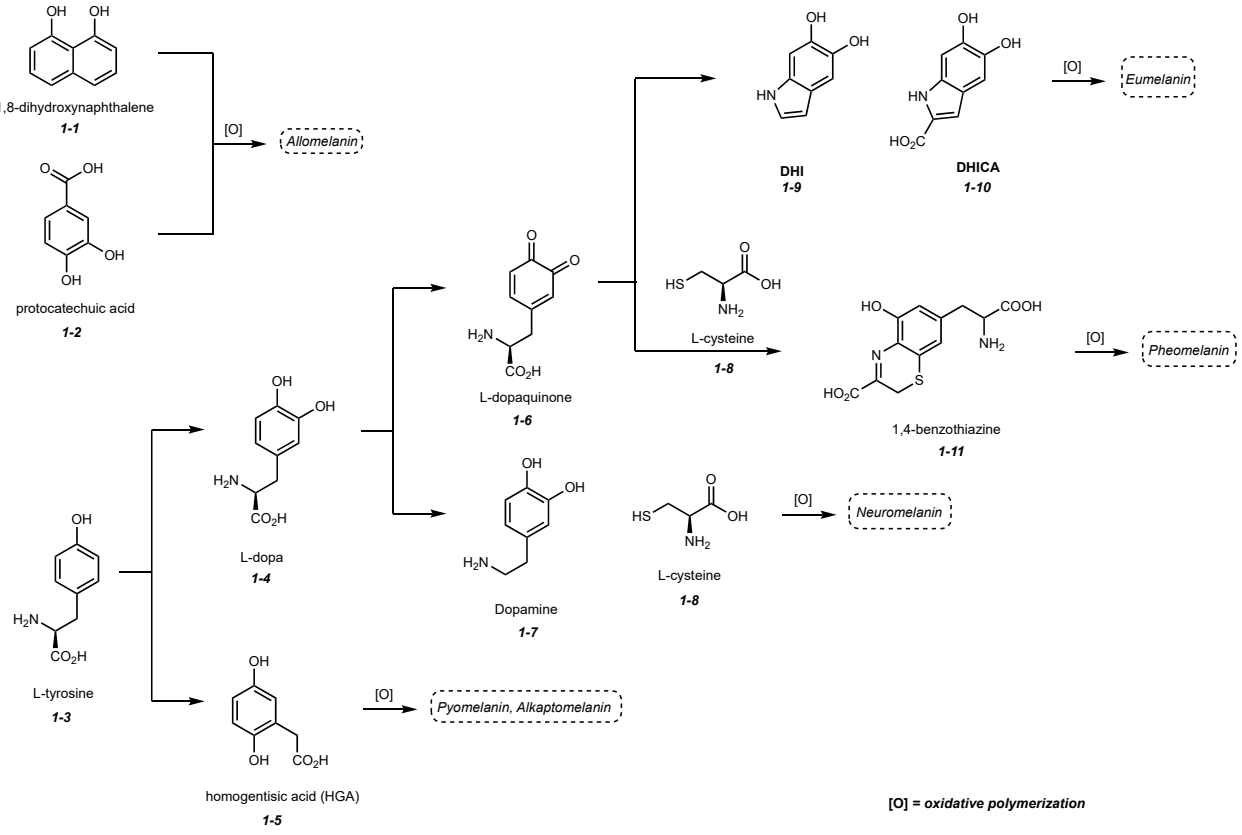

Scheme 1.1. Classification of melanins.

Black-brown *eumelanin* is the subclass of melanin most predominant in humans. Experiments by Raper in 1927 isolated the compounds 5,6-dihydroxyindole (**DHI**) **1-9** and 5,6-dihydroxyindole-2-carboxylic acid (**DHICA**) **1-10** from a natural sample of black eumelanin,[1] and further studies in 1948 established the currently-accepted eumelanogenic biosynthetic pathway as tyrosinase-catalyzed oxidation of L-tyrosine via **1-9** and **1-10** (Scheme 1.2).[2] Yellow-red *pheomelanin* is another category; it is also derived from L-tyrosine but in the presence of L-cysteine via benzothiazine heterocycles.[3] It is the pigment responsible for yellow-to-red mammalian hair and red bird feathers. *Neuromelanin* was found in nerve cells in 1955. Brown *pyomelanin* was isolated from the bacterium *pseudomonas aeruginosais* in 1972.[4] *Alkaptomelanin* is the equivalent of pyomelanin but produced by humans as opposed to microbes. Finally, *allomelanin* is a subtype of melanin, established in 1976, that is found in fungi, bacteria and plants. Pyomelanin and allomelanin are notably nitrogen-free melanins, deriving from oxidative polymerization of nitrogen-free precursors. This makes for six categories of melanin (Scheme 1.1). Henceforth in this document, it is *eumelanin* which is being discussed unless otherwise noted. Eumelanin plays a number of important biological roles and features unique and distinctive properties, notably i) broadband UV absorption, ii) ultrafast nonradiative decay, and iii) a persistent radical character.[5] Properties (i) and (ii) are what determine eumelanin's sun-screening ability, while (iii) makes it a powerful antioxidant.

1.1. Biosynthesis of Eumelanin and Challenges of Study

The biochemical pathway responsible for the biosynthesis of eumelanin in mammals as established through the studies of Raper and Mason is shown in Scheme 1.2. The process occurs within organelles called melanosomes, which are located within larger cells called melanocytes.[6,7] It begins with the amino acid L-tyrosine **1-3**, which through tyrosinase-catalyzed oxidation is transformed to L-dopaquinone **1-6**. L-dopaquinone then undergoes an intramolecular 1,4-addition of the amino group, followed by rearomatization to yield L-cyclo-dopa **1-12**. Redox exchange

between the two species **1-6** and **1-12** gives rise to L-dopachrome **1-13** and L-dopa **1-4**. L-dopa undergoes tyrosinase-catalyzed oxidation back to L-dopaquinone to continue the cycle. L-dopachrome **1-13**, then, is the branch point in the pathway from which the aforementioned eumelanin monomeric precursors arise: **DHI** (**1-9**) and **DHICA** (**1-10**). A nonenzymatic decarboxylative rearrangement of **1-13** yields **1-9** and CO_2. Enzymatic action by dopachrome tautomerase (Dct) or tyrosinase-related protein 2 (Tyrp2) alternatively transforms **1-13** to **1-10**. Aerobic oxidation of **1-9** and **1-10** is tightly coupled to a rapid and spontaneous polymerization that forms the ultimate eumelanin biopolymer. It is worth noting that the electron-withdrawing carboxyl group at C2 (indole numbering, see **1-10** in Scheme 1.2) of **DHICA** renders its oxidation much slower than that of **DHI**: therefore, it is suspected that **DHICA** oxidation in vivo is an enzymatic reaction.[8,9]

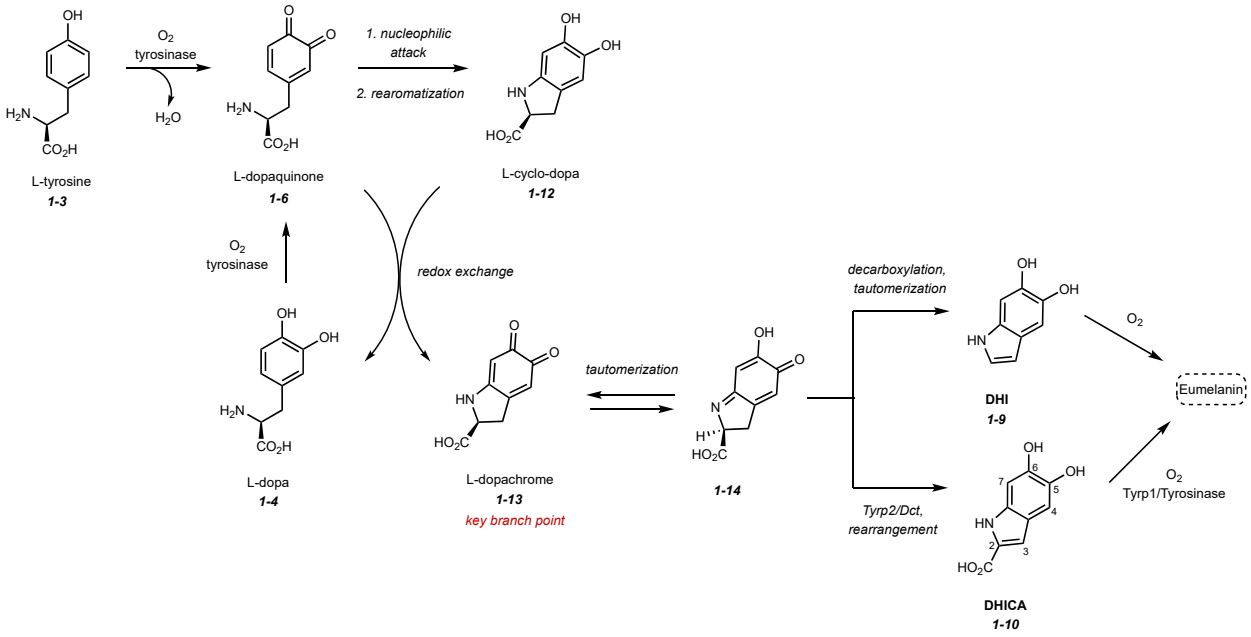

Scheme 1.2. Eumelanogenic pathway as proposed by Raper and Mason. **DHI 1-9** and **DHICA 1-10** are the last-known monomeric precursors in the pathway. Indole numbering is indicated on molecule **1-10**.

Impressively, unlike similar complex molecular systems such as DNA, proteins or other natural pigments, melanin still has yet to be described as a well-defined structure. The tight coupling of oxidative processes with spontaneous polymerization leads rapidly to the black-brown,

amorphous, heterogeneous material that is the natural melanin pigment; very poor solubility in organic solvents renders characterization of this biopolymer by many conventional characterization techniques impossible. **DHI** and **DHICA** remain, to this day, the last known monomeric units in the eumelanogenic pathway.

2. DHICA in Natural Eumelanin

While **DHI** and **DHI** melanins have been quite expansively studied in these last 30 years of melanin research, **DHICA** and its contribution to the eumelanin structure-function story has perhaps received less attention. We will offer next an overview of some of the syntheses of and studies on **DHICA** and its oligomers in the literature up to the current day. We will point out key differences between **DHICA** and **DHI** which make investigation of the former invaluable to continued efforts at the elucidation of the eumelanin mystery.

Sepia officianalis, or Sepia melanin, sourced from the black ink of the cuttlefish, has widely served as the representative standard of natural eumelanin. Many top-down research efforts have sought to characterize the natural biopolymer, using techniques such as chemical degradation, titrations, elemental analyses, and mass spectrometric analyses. Such studies have consistently agreed that Sepia melanin consists of a highly cross-linked set of irregular polymers built up of units of **DHI**, **DHICA**, pyrrolecarboxylic acids, leucodopachrome and uncyclized dopa units, linked randomly and at various states of oxidation, and intermixed with proteins and impurities.[10] The lack of clarity beyond this large structural picture, however, has complicated further study.

Mason had originally spotlighted **DHI** as being the unit which, upon oxidation, was responsible for forming the eumelanin polymer.[11] In 1962, however, analysis by Nicolaus and coworkers showed that melanin from *Sepia officinalis* has a greater content of carboxyl groups than does synthetic dopa melanin.[12] This was taken as evidence of carboxylated indole units, derived from dopachrome or **DHICA**, in the natural melanin. Further to this, Benathan and Wyler in 1980 found by quantitative titration the ratio of carboxyl to phenoxyl groups in Sepia melanin to be more than double that in dopa melanin.[13] In 1986, Ito used improved analytical techniques –

namely, elemental analysis and acid degradation followed by measurement of the amounts of CO_2 generated – to conclude that in fact more than half of the melanin polymer is made up of **DHICA**-derived units.[14] In 1992 Prota and coworkers used a biosynthetic approach, measuring the incorporation of specifically radiolabeled melanogenic precursors into melanins formed in melanocytes *in vivo*, to conclude the presence of physiologically significant amounts of **DHICA** in natural eumelanins.[15] Inherent limitations of the techniques used in these studies, however, prevented a reliable, quantitative measure of relative ratios. Other studies continued to corroborate this new understanding of **DHICA** inclusions in Sepia melanins[16,17] until ultimately, in 1997, continued investigations by Prota with use of advanced quantitative methods concluded the mixture of oligomeric structures to contain over 75% of **DHICA**-derived units and only 20% of **DHI**-derived units.[18] Structural investigation was carried out by acidic decarboxylation conditions – 6 M HCl, with heating – to selectively determine carboxyl groups linked to aromatic rings. A mild oxidation with alkaline hydrogen peroxide forms pyrrole-2,3,5-tricarboxylic acid (**PTCA**) **1-16** in the case mainly of disruption of **DHICA** units and minorly by **DHI** units; pyrrole-2,3-dicarboxylic acid (**PDCA**) **1-18** forms instead exclusively from disrupted **DHI** units. **PDCA**, therefore, is taken as a marker for quantitative measurement of the amounts of **DHI** (Scheme 1.3).

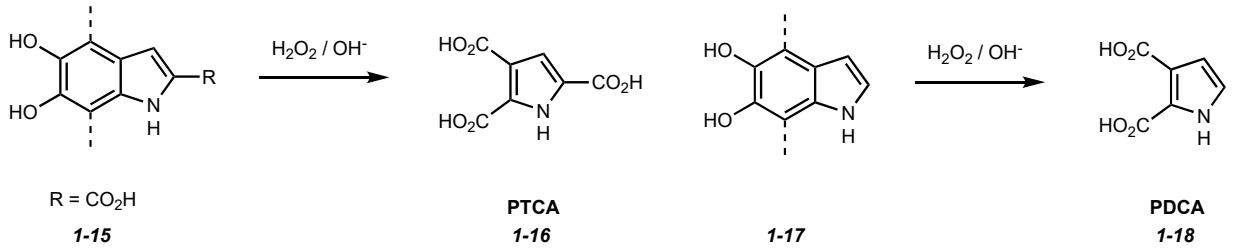

R = CO_2H
1-15

PTCA
1-16

1-17

PDCA
1-18

Scheme 1.3. Scheme adapted from Prota *et al*,, 1997: Pyrrolecarboxylic acids (**PTCA**, **PDCA**) obtained by acidic degradation of melanins for assignment of monomer makeup.[18]

The contribution of **DHICA** to the eumelanin framework had originally been greatly underestimated. Next in this Chapter, we will offer an overview of existing synthetic and analytical studies of both natural and synthetic melanins in the literature, with a focus on **DHICA**, and their various shortcomings. We will provide a context for the group's interest in melanin-related

systems and discuss recent development in the Lumb Group of a "blocking" strategy which allows attainment and characterization of stable blocked **DHI** derivatives and their corresponding oxidized forms, blocked indole-5,6-quinone (blocked **IQ**) derivatives.[19] It follows from the discussion above that it would be of great import to expand this blocking strategy to also access blocked **DHICA** derivatives, and their corresponding blocked 2-carboxy-indole-5,6-quinone (blocked **2-carboxy-IQ**) derivatives, in pursuit of the greater half of the eumelanin-network story. This has been the primary goal of my M.Sc., and the synthetic progress which has been made is the subject of this Thesis.

2.1 Existing Methods of Investigation

'Top-down' research efforts are based off of synthetic melanins, such as DOPA melanin – but, synthesis of such materials closely resembles that of the natural biosynthesis. Product structures are thus also ultimately unknown, and cannot be tailored nor modified. 'Bottom-up' synthetic studies are those starting from molecular or monomeric states of matter – for example, stopping biomimetic oxidation reactions at short times. In silico methods also seek to predict polymeric structure. Such studies have established certain hypothetical oligomeric subunits currently accepted in the field, such as the linear oligomer **1-19** (Scheme 1.4). Such structures at the catechol oxidation state as pictured, however, are unstable and readily autoxidize, precluding proper structure-function analysis. Further, they typically demonstrate optical and electronic properties reminiscent of **DHI**, rather than eumelanin. This points to oxidized subunits as responsible for the emergence of eumelanin's unique and distinctive properties. The porphyrin-like cyclic tetramer **1-20** has been proposed by Kaxiras *et al.* based off of density functional modeling.[20] Such a compound, however, has not yet been synthetically accessed. Work in the Lumb Research group (unpublished work by Dr. Haiyan Huang, Mr. Yiming Zhang) is currently seeking to synthesize a derivative for further study.

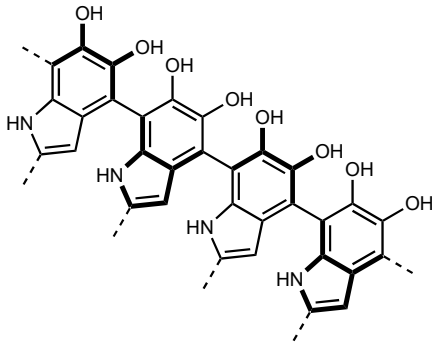

1-19
proposed linear structure of eumelanin

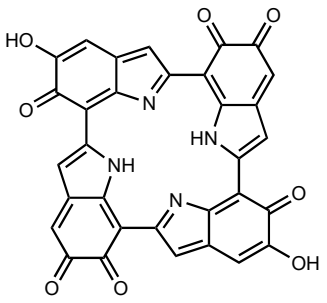

1-20
proposed cyclic structure of eumelanin

Scheme 1.4. Some current proposed hypothetical oligomeric structural subunits of eumelanin.

Due to the aforementioned coupling of oxidation with spontaneous polymerization, any well-defined, stable, oxidized subunit has been lacking in the field. This precludes studies which may allow us to properly understand the molecular origins of eumelanin's properties. Current materials and technological applications seeking to exploit the properties of melanin would greatly benefit from structure-function correlations. In addition, neuromelanin is implicated in the progression of diseases such as malignant melanoma, Alzheimer's and Parkinson's.[7,21] For example, a diminished concentration of neuromelanin pigmentation accompanied by an increased concentration of redox-active iron in the substantia nigra of the brain is correlated with the progression of Parkinson's disease. The redox activity of melanin makes it a good radical scavenger and chelator of metal ions. It is suspected that saturation of the iron binding sites of neuromelanin in individuals with Parkinson's leaves greater amounts of residual iron free to promote neurodegeneration via oxidative damage. The ability to characterize the iron complexes formed at neuromelanin's chelation to iron would be advantageous to better understanding the mechanisms of the disease – thus allowing more informed development of potential treatment.

Through a bottom-up approach, recent studies in the Lumb Group (work by Dr. Haiyan Huang and Ms. Xueqing Wang) have achieved a major advance in this regard. We have sought to address the melanin mystery by seeking synthetic access of discrete, oxidized monomeric or oligomeric **DHI**- and **DHICA**- derivates stable enough for proper physicochemical characterization (study detailed in Section 3.4).

3. Synthetic DHICA Materials

Efforts in the literature to elucidate the structure-function relationships of melanin are often driven by study of synthetic melanins. These are materials inspired by the natural biopolymer, but produced by abiotic oxidative polymerization. Their synthesis varies quite largely in the literature: different monomeric precursors may be used, and reaction conditions vary in pH, temperature, oxidants, reaction times, and subsequent isolation procedures used.[22, 23, 24] Though the resultant polymers reliably reproduce many of the macroscopic properties of natural melanin, it is impossible to know the extent to which they resemble each other at the molecular level; it is necessary to be conservative, therefore, in allowing data collected from synthetic melanins to inform understandings of natural melanins.

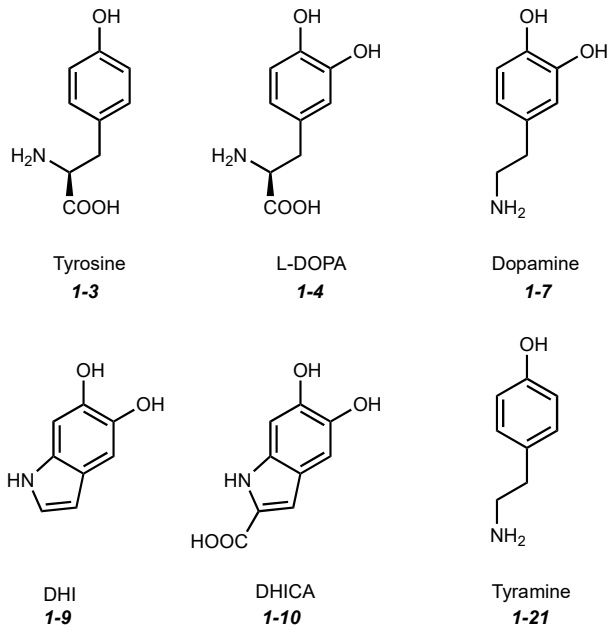

Scheme 1.5. Main synthetic melanin precursors.

Some common monomers used for synthesis of synthetic eumelanins aside from **DHI** and **DHICA** include tyrosine **1-3**, L-dopa **1-4**, dopamine **1-7**, and tyramine **1-21** (Scheme 1.5). Oxidants used include tyrosinase, chemical oxidants, or ambient oxygen under basic conditions. Tyrosinase is one of the most commonly-used oxidants for preparation of synthetic melanins. Peroxidase/hydrogen peroxide systems may also be used in preparation of **DHI** and **DHICA** melanins.[25] Chemical oxidants such as potassium ferricyanide or periodate may also be used. Suitable mediums include phosphate buffers of 0.05-0.1 M concentrations, at neutral pH. The addition of poly(vinyl alcohol) to the buffer can aid in controlling aggregation and precipitation during oxidative polymerization, allowing isolation of water-soluble synthetic eumelanins.[26] Work-up procedures are typically based on precipitations with dilute acids.[14]

3.1 DHICA Homopolymers

Synthetic Approaches

Pure **DHICA** melanins may be prepared. These are homopolymers resulting from polymerization of the **DHICA** monomer. Ito has reported preparation of synthetic eumelanin using **DHICA** as precursor and mushroom tyrosinase (obtained from commercial sources) as oxidant[14]: To a solution of the indole in 0.1 M sodium phosphate buffer (pH 6.8) is added mushroom tyrosinase at 25 ºC. This reaction is mixture is stirred vigorously for 4 hours, before the oxidation is stopped by addition of 6 M HCl. This acidic mixture (pH approximately 1) is then kept at 4 ºC overnight to precipitate pigment formed. The precipitate is then collected by centrifugation, and washed with 1 M HCl. Napolitano reported slight modification of the preceding conditions[27], allowing the reaction mixture to stir under a stream of oxygen. Following oxidation the solution is acidified to pH 3, collected by centrifugation, and then washed with water.

An alternative is the use of a horseradish peroxidase/hydrogen peroxide system for oxidation.[27] The **DHICA** monomer is dissolved in 0.1 M phosphate buffer (pH 6.8), and a solution of the enzyme and 30 % H_2O_2 added. This mixture is stirred for 2 hours at 25 ºC. The melanin

formed is precipitated by acidification of the mixture to pH 3, then collected by centrifugation and washed with water. The collected melanin is dried over silica gel and sodium hydroxide overnight. Rosei *et al.* reported **DHICA** melanin synthesis modified from those by Sealy for dopa-melanin synthesis.[28] **DHICA** was dissolved in water and 1 M potassium hydroxide was added to increase the pH of the solution to pH 8. This was then incubated at 37 ºC under a stream of oxygen for 72 hours, dialyzed against deionized water, and finally lyophilized. Rosei also reported the ability of lipoxygenase (LOX) enzyme in the presence of hydrogen peroxide to oxidize **DHI** and **DHICA** to melanin materials.

There are myriad examples of preparation of synthetic eumelanin films using ammonia-induced solid-state polymerization.[28-34] Other examples report the use of inorganic materials as polymerization catalysts, pointing to formation of metal-**DHICA** charge transfer complexes which act as precursors to a resultant hybrid melanin polymer.[30] In 2015, Luciani and coworkers demonstrated the efficacy of titanium dioxide in catalyzing **DHICA** polymerizations through oxidative reactions.[32]

Beyond those above, the variety of conditions used for the preparation of **DHICA** synthetic eumelanins leads to products of a variety of structural features and properties, even though of the same precursor. One must be cautious, therefore, in drawing comparisons between pigments prepared under differing conditions. Though these homopolymers can be studied for their physical and optical properties – and may be used to inspire materials research – they are still unable to inform directly on the structure-function-property relationships of natural eumelanin.

Properties

Oxidation of **DHICA** monomers leads to brown, *soluble* materials rather than the black, insoluble materials of DHI melanins. Computed absorption spectra for these **DHICA**-derived structures demonstrate absorbances mainly below 400 nm. It is suggested that this is due to inter-unit dihedral angles of roughly 47 degrees with local orthoquinone moieties, which disrupts inter-unit pi electron delocalization.[35] It is interesting to note, that this spectroscopic property is reminiscent of the characteristic shoulder above 310 nm in absorption spectra of natural eumelanin samples from Sepia melanin.[10]

Studies in 2010 by Xu and coworkers revealed **DHICA** melanins to have far more potent free radical scavenging abilities than do **DHI** melanins.[36] Numerous studies have suggested that this and other key photophysical properties of melanin material arise largely from its primary structure: e.g., the degree of planarization and resultant electron-delocalization within the network. The influence of its secondary, supramolecular structure had largely been assumed to be of less importance.[37] Studies by d'Ischia and coworkers in 2013, however, revealed an effect of dilution on the visible absorption spectra of solubilized eumelanins.[38] It was observed that the spectrum of **DHICA** melanin varied significantly and non-linearly with dilution; that of **DHI** melanin did not. This suggested an aggregation-dependent effect. The authors embarked on the first systematic comparison of **DHI** and **DHICA** melanin aggregation behaviors. It was of interest to see whether this might reveal the reason behind the superior radical-scavenging abilities of **DHICA** melanin.

The mode of aggregation of oligomeric species forming with oxidative polymerization of **DHI** and **DHICA** was monitored by thin-electron microscopy (TEM). After a reaction time of 2 hours, **DHI** polymers showed "onion-like" aggregates of approximately 50 nm in diameter. **DHICA** polymers, on the other hand, showed more elongated structures, of at least 100 nm in length (Scheme 1.6).[38]

The carboxylic acid at the C2 position is largely responsible for the observed properties of **DHICA** melanins: because of it, reactivity and thus chain growth is directed to the C4 and C7 positions. The inter-ring dihedral angles twist to minimize electrostatic interactions. The twisted chains therefore are not amenable to pi-stacking as are **DHI** polymeric structures. This makes for weaker intermolecular interactions overall, and leads to electronically-isolated monomer-like regions within the oligomeric scaffold. EPR and power saturation studies suggested that free-radical character existed in more restricted, localized regions, unlike the broad delocalization of pi-electron systems and variety of free radical species in **DHI** melanins. Ultimately, d'Ischia and coworkers suggest that it is, interestingly, this "less-effective chemical disorder" that accounts for the superior antioxidant capabilities of **DHICA** as opposed to **DHI** melanin.[38] They suggest that weaker aggregates allow the **DHICA** units to be more accessible to free radicals.

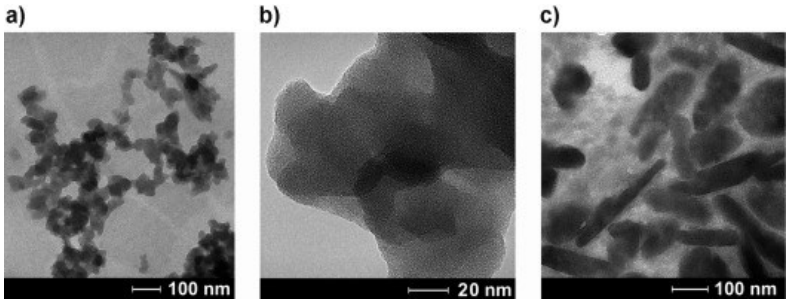

Scheme 1.6. TEM images of **DHI** (a, b) and **DHICA** (c) polymers, taken from studies by d'Ischia and coworkers.[38]

Computational studies using density functional theory (DFT) and molecular dynamics (MD) simulation can be powerful tools for prediction of physicochemical properties of materials. Challenges, however, in the computational modeling of synthetic eumelanins unfortunately slows research progress from the computational front: firstly, for the lack of any known well-defined structure for modeling.[39c] Secondly, the amorphous and hierarchical nature of the biopolymer network commands very large-scale simulations, with hundreds of molecules necessary to properly replicate the macro-properties.[40]

3.2 DHICA Oligomers

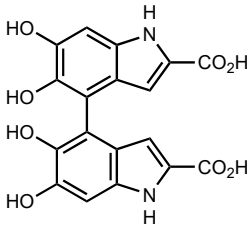

1-22

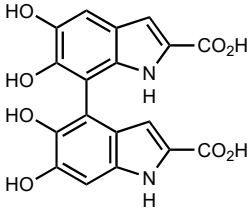

1-23

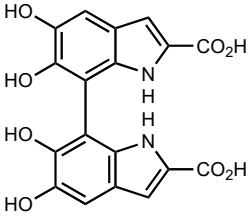

1-24

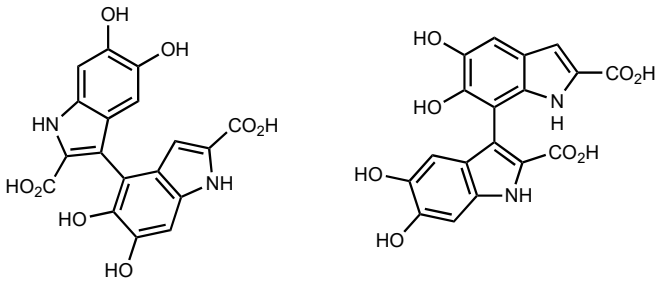

1-25 ***1-26***

Scheme 1.7. Examples of dimers isolated from biomimetic oxidations of **DHICA**.[41]

Synthetic Approaches

Since the 1980's, a finite set of oligomers have been isolated from oxidations of the **DHICA** compound.[42,43] Examples **1-22** to **1-34** are illustrated in Schemes 1.7 and 1.8. Typically these are obtained by stopping biomimetic oxidation reactions at short times. In 1987, Prota *et al*. successfully isolated an acetate-protected, C2-methyl-ester derivative of a 4,7'-coupled dimer of **DHICA** (as compound **1-22** in Scheme 1.7).[44] The procedure involved autoxidation of **DHICA** in 0.5 M sulfonic acid buffer at neutral pH under oxygen, in the presence of cobalt(II) sulfate. A deep violet precipitate is collected, then reduced with dithionate, esterified with methanolic hydrochloric acid, and acetylated.

Studies by Prota, d'Ischia, Pezzella, Napolitano and others in the years since have expanded the library of known dimeric and trimeric **DHICA** oligomers. In 1996, 3,4' and 3,7' dimers **1-25** and **1-26** (Scheme 1.7) were isolated; this implication of the C3 position in bond formation was yet unprecedented.[45] Structural characterizations of subsequently isolated regioisomeric trimers revealed the presence of a significant rotational barrier around interunit bonds, thus revealing **DHICA** oligomers to be chiral in nature.[45a] Optical activity is expected due to this chirality; this fact provides rationale for the non-linear optical behavior observed of melanin intermediates. In 2003, a regiosymmetric 4,4':7',7'':4'',4''' coupled linear tetramer was isolated (atropisomers **1-35** to **1-37**, Scheme 1.9). It was necessary to acetylate the catechol in order to more easily isolate the tetramer using preparative HPLC, due to its high propensity for oxidation.

The authors point to how isolation of this oligomer and the preceding trimers validate the supposed structural model of eumelanin as a mixture of linear **DHICA** oligomers.[43]

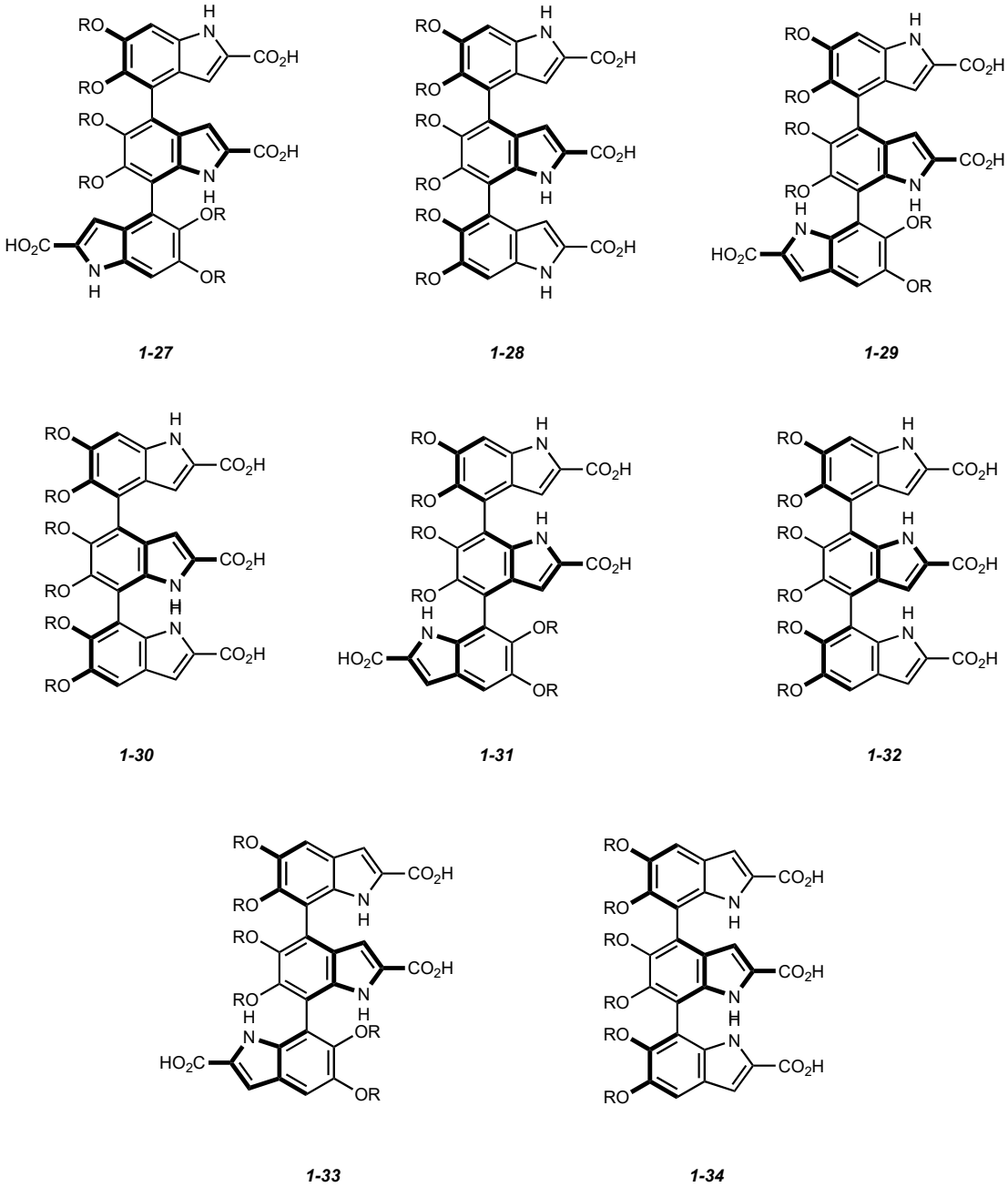

Scheme 1.8. Trimers isolated from biomimetic oxidations of **DHICA**.[42,43] R=$COCH_3$. Only one enantiomer of each atropisomer is represented.

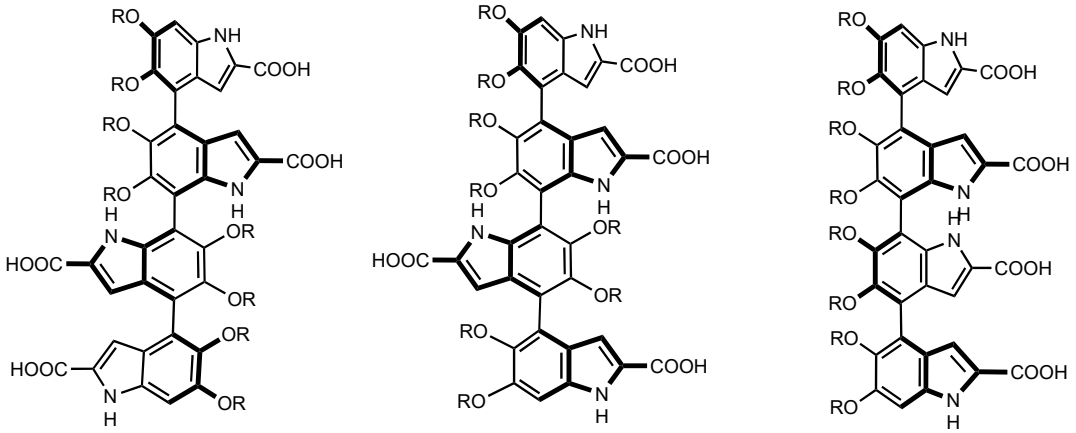

Scheme 1.9. Atropisomers of the linear **DHICA** tetramer isolated by Pezzella *et al.* Only one enantiomer of each atropisomer is represented.

Properties

The molecular scaffolds of pure **DHI**- and pure **DHICA**- oligomers are indeed quite distinct. Upon oxidation, **DHI** dimers will generate compact, pi-stacked, largely planar species. These demonstrate strong absorption in the visible light region.[46] The **DHI** units may be coupled by any of the 4,4', 4,7', 7,7', 2,4' or 2,7' linking patterns. **DHICA** chain growth, on the other hand, occurs only primarily through 4,4' and 4,7' linkages, creating twisted linear oligomeric chains.

Mechanisms of excited-state deactivation in **DHICA** oligomers are distinct from those of **DHI**. Evidence presented by Meredith, Sundström and others has suggested that energy dissipation mechanisms in **DHICA** monomers are the result of intramolecular proton transfer (ESIPT).[47,48] The deactivation mechanisms of the **DHICA** monomer, an acetylated dimer, and an acetylated trimer were probed by ultrafast time-resolved fluorescence spectroscopy. ESIPT is a very efficient energy dissipation process and is relevant to the photoprotection of natural eumelanin. ESIPT processes are often facilitated by an intramolecular hydrogen bond existing in the ground state of a molecule.[49] This and the energy level diagram as proposed by Sundström *et al.* for excited state decay are illustrated in Scheme 1.10. It has in fact been shown for **DHICA** that there is an excited-

state equilibrium between the neutral hydrogen-bonded form, and the zwitterionic form **1-38** in which the carboxylic hydrogen has been transferred to the nitrogen.[50] Such a mechanism is not available to **DHI**, given the open C2 position.

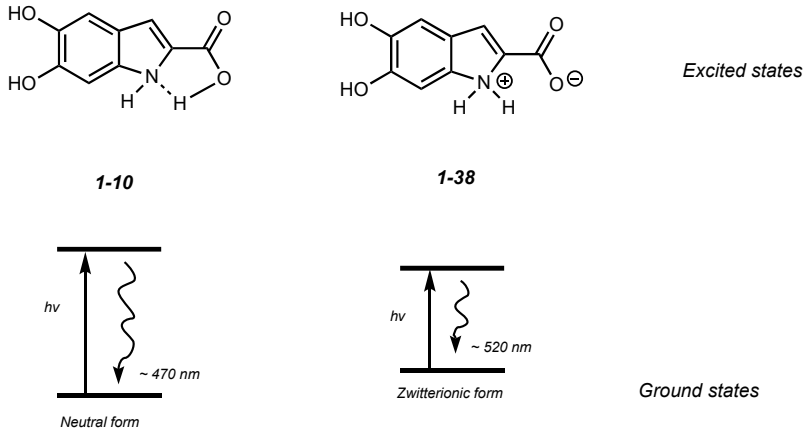

Scheme 1.10. Energy-level diagram of proposed excited-state decay.

The electron-withdrawing carboxylic acid at C2 hinders reactivity of the pyrrole moiety, minimizing reactivity at the C3 position and directing coupling primarily to 4,4', 4,7', and 7,7' patterns. Oligomers of **DHICA** exhibit significantly different structures from oligomers of **DHI**. The planar stacking possible in oligomers of **DHI** based on 2,4', 2,7', and 2,2' coupling patterns is not observed. Instead, the biphenyl-type coupling between **DHICA** units results in atropisomerism at the interunit bonds of **DHICA** oligomers. The number of stereoisomers existing for a single regioisomer increases exponentially with increased chain length. The concept as illustrated by Pezzella *et al.* is reproduced in Scheme 1.11.[51]

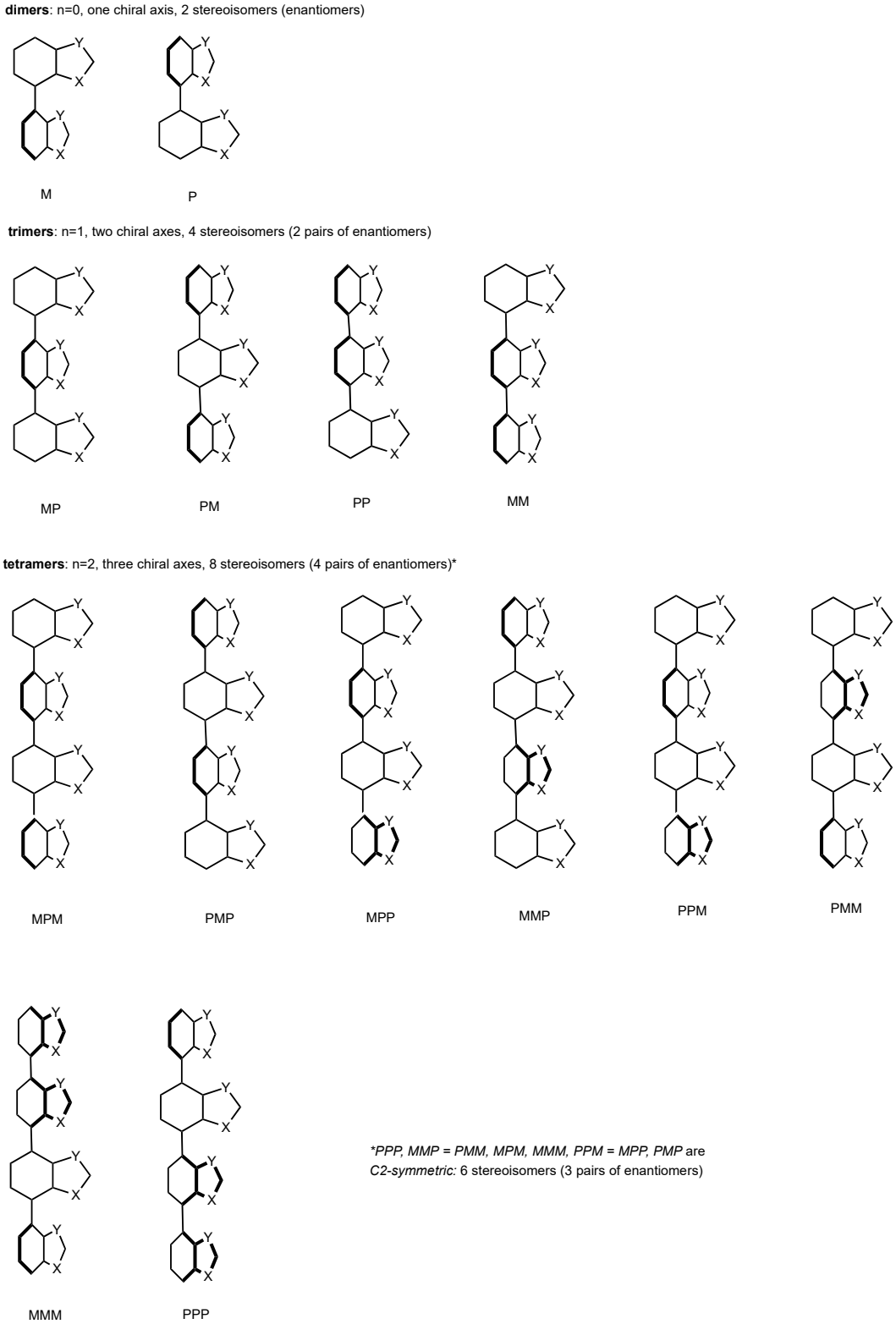

Scheme 1.11. Hierarchical illustration of atropisomerism in oligomers of **DHICA**, reproduced from Pezzella *et al*.

The optical and electronic properties of **DHI** oligomers at the catechol oxidation state are reminiscent of those of **DHI**, and not of natural eumelanin. This points to the importance of oxidized subunits for the emergence of eumelanin's hallmark properties.[52]

3.3 DHICA Monomer

Synthetic Approaches

The first foray into the synthesis of **DHICA** and related derivatives was by Beer and coworkers in 1949.[53] It was based off of the reductive cyclization of 2-nitro-4,5-dihydroxyphenylpyruvic acid **1-39** (Scheme 1.12). Reduction using Fe powder in ethanol and acetic acid yields **1-40**, which can be deacetylated by sodium hydroxide-sodium hydrosulphite to yield **DHICA**. The authors noted the latter to be remarkably stable, and slow to oxidize; eventually, over the course of 24 hours under oxidizing conditions, they observed formation of a dark-brown

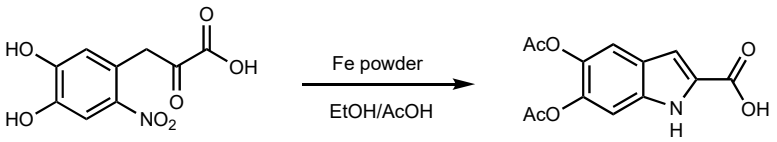

2-nitro-4,5-dihydroxyphenylpyruvic acid
1-39

5,6-diacetoxyindole-2-carboxylic acid
1-40

Scheme 1.12. Synthesis of 5,6-diacetoxyindole-2-carboxylic acid **1-40** by Beer and coworkers, 1949.

solution but not one insoluble as of the melanin-type.[54] They cited this distinct behavior in putting forth a theory on the unlikelihood of **DHICA** as a precursor to melanin, as previously suggested by Raper and Mason. **DHICA** was later confirmed, however, to be a precursor by subsequent studies.[10a]

Gram-scale synthesis of **DHICA** was reported by Benigni and Minnis in 1965.[55] Condensation of 4,5-dibenzyloxy-2-nitrotoluene **1-41** with diethyl oxalate, promoted by potassium ethoxide, results in 2-nitro-4,5-dibenzyloxyphenylpyruvic acid **1-42**. Subsequent reductive cyclization with Fe powder in ethanol and acetic acid results in **1-43**, and catalytic hydrogenation on Pd/C finally yields **DHICA**– although overall yields of less than 20 % were reported (Scheme 1.13).

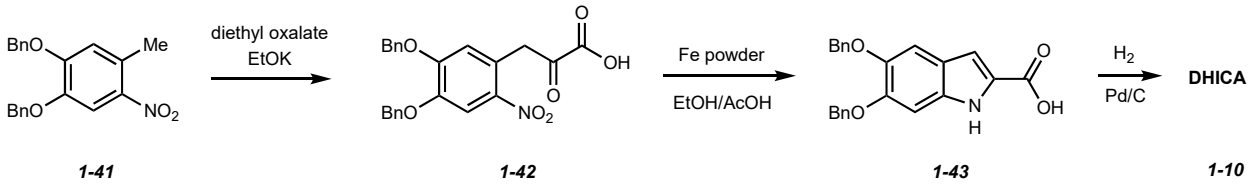

Scheme 1.13. Synthesis of 5,6-dibenzyloxyindole-2-carboxylic acid **1-43** by Benigni and Minnis, 1965.

In 2004, a novel synthetic route for **DHICA** was reported from a study by Sechi and coworkers on HIV-1 integrase inhibitors, and its biological activity evaluated. A Knoevenagel/Hemetsberger-type reaction of dialkoxybenzaldehydes as **1-44** with methyl azidoacetate gives azidocinnamate intermediates as **1-45**. These are then cyclized to the relevant indole derivatives through thermal decomposition of the azido group to yield **1-46** (Scheme 1.14). Ether cleavage using boron tribromide and saponification using potassium hydroxide can finally reveal deprotected **DHICA**.[56,57]

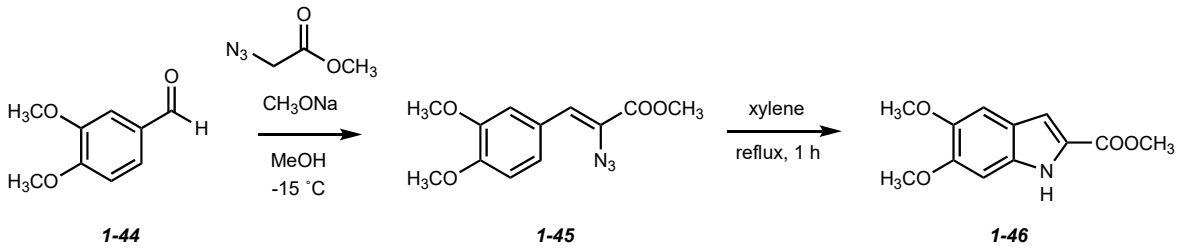

Scheme 1.14. Knoevenagel/Hemetsberger reaction to attain protected **DHICA** derivatives, by Sechi *et al.*

Properties

Properties of the **DHICA** molecule have already been discussed above, in the contexts of **DHICA** synthetic melanins and oligomers, and in comparison to the **DHI** molecule.

3.4 The Blocking Strategy

Experimental oxidation of **DHICA** compounds in the literature is always in the context of the polymeric materials obtained. Smaller oligomers which may also be isolated are at the catechol oxidation state. As noted earlier in the Chapter, oxidized subunits have been implicated in the emergence of eumelanin's hallmark properties. Though computational studies have modeled and predicted its theoretical properties and behaviors, to the best of our knowledge an oxidized **DHICA** unit, **2-carboxy-IQ**, remains unreported in synthetic literature.

As discussed above, research in the Lumb Group has aimed to decouple oxidation from rapid and spontaneous polymerization of melanin precursors. A "blocking" strategy successfully allows, now, synthetic access of an **IQ** derivative electronically faithful to the parent system but stable enough to be spectroscopically studied.[19] Ortho-substituted aromatic rings at the C2, C4 and C7 positions sterically impede covalent bond formation and chain growth which would normally occur with oxidation. Orthogonality between the π-planes of the aryl blocking groups and that of the indole core minimizes electronic perturbation of the parent **IQ** system (**1-48**, Scheme 1.15). These compounds, quite notably, exhibit optical and electronic properties that resemble the paramagnetism, broadband absorption, and ultrafast excited-state decay which are hallmarks of the eumelanin biopolymer. This result opens the path to a bottom-up understanding of the emergent properties of eumelanin.

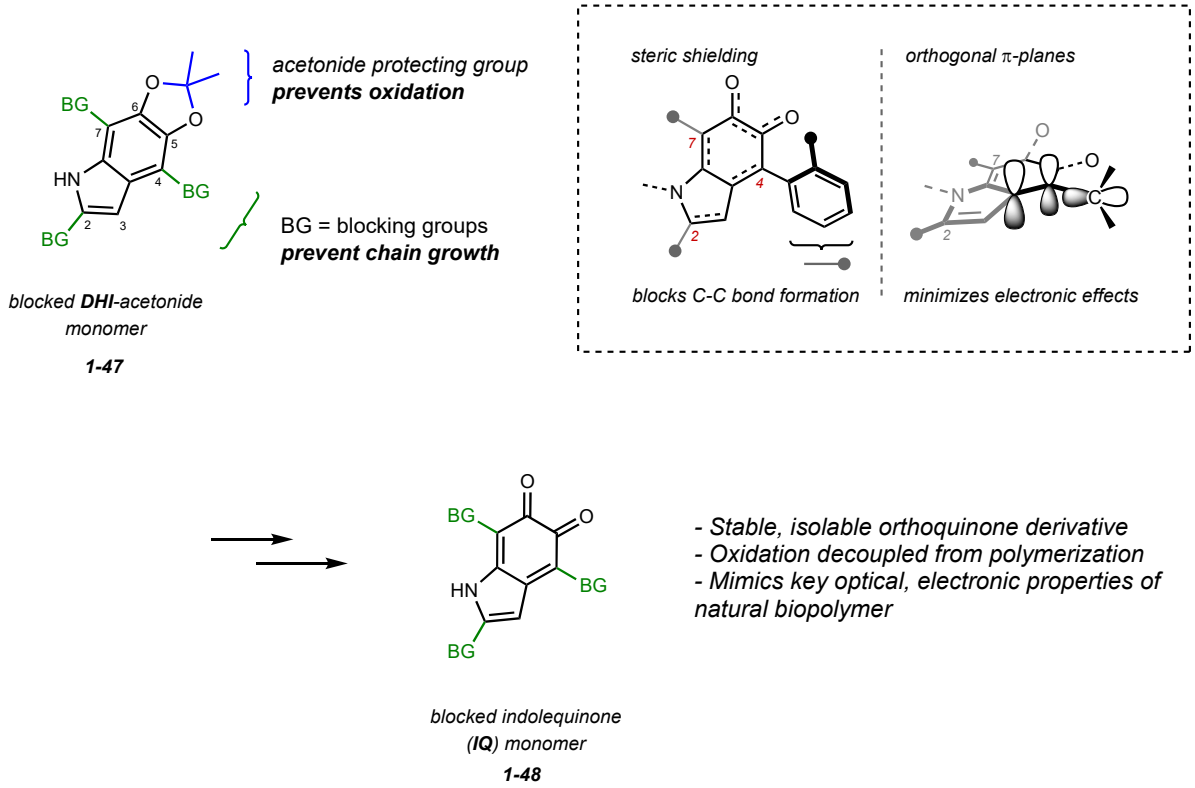

Scheme 1.15. Blocking strategy as developed by Wang *et al*.: blocking groups prevent chain growth at reactive positions, with minimal perturbance of the electronic structure of the indole core.[19]

My work during the M.Sc. has the overall goal of expansion and establishment of a robust library of stable melanin-related small molecules using this blocking strategy. The primary focus has been efforts access a blocked **2-carboxy-IQ** compound, whereby the C2 position is occupied by a carboxylic acid instead of a blocking group as in blocked **IQ**. We believe that the optical and electronic properties of such hypothetical oxidized, blocked **DHICA** derivatives would complement those so far proffered by blocked **DHI** derivatives, to round out the insights into the structure-function relationships of eumelanin. In the Chapter to follow we will discuss progression of the synthetic efforts towards this goal. Lastly, in Chapter 3, we will discuss the future work anticipated in continuation and expansion of this project.

4. Conclusions

Realization of the **DHI** blocking strategy and of synthetic access to a monomeric derivative at the orthoquinone oxidation state has underlined the role of oxidized subunits in the emergence of eumelanin's hallmark biological functions. Here we have presented context for the role of **DHICA** in the natural eumelanin biopolymer, and a summary of some key synthetic studies based upon it in the literature. It follows that synthetic access of discrete, stable, blocked **DHICA** and **2-carboxy-IQ** monomers using the established blocking strategy would be a valuable addition to the study.

5. References

1. Raper, H. S., The Tyrosinase-tyrosine Reaction: Production from Tyrosine of 5: 6-Dihydroxyindole and 5: 6-Dihydroxyindole-2-carboxylic Acid—the Precursors of Melanin. *Biochem. J.* **1927,** *21* (1), 89-96.
2. Mason, H. S., The Chemistry of Melanin: III Mechanism of the Oxidation of Dihydroxyphenylalanine by Tyrosinase. *J. Biol. Chem.* **1948,** *172* (1), 83-99.
3. Deibel, R-M. B. and Chedekel, M.R., Biosynthetic and structural studies on pheomelanin. *J. Am. Chem. Soc.* **1982,** 104 (25), 7306-7309.
4. Schmaler-Ripcke, J.; Sugareva, V.; Gebhardt, P.; Winkler, R.; Kniemeyer, O.; Heinekamp, T.; Brakhage, A. A., Production of Pyomelanin, a Second Type of Melanin, via the Tyrosine Degradation Pathway in Aspergillus fumigatus. *Appl. and Environ. Microbiol.* **2009,** *75* (2), 493-503.
5. Meredith, P.; Sarna, T., The physical and chemical properties of eumelanin. *Pigment Cell Res.* **2006,** *19* (6), 572-594.
6. Prota, G., Chapter 2 - Melanin Producing Cells. *Melanins and Melanogenesis*, Ed. Academic Press: San Diego, 1992; pp 14-33.

7. Westerhof, W., The discovery of the human melanocyte. *Pigment Cell Res.* **2006,** *19* (3), 183-193.
8. Jiménez-Cervantes, C.; Solano, F.; Kobayashi, T.; Urabe, K.; Hearing, V. J.; Lozano, J. A.; García-Borrón, J. C., A new enzymatic function in the melanogenic pathway. The 5,6-dihydroxyindole-2-carboxylic acid oxidase activity of tyrosinase-related protein-1 (TRP1). *J. Biol. Chem.* **1994,** *269* (27), 17993-18000.
9. Kobayashi, T.; Urabe, K.; Winder, A.; Jiménez-Cervantes, C.; Imokawa, G.; Brewington, T.; Solano, F.; García-Borrón, J. C.; Hearing, V. J., Tyrosinase related protein 1 (TRP1) functions as a DHICA oxidase in melanin biosynthesis. *EMBO J.* **1994,** *13* (24), 5818-5825.
10. **(a)** Pezzella, A.; d'Ischia, M.; Napolitano, A.; Palumbo, A.; Prota, G., An integrated approach to the structure of Sepia melanin. Evidence for a high proportion of degraded 5, 6-dihydroxyindole-2-carboxylic acid units in the pigment backbone. *Tetrahedron* **1997**, 53 (24), 8281– 8286. (b) Nofsinger, J. B.; Forest, S. E.; Simon, J. D., Explanation for the disparity among absorption and action spectra of eumelanin. *J. Phys. Chem. B.* **1999**, *103* (51), 11428-11432.
11. Palumbo, A.; d'Ischia, M.; Misuraca, G.; Prota, G.; Schultz, T. M., Structural modifications in biosynthetic melanins induced by metal ions. *Biochim. Biophys. Acta Gen. Sub.* **1988**, *964* (2), 193-199.
12. Piattelli, M.; Fattorusso, E.; Magno, S.; Nicolaus, R. A., The structure of melanins and melanogenesis—II: Sepiomelanin and synthethic pigments. *Tetrahedron*, **1962**, *18* (8), 941-949.
13. Benathan, M. & Wyler, H., Quantitative approaches to melanin structure. *Yale J. Biol. Med.* **1980**, *53* (5) 389-390.
14. **(a)** d'Ischia, M.; Wakamatsu, K.; Napolitano, A.; Briganti, S.; Garcia-Borron, J.C.; Kovacs, D.; Meredith, P.; Pezzella, A.; Picardo, M.; Sarna, T.; Simon, J.D., Ito, S., Melanins and melanogenesis: methods, standards, protocols. *Pigment Cell Melanoma Res.* **2013**, *26* (5), 616-633. **(b)** Ito, S. Reexamination of the structure of eumelanin. *Biochim. Biophys. Acta Gen. Sub.* **1986**, *883* (1), 155-161.
15. Tsukamoto, K.; Palumbo, A.; D'Ischia, M.; Hearing, V. J.; Prota, G., 5, 6-Dihydroxyindole-2-carboxylic acid is incorporated in mammalian melanin. *Biochem. J.* **1992**, *286* (2), 491-495.

16. Prota, G., Photooxidation of 5, 6-dihydroxy-1-methyl-indole. *Tetrahedron* **1987**, *43* (2), 431-434.
17. Palumbo, A.; d'Ischia, M.; Misuraca, G.; Prota, G., Effect of metal ions on the rearrangement of dopachrome. *Biochim. Biophys. Acta Gen. Sub.* **1987**, *925* (2), 203-209.
18. Pezzella, A.; d'Ischia, M.; Napolitano, A.; Palumbo, A.; Prota, G., An integrated approach to the structure of Sepia melanin. Evidence for a high proportion of degraded 5, 6-dihydroxyindole-2-carboxylic acid units in the pigment backbone. *Tetrahedron*, **1997**, *53* (24), 8281-8286.
19. Wang, X.; Kinziabulatova, L.; Bortoli, M.; Manickoth, A.; Barilla, M. A.; Huang, H.; Blancafort, L.; Kohler, B.; Lumb, J.-P. Indole-5, 6-quinones display hallmark properties of eumelanin. *Nat. Chem.* **2023**, *15* (6), 787–793.
20. Kaxiras, E.; Tsolakidis, A.; Zonios, G.; Meng, S., Structural model of eumelanin. *Phys. Rev. Lett.* **2006,** *97* (21), 218102.
21. **(a)** d'Ischia, M.; Napolitano, A.; Ball, V.; Chen, C. T.; & Buehler, M. J., Polydopamine and eumelanin: From structure–property relationships to a unified tailoring strategy. *Acc. Chem. Res.* **2014**, *47* (12), 3541-3550. **(b)** Okuda, H.; Wakamatsu, K.; Ito, S.; Sota, T., Possible oxidative polymerization mechanism of 5, 6-dihydroxyindole from ab initio calculations. *J. Phys. Chem. A.* **2008**, *112* (44), 11213-11222.
22. Bernsmann, F.; Ball, V.; Addiego, F.; Ponche, A.; Michel, M.; Gracio, J. J. d. A.; Toniazzo, V.; Ruch, D., Dopamine−Melanin Film Deposition Depends on the Used Oxidant and Buffer Solution. *Langmuir* **2011,** *27* (6), 2819-2825.
23. Bernsmann, F.; Ponche, A.; Ringwald, C.; Hemmerlé, J.; Raya, J.; Bechinger, B.; Voegel, J.-C.; Schaaf, P.; Ball, V., Characterization of Dopamine−Melanin Growth on Silicon Oxide. *J. Phys. Chem C.* **2009,** *113* (19), 8234-8242.
24. Liebscher, J.; Mrówczyński, R.; Scheidt, H. A.; Filip, C.; Hădade, N. D.; Turcu, R.; Bende, A.; Beck, S., Structure of Polydopamine: A Never-Ending Story? *Langmuir* **2013,** *29* (33), 10539- 10548.
25. Cao, W.; Zhou, X.; McCallum, N. C.; Hu, Z.; Ni, Q. Z.; Kapoor, U.; Heil, C.M.; Cay, K.S.; Zand, T.; Mantanona, A.J.; Jayaraman, A.D.; Deheyn, D.D.; Shawkey, M.D.; Burkart, M.D.; Rinehart, J.D.; Gianneschi, N. C., Unraveling the structure and function of melanin through synthesis. *J. Am. Chem. Soc.* **2021**, *143* (7), 2622-2637.

26. Arzillo, M.; Mangiapia, G.; Pezzella, A.; Heenan, R. K.;Radulescu, A.; Paduano, L.; d'Ischia, M., Eumelanin Buildup on the Nanoscale: Aggregate Growth/Assembly and Visible Absorption Development in Biomimetic 5,6-Dihydroxyindole Polymerization. *Biomacromolecules* **2012**,*13* (8), 2379−2390.
27. Napolitano, A.; Pezzella, A.; Vincensi M. R.; Prota G., Oxidative degradation of melanins to pyrrole acids: a model study. *Tetrahedron* **1995**, *51* (20), 5913-5920.
28. **(a)** Blarzino, C.; Mosca, L.; Foppoli, C.; Coccia, R.; De Marco, C.; Rosei, M. A., Lipoxygenase/H2O2-catalyzed oxidation of dihydroxyindoles: Synthesis of melanin pigments and study of their antioxidant properties. *Free Radic. Biol. Med.* **1999**, *26* (3−4), 446−453. **(b)** Sealy, R. C., Radicals in melanin biochemistry. *Meth. Enzymol*. Academic Press, 1984 Vol. 105, pp 479–483.
29. Xu, R.; Prontera, C. T.; Di Mauro, E.; Pezzella, A.; Soavi, F.; Santato, C. An electrochemical study of natural and chemically controlled eumelanin. *APL Mater.* **2017**, *5* (12), 126108.
30. Vitiello, G.; Pezzella, A.; Zanfardino, A.; Silvestri, B.; Giudicianni, P.; Costantini, A.; Varcamonti, M.; Branda, F.; Luciani, G., Antimicrobial activity of eumelanin-based hybrids: The role of TiO2 in modulating the structure and biological performance. *Mater. Sci. Eng. C.* **2017**, *75*, 454−462
31. Panzella, L.; Melone, L.; Pezzella, A.; Rossi, B.; Pastori, N.; Perfetti, M.; D'Errico, G.; Punta, C.; d'Ischia, M., Surface Functionalization of Nanostructured Cellulose Aerogels by Solid State Eumelanin Coating. Biomacromolecules **2016**, *17* (2), 564−571.
32. Vitiello, G.; Pezzella, A.; Zanfardino, A.; Varcamonti, M.; Silvestri, B.; Costantini, A.; Branda, F.; Luciani, G., Titania as a driving agent for DHICA polymerization: a novel strategy for the design of bioinspired antimicrobial nanomaterials. *J. Mater. Chem. B.* **2015**, *3* (14), 2808−2815.
33. Wunsche, J.; Deng, Y. X.; Kumar, P.; Di Mauro, E.; Josberger, E.; Sayago, J.; Pezzella, A.; Soavi, F.; Cicoira, F.; Rolandi, M.; Santato, C., Protonic and Electronic Transport in Hydrated Thin Films of the Pigment Eumelanin. *Chem. Mater.* **2015**, *27* (2), 436−442.
34. Gargiulo, V.; Alfe, M.; Di Capua, R.; Togna, A. R.; Cammisotto, V.; Fiorito, S.; Musto, A.; Navarra, A.; Parisi, S.; Pezzella, A., Supplementing pi-systems: eumelanin and graphene-like integration towards highly conductive materials for the mammalian cell culture bio-interface. *J. Mater. Chem. B.* **2015**, *3* (25), 5070−5079.

35. Pezzella, A.; Panzella, L.; Crescenzi, O.; Napolitano, A.; Navaratnam, S.; Edge, R.; Land, E.J.; Barone, V.; d'Ischia, M., Lack of visible chromophore development in the pulse radiolysis oxidation of 5, 6-dihydroxyindole-2-carboxylic acid oligomers: DFT investigation and implications for eumelanin absorption properties. *J. Org. Chem.* **2009**, *74* (10), 3727-3734.
36. Jiang, S.; Liu, X.M.; Dai, X.; Zhou, Q.; Lei, T.C.; Beermann, F.; Wakamatsu, K.; Xu, S.Z., Regulation of DHICA-mediated antioxidation by dopachrome tautomerase: implication for skin photoprotection against UVA radiation. *Free Radical Biol. Med.* **2010**, *48* (9), 1144 – 1151.
37. Watt, A. A.; Bothma, J. P.; Meredith, P., The supramolecular structure of melanin. *Soft Matter*, **2009**, *5* (19), 3754-3760.
38. Panzella, L.; Gentile, G.; D'Errico, G.; Della Vecchia, N. F.; Errico, M. E.; Napolitano, A.; Carfagna, C.; d'Ischia, M., Atypical structural and π-electron features of a melanin polymer that lead to superior free-radical-scavenging properties. *Angew, Chem. Int. Ed*. **2013**, *52* (48), 12684-12687.
39. **(a)** d'Ischia, M.; Napolitano, A.; Pezzella, A.; Land, E.J.; Ramsden, C.A.; Riley, P.A., 5, 6-dihydroxyindoles and indole-5, 6-diones. *Adv. Heterocycl. Chem.* **2005**, *89,* 1-63. **(b)** Panzella, L.; Pezzella, A.; Napolitano, A.; d'Ischia, M., The First 5, 6-Dihydroxyindole Tetramer by Oxidation of 5,5',6,6'-Tetrahydroxy-2,4'-biindolyl and an Unexpected Issue of Positional Reactivity en Route to Eumelanin-Related Polymers. *Org. Lett.* **2007** *9* (7), 1411-1414. **(c)** Pezzella, A.; Panzella, L.; Natangelo, A.; Arzillo, M.; Napolitano, A.; d'Ischia, M., 5,6-Dihydroxyindole Tetramers with "Anomalous" Interunit Bonding Patterns by Oxidative Coupling of 5,5', 6,6'-Tetrahydroxy-2,7'-biindolyl: Emerging Complexities on the Way toward an Improved Model of Eumelanin Buildup. *J. Org. Chem.* **2007**, *72* (24), 9225-9230.
40. Wang, J. & Blancafort, L., Stability and optical absorption of a comprehensive virtual library of minimal eumelanin oligomer models. *Angew. Chem*. **2021,** *133* (34), 18948-18957.
41. Pezzella, A.; Napolitano, A.; d'Ischia, M.; Prota, G., Oxidative polymerisation of 5, 6-dihydroxyindole-2-carboxylic acid to melanin: A new insight. *Tetrahedron*, **1996**, *52* (23), 7913-7920.

42. Pezzella, A.; Vogna, D.; Prota, G., Atropoisomeric melanin intermediates by oxidation of the melanogenic precursor 5, 6-dihydroxyindole-2-carboxylic acid under biomimetic conditions. *Tetrahedron* **2002**, *58* (19), 3681-3687.
43. Pezzella, A.; Vogna, D.; Prota, G., Synthesis of optically active tetrameric melanin intermediates by oxidation of the melanogenic precursor 5,6-dihydroxyindole-2-carboxylic acid under biomimetic conditions. *Tetrahedron: Asymmetry* **2003**, *14* (9), 1133-1140.
44. Palumbo, P.; d'Ischia, M.; Crescenzi, O.; Prota, G., Isolation of a new intermediate in the oxidative conversion of 5, 6-dihydroxyindole-2-carboxylic acid to melanin. *Tetrahedron Lett.* **1987**, *28* (4), 467-470.
45. **(a)** Pezzella, A.; Vogna, D.; & Prota, G., Atropoisomeric melanin intermediates by oxidation of the melanogenic precursor 5, 6-dihydroxyindole-2-carboxylic acid under biomimetic conditions. *Tetrahedron*, **2002**, *58* (19), 3681-3687. **(b)** Pezzella, A.; Napolitano, A.; d'Ischia, M.; Prota, G., Oxidative polymerisation of 5, 6-dihydroxyindole-2-carboxylic acid to melanin: A new insight. *Tetrahedron*, **1996**, *52* (23), 7913-7920; **(c)** Napolitano, A.; Crescenzi, O.; Prota, G., Copolymerisation of 5, 6-dihydroxyindole and 5, 6-dihydroxyindole-2-carboxylic acid in melanogenesis: isolation of a cross-coupling product. *Tetrahedron Lett.* **1993**, *34* (5), 885-888. **(d)** Palumbo, P.; d'Ischia, M.; Prota, G., Tyrosinase-promoted oxidation of 5, 6-dihydroxyindole-2-carboxy1ic acid to melanin. Isolation and characterization of oligomer intermediates. *Tetrahedron,* **1987**, *43* (18), 4203-4206.
46. Pezzella, A.; Panzella, L.; Crescenzi, O.; Napolitano, A.; Navaratnam, S.; Edge, R.; Land, E.J.; Barone, V.; d'Ischia, M., Short-lived quinonoid species from 5, 6-dihydroxyindole dimers en route to eumelanin polymers: integrated chemical, pulse radiolytic, and quantum mechanical investigation. *J. Am. Chem. Soc.* **2006**, *128* (48), 15490-15498.
47. Olsen, S.; Riesz, J.; Mahadevan, I.; Coutts, A.; Bothma, J. P.; Powell, B. J.; McKenzie, R.H.; Smith, S.C.; Meredith, P., Convergent proton-transfer photocycles violate mirror-image symmetry in a key melanin monomer. *J. Am. Chem. Soc.* **2007**, *129* (21), 6672-6673.
48. Gauden, M.; Pezzella, A.; Panzella, L.; Neves-Petersen, M.T.; Skovsen, E.; Petersen, S.B.; Mullen, K.M.; Napolitano, A.; d'Ischia, M.; Sundstrom, V., Role of solvent, pH, and molecular size in excited-state deactivation of key eumelanin building blocks: implications for melanin pigment photostability. *J. Am. Chem. Soc.* **2008**, *130* (50), 17038-17043.

49. **(a)** Weller, A., Innermolekularer protonenübergang im angeregten zustand. *Zeitschrift für Elektrochemie,* Ber. Bunsenges. Phys. Chem. **1956**, *60* (9-10), 1144-1147. **(b)** Kosower, E. M.; Huppert, D. Excited state electron and proton transfers. *Annu. Rev. Phys. Chem.* **1986**, *37*(1), 127-156.
50. Bangal, P. R.; Chakravorti, S., Excited state proton transfer in indole-2-carboxylic acid and indole-5-carboxylic acid. *J. Phys. Chem. A*. **1999**, *103* (43), 8585-8594.
51. d'Ischia, M.; Napolitano, A.; Pezzella, A., 5,6-Dihydroxyindole chemistry: unexplored opportunities beyond eumelanin. *Eur. J. Org. Chem.* **2011** *2011* (28), 5501-5516.
52. Wang, J.; Blancafort, L., Stability and optical absorption of a comprehensive virtual library of minimal eumelanin oligomer models. *Angew. Chem. Int. Ed.* **2021**, *60*, 18800-18809.
53. Napolitano, A.; Pezzella, A.; Land, E. J.; Ramsden, C. A.; Riley, P. A., 5, 6-dihydroxyindoles and indole-5, 6-diones. *Adv. Heterocycl. Chem.*, **2005**, *89*, 20-23.
54. Beer, R. J. S.; McGrath, L.; Robertson, A.; Woodier, A. B., 441. The chemistry of the melanins. Part II. The synthesis of 5: 6-dihydroxyindole-2-carboxylic acid and related compounds. *J. Chem. Soc. (Resumed)*, **1949**, 2061-2066.
55. Benigni, J. D.; Minnis, R. L., The syntheses of 5, 6-dihydroxyindole and some of its derivatives. *J. Heterocycl. Chem.* **1965**, *2* (4), 387-392.
56. Sechi, M.; Angotzi, G.; Dallocchio, R.; Dessì, A.; Carta, F.; Sannia, L.; Mariani, A.; Fiori, S.; Sanchez, T.; Movsessian, L.; Plasencia, C.; Neamati, N., Design and synthesis of novel dihydroxyindole-2-carboxylic acids as HIV-1 integrase inhibitors. *Antivir. Chem. and Chemother.* **2004**, *15* (2), 67-81.
57. Hemetsberger, H.; Knittel, D.; Weidmann, H., Enazides, III: Thermolysis of α-azido-cinnamates. Synthesis of indol carboxylates. *Monatsh. Chem.* **1970**, *101*, 161-165.
58. **(a)** Hatcher, L. Q.; Simon, J. D., Ultra-low temperature oxidation of 5, 6-dihydroxyindole: A novel approach to study synthetic melanogenesis. *Photochem. Photobiol*. **2008**, *84* (3), 608-612. **(b)** Lu, Y., Biosynthetic inorganic chemistry. *Angew. Chem. Int. Ed.* **2006**, *45* (34), 5588-5601.

Chapter 2: Synthesis of Blocked DHICA Derivatives

1. Introduction

Chapter 1 reviews the biological context of eumelanin, and offers an overview of some past and current studies on these last-known monomeric units in the eumelanogenic pathway. A proper understanding of the structure-function-property relationships of the biopolymer remains elusive due to its inability to be characterized by conventional characterization methods. This knowledge gap precludes the rational design of functional materials, such as biocompatible semiconductors or sun-screening materials, as well as the understanding of human disease, such as melanoma or Parkinson's.

As discussed in Chapter 1, previous work in the group (by Ms. Xueqing Wang) has successfully achieved access to oxidized "blocked" **DHI** derivatives.[1] These compounds have already offered invaluable insight into the structure-function relationships of the natural biopolymer. Familiarization with the synthetic route and contribution of material for blocked **DHI** research efforts made up a significant portion of training for my M.Sc.

DHI, however, only covers part of the eumelanin story. The electronics of the second monomer implicated in the biosynthetic pathway – **DHICA** – differs significantly from the electronics of **DHI** due to the presence of the electron-withdrawing carboxylic acid group at the C2 position. And in 1986, studies by Ito *et al*. established the presence of **DHICA**-derived subunits to make up over half of the natural eumelanin network.[2] It is next certainly of interest to address the **DHICA** counterpart of the eumelanin polymeric network by attaining access also to "blocked" **DHICA** derivatives. My work in this M.Sc. program has focused on the latter. Chapter 2 will discuss the progress that has been made towards attaining the final target blocked, oxidized **DHICA** monomer (*blocked 2-carboxy-indole-5,6-quinone*, **2-carboxy-IQ-Me**). The aforementioned compound name is given the *-Me* suffix in reference to the ortho-tolyl blocking

group as drawn in the retrosynthesis of Scheme 2.1. This aryl blocking group was the one predominantly used in blocked **DHI** studies for its ease of installment and its stability following deprotection and oxidation. It can be noted here that it is the blocking group used in all further blocked **DHICA** research efforts discussed in this Thesis.

I will first detail the previously-established synthetic route for the blocked, oxidized **DHI** derivatives (*blocked indole-5,6-quinone*, **IQ-Me**) (Schemes 2.2, 2.3)[1], as my own synthetic route will draw from it. The progress that has been made towards attaining **2-carboxy-IQ-Me** will be explained next. Although the final orthoquinone target has not yet been attained, we have successfully developed and optimized conditions for key transformations in the pathway. Initial synthesis of the C2-unsubstituted indole core is based upon the Leimgruber-Batcho indole synthesis.[3] The routes diverge at the sixth transformation in the pathway (Scheme 2.1). We see this divergent synthetic approach to be of notable advantage as it means that both blocked derivatives may be synthetically accessed from the key late-stage intermediate **2-4**, streamlining future study. The Chapter will move on to discuss the bismuth-mediated chemistry for selective removal of the boronic ester handle at C2 (indole numbering, see Scheme 2.3) of intermediate **2-4**. Optimization of the subsequent Suzuki-Miyaura coupling for installation of the aryl blocking

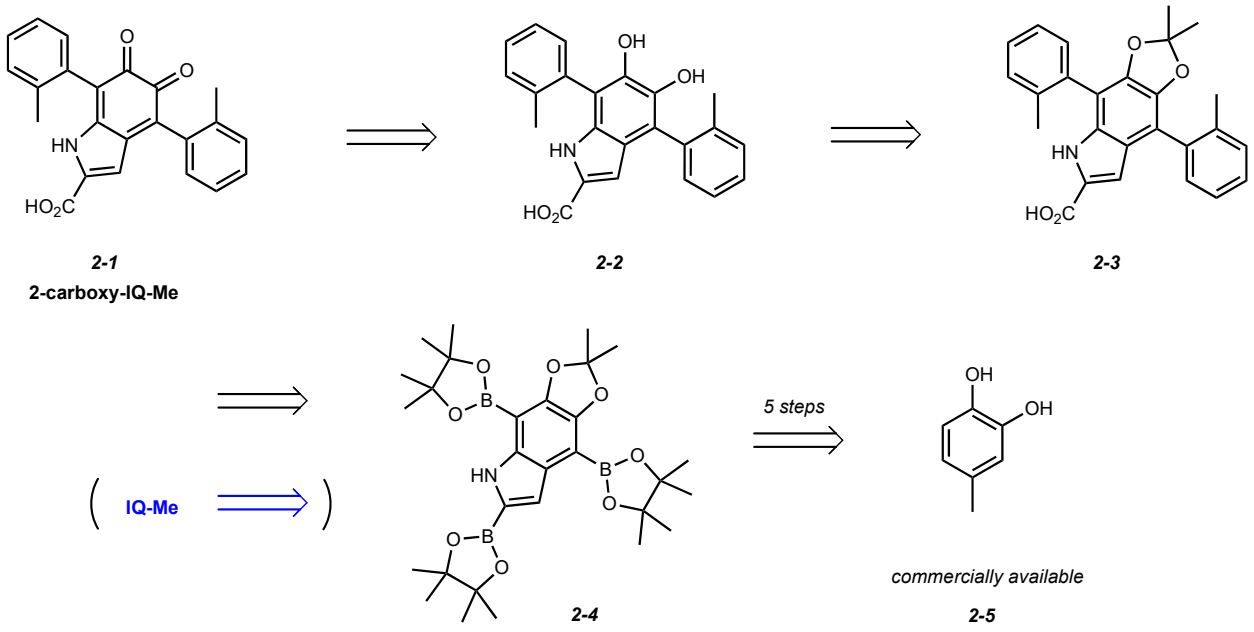

Scheme 2.1. Proposed retrosynthesis of **2-carboxy-IQ-Me**. The route shares precursor **2-4** with **IQ-Me**.

groups at C4 and C7 is discussed in Section 3.2. Section 3.3 will describe the efforts to establish conditions for the key C2 carboxylation. Section 3.4 will detail the efforts to then remove the nitrogen- and the dihydroxy- protecting groups from our C2-carboxylated substrate. We will discuss the obstacles in removal of these groups. There arose also during the study the possibility of alternative C2 functionalization; some preliminary studies are discussed in Sections 3 and 4, and then will be further addressed in Chapter 3.

2. Synthesis of Blocked DHI Derivatives

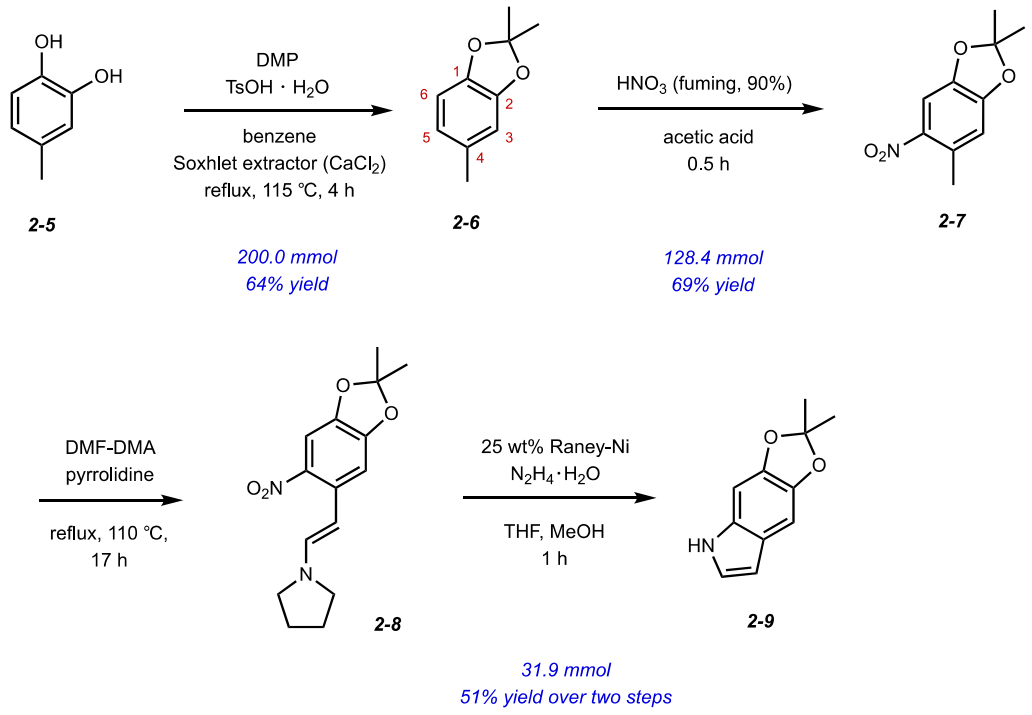

Scheme 2.2. Synthetic pathway to reach the acetonide-protected **DHI** core **2-9**.

The synthetic route for obtaining acetonide-protected indole core **2-9** is modified from the method of Leimgruber *et al*. and was work done by past group member Dr. Haiyan Huang.[3a] Commercially-available 4-methylcatechol **2-5** was acetonide-protected using conditions slightly

modified from those of Frey *et al.*[3c] Compound **2-6** was then nitrated at the C5 position (see numbering on substrate **2-6**, Scheme 2.2)[3b] using fuming nitric acid. The nitration is selective for this position due to electron-donation from both the alkyl group *ortho* and the oxygen *para*, in addition to the smaller steric penalty as compared to C3. Condensation with DMF-DMA followed by displacement of pyrrolidine yielded the enamine **2-8**. The crude of this reaction could be advanced to a reduction of the -NO_2 functional group to an amine using Raney Nickel; this subsequently led to a cyclization to form the acetonide-protected dihydroxyindole core ("**DHI**-acetonide") **2-9** in 51% yield over two steps.

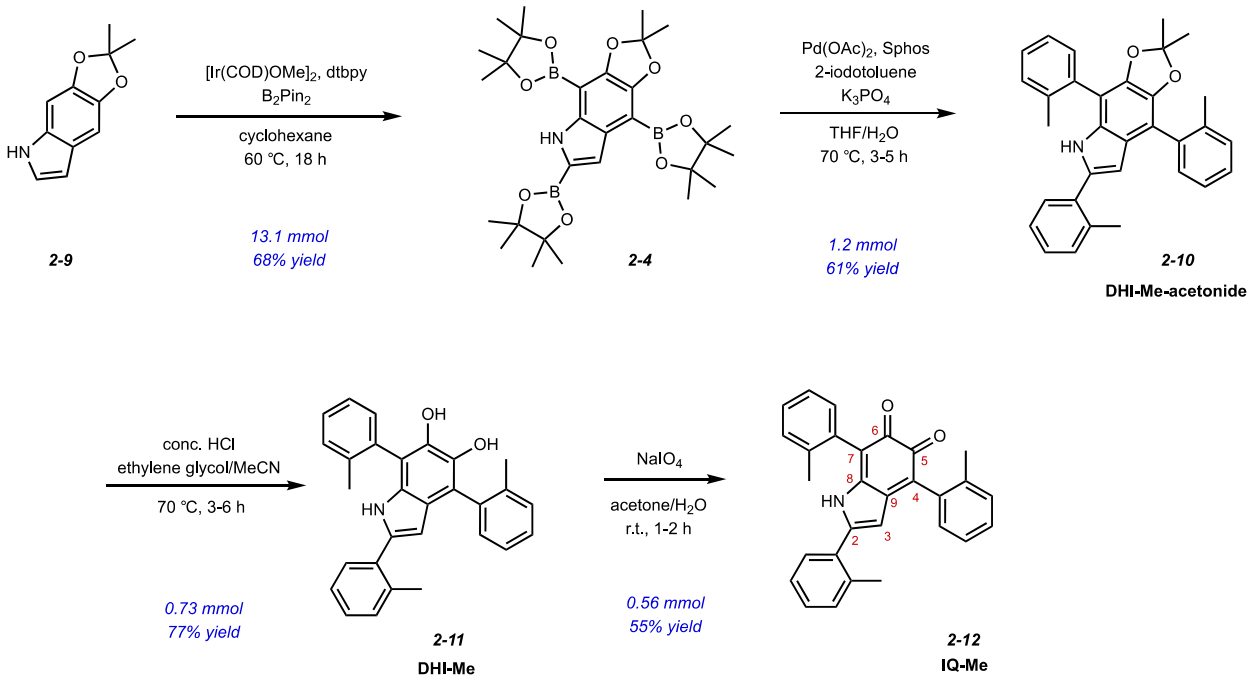

Scheme 2.3. Transformation of the indole core **2-9** into blocked **IQ** derivatives.[1] Indole carbon numbering is indicated on substrate **2-12**.

The synthetic route proceeding from **2-9** towards blocked **IQ** derivatives was developed by group member Ms. Xueqing Wang. An iridium-catalyzed borylation reaction at 60 ºC installed convenient boronic-ester handles at all of the C2, C4, and C7 positions within 18 hours. Kinetically, C2 is installed first, followed by C7, and finally C4. Due to electron donation from the C6 hydroxyl group, borylation at the most electron-rich C2 position is facile; the NH of the

indole ring then serves to guide borylation to the adjacent positions of C7, before C4, borylation. The boronic-ester handles are used as coupling handles for installation of aryl blocking groups. Compound **2-4** underwent a classic Suzuki-Miyaura coupling reaction with 2-iodotoluene to afford **DHI**-**Me**-acetonide **2-10** in 61% yield. The acetonide protecting group was removed under acidic conditions at 70 ºC to access **DHI-Me 2-11** as a white solid; this precursor was then able to be oxidized with 2.2 equivalents of sodium periodate to access **IQ-Me 2-12**.

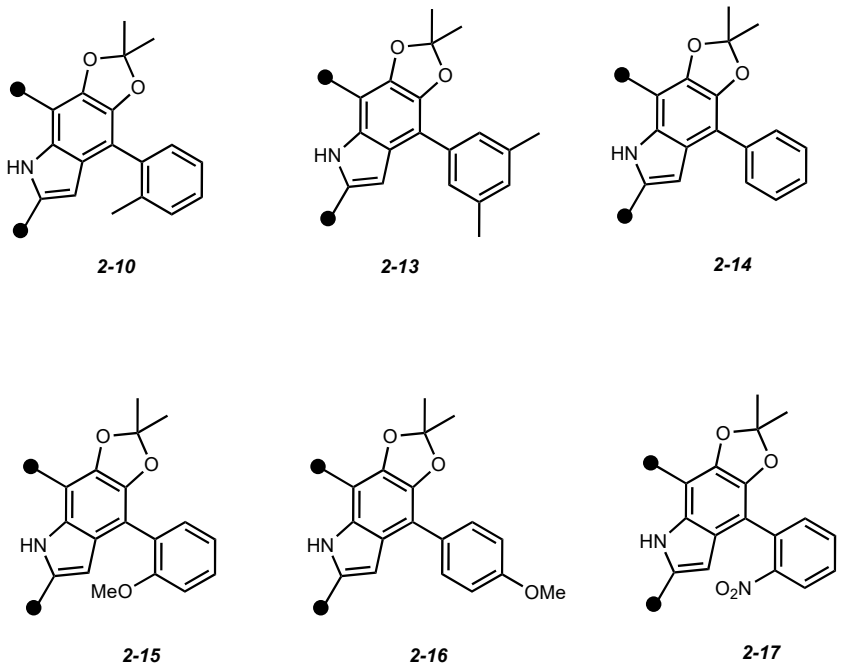

Scheme 2.4. Library of blocked **DHI**-acetonide derivatives established by Ms. Xueqing Wang. Black dots indicate the same aryl substitution as shown at the C4 position of each substrate.

It is worth noting that besides 2-iodotoluene, different aryl iodides have been used as coupling partners for the Suzuki-Miyaura reaction, providing a small library of blocked **DHI**-acetonide derivatives **2-10** to **2-17** available for downstream synthesis (Scheme 2.4). Blocking groups within the library included various 2-, 4-, and 6- substitutions around the aryl ring.

3. Development of Synthetic Route Towards Blocked DHICA Derivatives

Blocked **DHICA** derivatives differ structurally by the presence of a carboxylic acid at the C2 position instead of an aryl blocking group. We were pleased to discover robust conditions for a selective C2 protodeborylation (work by colleague Ms. Xueqing Wang), such that synthetic efforts toward blocked **DHICA** could be started from the point of the tris-borylated indole-acetonide **2-4**. We considered this to be a practical advantage in terms of time and resource management, as substrate **2-4** can be prepared in five steps and on large scales (Schemes 2.2, 2.3). As the library expands, a variety of melanin-related compounds can be accessible from a late-stage intermediate.

3.1. Bismuth-mediated protodeborylation

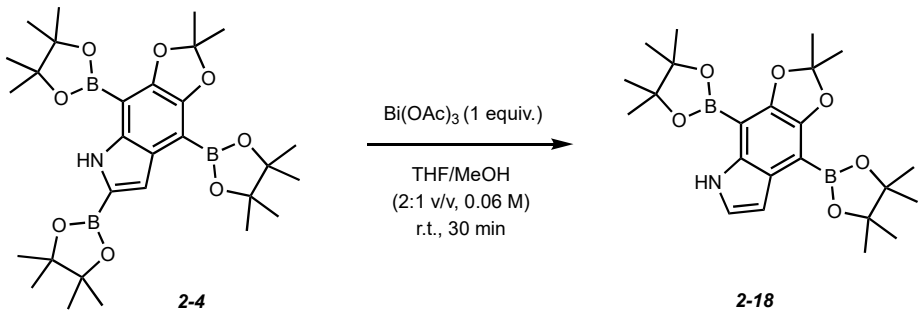

Scheme 2.5. Conditions for bismuth-mediated selective removal of the C2 boronic ester.

The conditions for protodeborylation of compound **2-4** are slightly modified from those of Watson *et al.*[4] To our delight, facile removal of the C2-Bpin was observed with use of 1 equivalent of $Bi(OAc)_3$ in THF/MeOH (2:1 mixture) within 30 minutes, yielding the desired C2-H, C4,7-borylated substrate **2-18** (Scheme 2.5). Longer reaction times and/or heating have shown to lead second to C7, and lastly to C4 deborylation. The latter selectivity can be again attributed to the

inherent nucleophilicity of C2, as well as a directing effect of the indole NH. This same association also guides deborylation to the C7 position to a lesser extent. We propose the mechanism as illustrated in Scheme 2.6. An initial ligand exchange between bismuth acetate and methanol is followed by coordination of an oxygen of the resultant **2-21** with the hydrogen of the indole nitrogen **2-22** to favor subsequent transfer of a methoxy-group to the boron at the adjacent C2 position, resulting in a tetravalent boron **2-23** that can undergo protodeborylation to yield **2-18**.

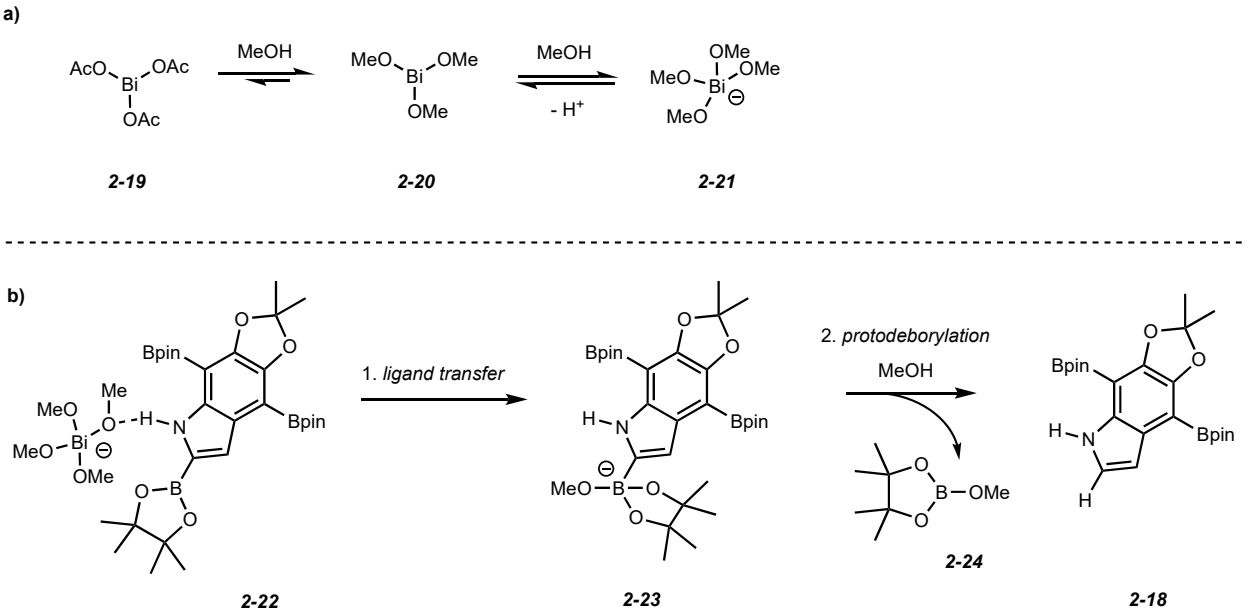

Scheme 2.6. Suggested mechanism of the bismuth-mediated protodeborylation. The C2 deborylation is shown. **a)** formation of 'ate'-complex. **b)** Ligand transfer guided by indole NH to C2 for protodeborylation.

While previously synthesis of compound **2-18** in the lab achieved yields of over 80% when run under air and without effort to exclude moisture, initial runs of the reaction in my hands following suit were low-yielding (only 40 – 50%). It might be expected that the presence of water in the reaction would promote the initial ligand addition. In optimization efforts, therefore, we experimented with running the reaction in the absence of oxygen and moisture. Unexpectedly, several of such trials in fact achieved improved yields. Subsequent trials run again *without* effort

to exclude air and moisture, however, also showed improved yields. Ultimately, this and the inconsistency of parameters such as scale (reactions were run with the intent of pushing material forward, rather than proper optimization) precluded the verification of mechanistic considerations. Prolonged reaction times (greater than 1 hour) led to mixtures of **2-18** and mono-C4-borylated **DHI**-acetonide **2-25** (Scheme 2.7). These two substrates are similar in polarity and so mixtures were difficult to separate; it could be advantageous to stop reactions prior to depletion of starting material (monitoring by TLC) in order to minimize bis-deborylation. Starting material **2-4** and product **2-18** were easily separated.

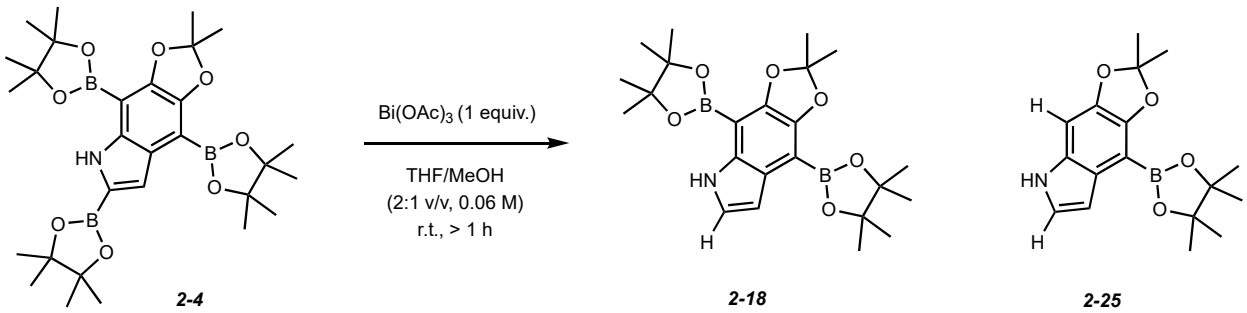

Scheme 2.7. A byproduct of protodeborylation reactions is the mono-borylated substrate **2-25**. Ratio of **2-25** to **2-18** increases with reaction time.

3.2. Optimization of Suzuki Coupling

A Suzuki-Miyaura coupling again was used to transform the boronic-ester handle at the C4 and C7 position to the desired aryl blocking group. The conditions and equivalents from coupling of the tris-borylated substrate **2-4** in blocked **DHI** studies (Section 2, Scheme 2.3) had been slightly adapted for application to the bis-borylated substrate (work by Ms. Xueqing Wang) to use fewer equivalents of aryl-iodide and base. Seeking to improve yields of this reaction in my hands, we explored adjustments to the amount of base (K_3PO_4) used. We hypothesized that greater amounts of base would increase the formation of the palladium hydroxide species involved in the transmetalation, thus facilitating the coupling (Table 2.1). Concentration of the aqueous base was

kept at 1 M, and the v/v ratio of aqueous to organic solvent at 3:1, for an overall reaction concentration of 0.04 M. It is important to note that these trials were run for the purpose of pulling material forward, rather than the express purpose of optimization, and were limited to the current amounts of substrate at hand, hence, unfortunately, the variable of scale was not kept a constant.

Table 2.1. Variation of equivalents of base, Suzuki coupling reaction; reaction mixture concentration 0.04 M.

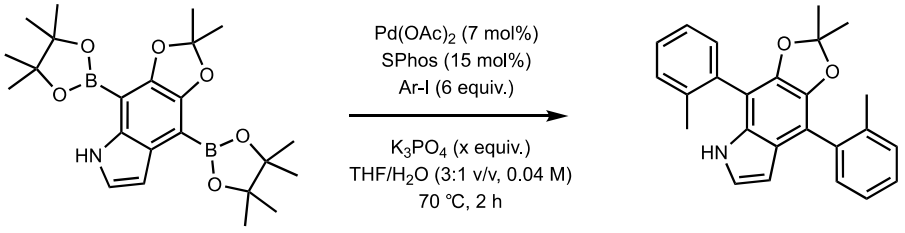

2-18 ***2-26***

Entry	*Scale (mmol)*	*x, equiv. K_3PO_4*	*Yield (%)*
1	0.6	5	66
2	1.1	5	37
3	1.1	5	31
4	0.6	7	24
5	1.3	7	28
6	1.4	7	51
7	1.5	7	43

While fewer equivalents served for higher yields in smaller-scale reactions (66% in entry 1 as opposed to only 24% in entry 4), there was no notable pattern amongst > 1 mmol scale reactions. Both the lowest yield (28%, entry 5) and the highest yield (51%, entry 6) resulted from the use of seven equivalents of base. Ultimately no clear trend was identified, and the results of the optimization were deemed inconclusive.

We hypothesized also that the efficiency of the coupling might be hindered by the high dilution of the reaction mixture. We therefore increased the overall concentration from 0.04 M to 0.2 M, with 7 equivalents of base, and a 5.6 M aqueous base concentration, to obtain average yields of 50%. From there we considered lengthening the reaction time; however, only minimal improvements in yield were observed (Table 2.2).

Table 2.2. Variation of time, Suzuki coupling reaction; reaction mixture concentration 0.2 M.

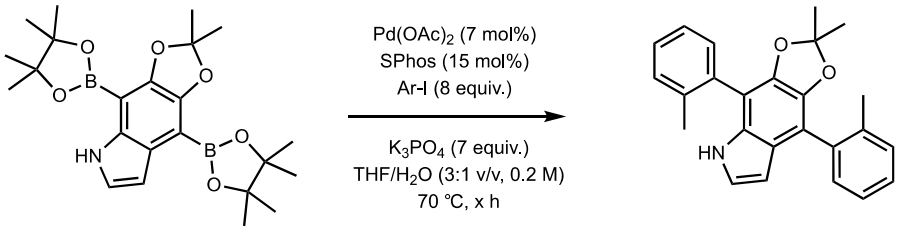

2-18 ***2-26***

Entry	*Scale (mmol)*	*x, Time (h)*	*Yield (%)*
1	0.1	2	50 (*average*)
2	0.2	4	37
3	0.3	3	52
4	0.4	5	50
5	0.5	3	27
6	0.5	3.5	51
7	0.8	3.5	58
8	1.0	3.5	42
9	1.2	4	62

3.3. Exploration of C2 Carboxylation Methods

With the synthetic route to substrate **2-26** established, the next task was installation of the carboxylic acid at C2. With the inherent electronic activation of the C2 position in our indole

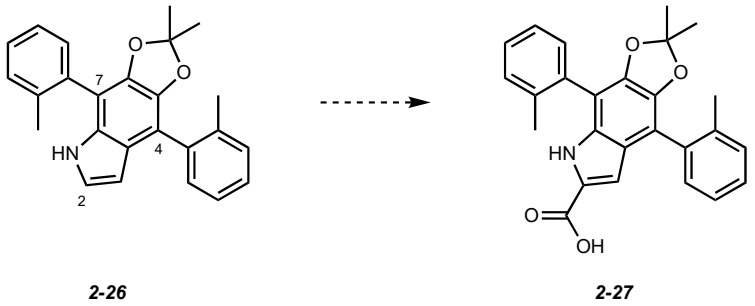

2-26 ***2-27***

Scheme 2.8. Desired subsequent installment of carboxylic acid at C2.

derivative **2-26** (as opposed to C3 in indole **2-28**) and blocking groups installed at C4 and C7, we anticipated good regioselectivity for this transformation. Conditions outlined by Katritzky in 1985 for the carboxylation of indole using *tert*-butyllithium and *n*-butyllithium were first considered (Scheme 2.9a).[5] The proposed mechanism of the transformation goes as follows: i) carboxylation of the indole nitrogen **2-31**, then ii) deprotonation at C2 **2-32**, followed by iii) carboxylation at C2 **2-33**, and finally iv) decarboxylation at the indole nitrogen upon workup to yield **2-34** – all in one pot. The *in situ* protection in the first step masks the reactive indole nitrogen, and is easily removable. It is important to highlight the ability of the nitrogen carboxylate group to direct lithiation to the C2 carbon (**2-31**, Scheme 2.9b). These conditions would eliminate the need for an additional two steps in the linear route for protection and deprotection of the indole nitrogen under alternative conditions.

However, initial attempts applying Katritzky's conditions to our more complex substrate **2-26** were unsuccessful, resulting in either recovered starting material or an unstable product which decomposed before it could be fully characterized. The rise of a broad featureless signal in the aromatic region of the ^{1}H NMR over time suggested decomposition to a complex mixture.

We considered photochemical conditions. The conditions for dearomative hydrocarboxylation of heteroarenes via photochemical activation of formate as reported by Wickens *et al.* were of interest. Photocatalyst 1,3-dicyano-2,4,5,6-tetrakis(diphenylamino)-benzene (4DPAIPN) **2-43** with co-catalyst methyl mercaptobenzoate **2-44** and potassium formate

2-46 in water and DMSO with blue LED light can be used to carboxylate indole (Scheme 2.10a).[6] The proposed mechanism proceeds through photoexcitation of the photocatalyst, followed by

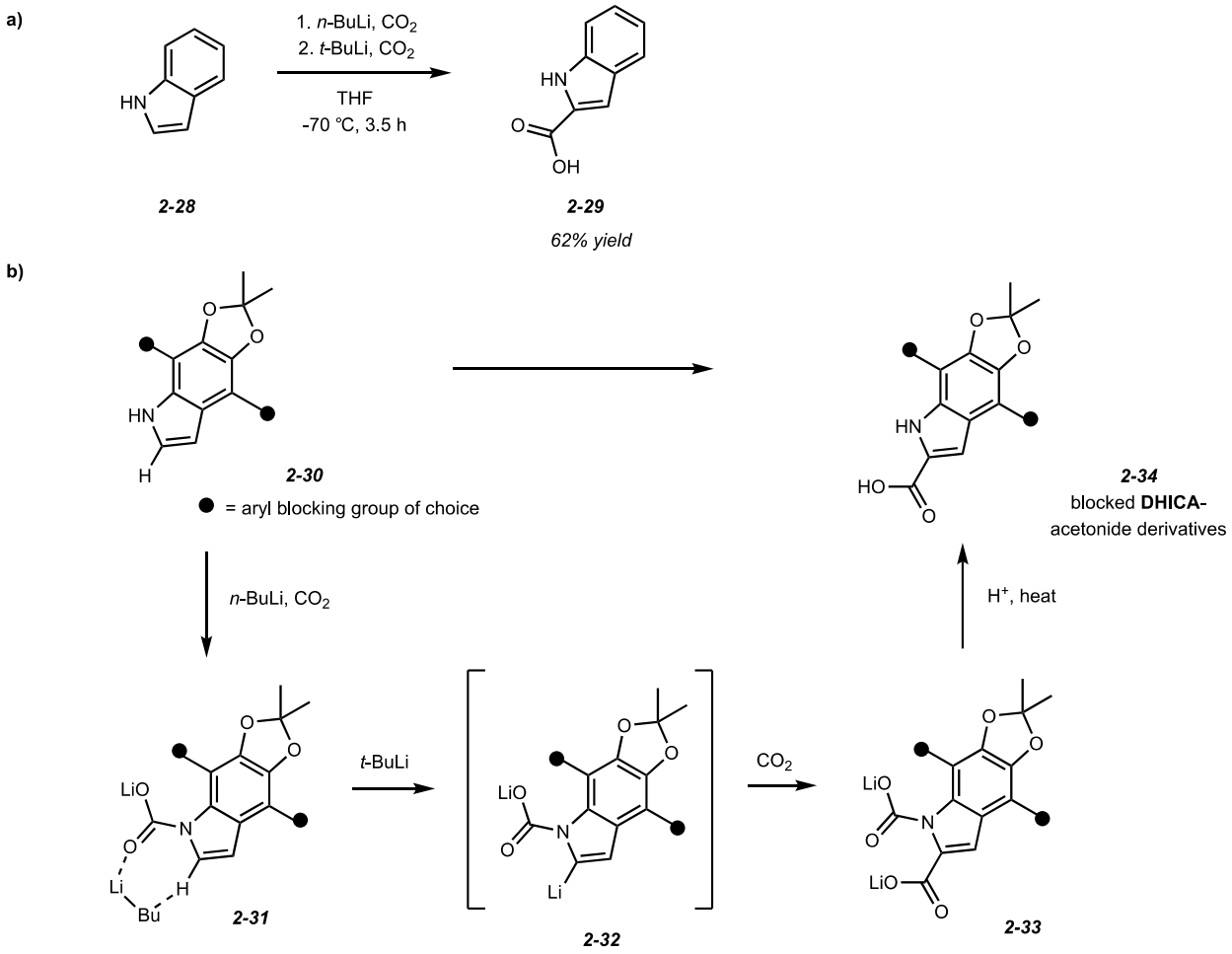

Scheme 2.9. **a)** C3 carboxylation of indole from Katritzky *et al.* Yield shown for product **2-29** is our yield from reproducing these conditions with the reported substrate at 4.3 mmol scale. **b)** Depiction of the *in situ* protection of the indole nitrogen, plus the guiding effect for desired C2 carboxylation.

generation of the sulfur radical **2-45** which can then perform a hydrogen atom transfer (HAT) on the formate to generate the carbonyl radical species **2-47**. This nucleophilic radical then attacks the C2 position of the indole to form the carboxylated product **2-50** (Scheme 2.10d). The photocatalyst 4DPAIPN can be prepared for use from readily available reagents in one step. Conditions used were taken from Grotjahn and König, using tetrafluoroisophthalonitrile **2-40** and

diphenylamine **2-41** with sodium bis(trimethylsilyl)amide **2-42** to form the desired photocatalyst (Scheme 2.10c).[7]

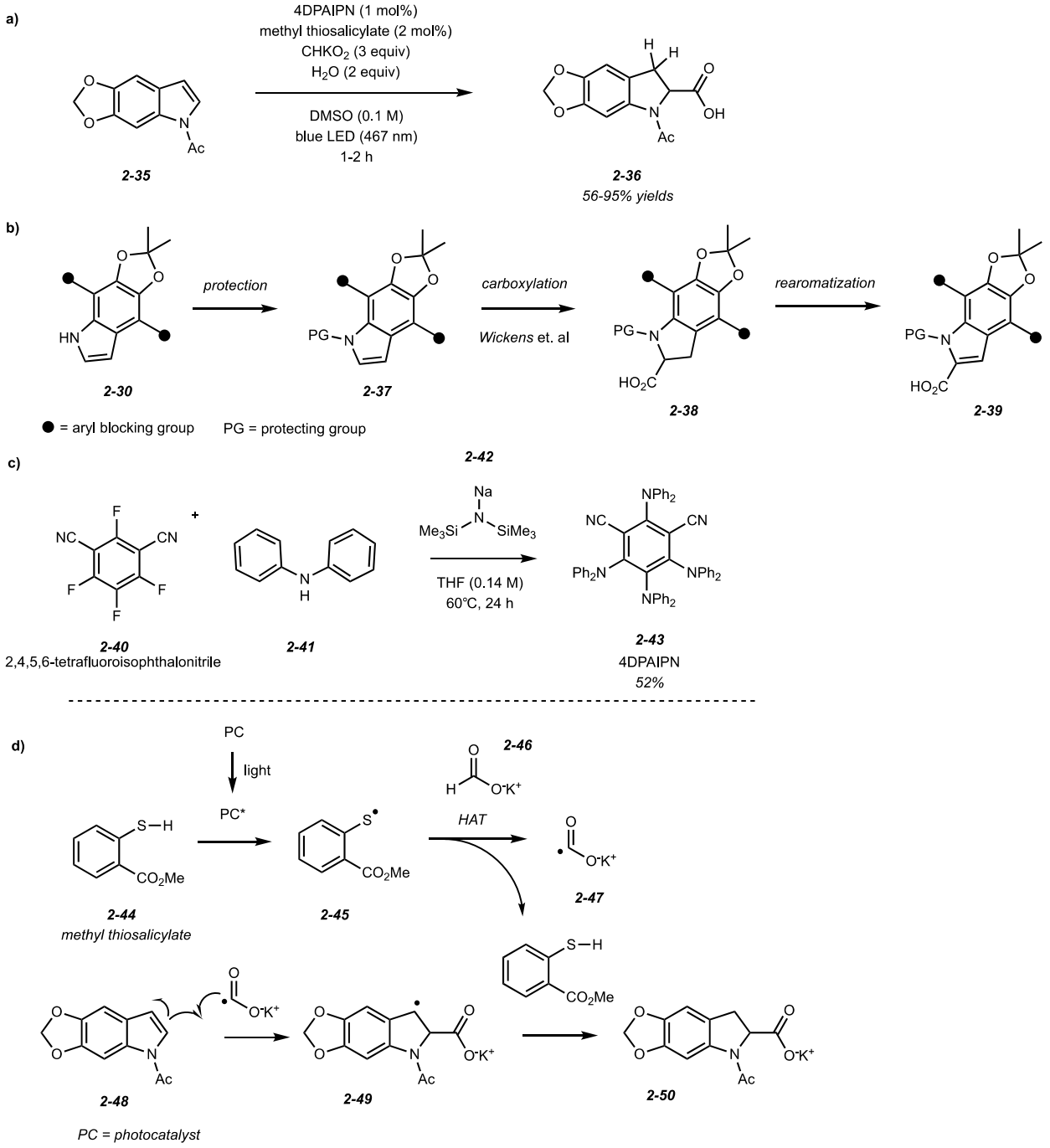

Scheme 2.10. a) Photochemical conditions for carboxylation reported by Wickens *et al.* Yields are those reported. **b)** The synthetic approach as would apply to our substrate **2-26** using Wickens' conditions. **c)** Conditions for synthesis of photocatalyst 4DPAIPN **2-43**. Yield is our work. **d)** Suggested mechanism of photocatalytic carboxylation from Wickens *et al*.

These conditions would require protection of the indole nitrogen of our substrate **2-26** to prohibit undesired reactivity. We were pleased to find that installment of a *tert*-butyloxycarbonyl (Boc) protecting group proceeded efficiently and reproducibly on substrate **2-26** to yield substrate **2-51**, with consistently > 95% conversion from starting material, using 1.2 equivalents of di-*tert*-butyl dicarbonate and a catalytic amount of 4-dimethylaminopyridine in THF and running overnight at room temperature (Scheme 2.11). As most other alternative carboxylation methods would likely also first require protection of the substrate's nitrogen, this result eased a concern of further synthetic exploration. Interestingly, NMR experiments revealed that the C3 proton on **2-51** corresponds both to a doublet at 6.19 ppm and a second doublet at 6.16 ppm (Scheme 2.12). We propose that this is due to the existence of two different rotamers depending on the orientation of the Boc protecting group.

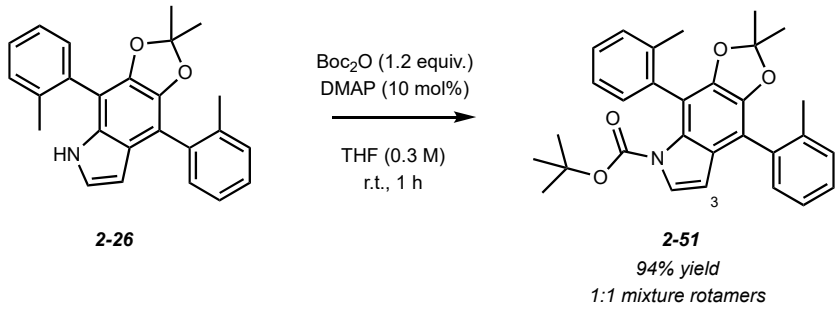

Scheme 2.11. Conditions for protection of the indole nitrogen. NMR indicates the presence of Boc rotamers.

Preliminary attempts at applying the photochemical carboxylation conditions from Wickens *et al.* to substrate **2-51** returned only starting material and thus the route was not pursued. In any case, these conditions would have been suboptimal because the carboxylation reduces the enamine double bond, and an extra step would be required to rearomatize to the desired blocked **DHICA**-acetonide substrate **2-39** (Scheme 2.10b).

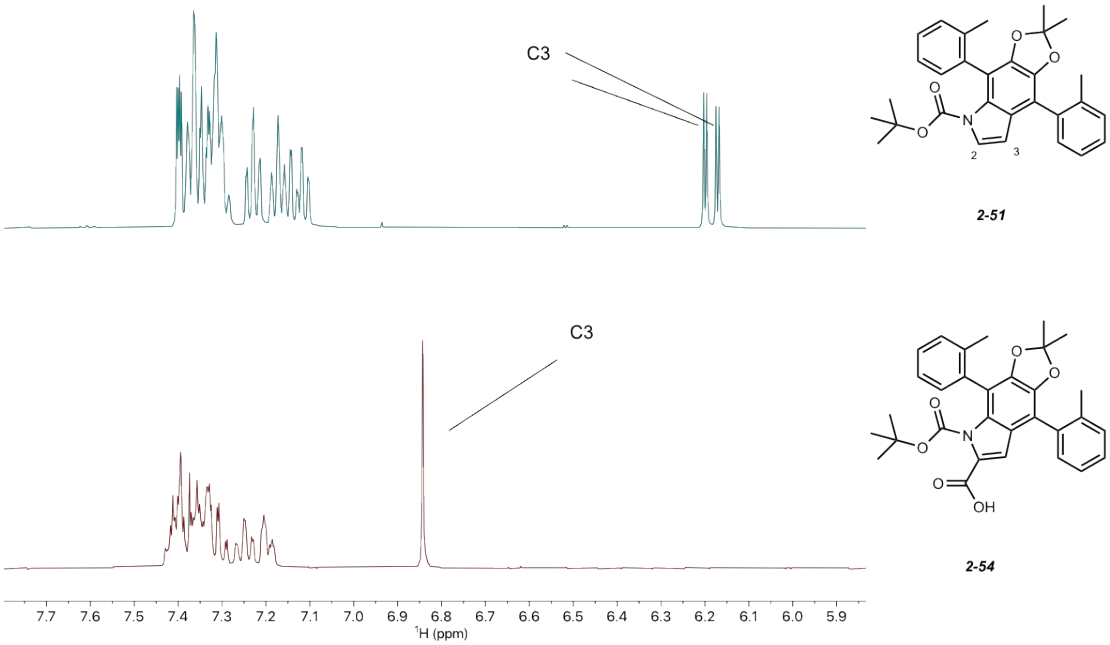

Scheme 2.12. Carboxylated substrate **2-54** as compared to substrate **2-51** by ^{1}H NMR.

We came back to the organolithiation strategy, taking example from conditions previously developed by the group for C2 silylation of the monomer **2-52** (unpublished work by Dr. Haiyan Huang) (Scheme 2.13a). We thought that C2 deprotonation of **2-51** using lithium diisopropylamide (LDA) followed by subsequent addition of a CO_2 electrophile would lead to the desired carboxylation. Substrate **2-51** was cooled to –78 ºC in THF and LDA was added to form the C2 carbanion. The resulting reaction mixture was sparged with CO_2 gas for 30 minutes. This procedure yielded, pleasantly, the desired product **2-54**. This operationally simple protocol reproducibly achieved conversions from starting material of greater than 90%, and average isolated yields of 69%. Interestingly, substrate **2-54** no longer shows doubling of the C3 proton signal by ^{1}H NMR. We take this as evidence that the doubling of signals observed for **2-51** was indeed due to the orientation of the Boc group; we speculate that hydrogen bonding, or potentially dipole minimization, with the carboxylic acid in place at C2 now limits the rotational freedom of the Boc group and locks substrate **2-54** into a single rotamer (Scheme 2.13c). Discovering conditions to achieve this carboxylation and attain this precursor to a blocked **DHICA** monomer was an important result.

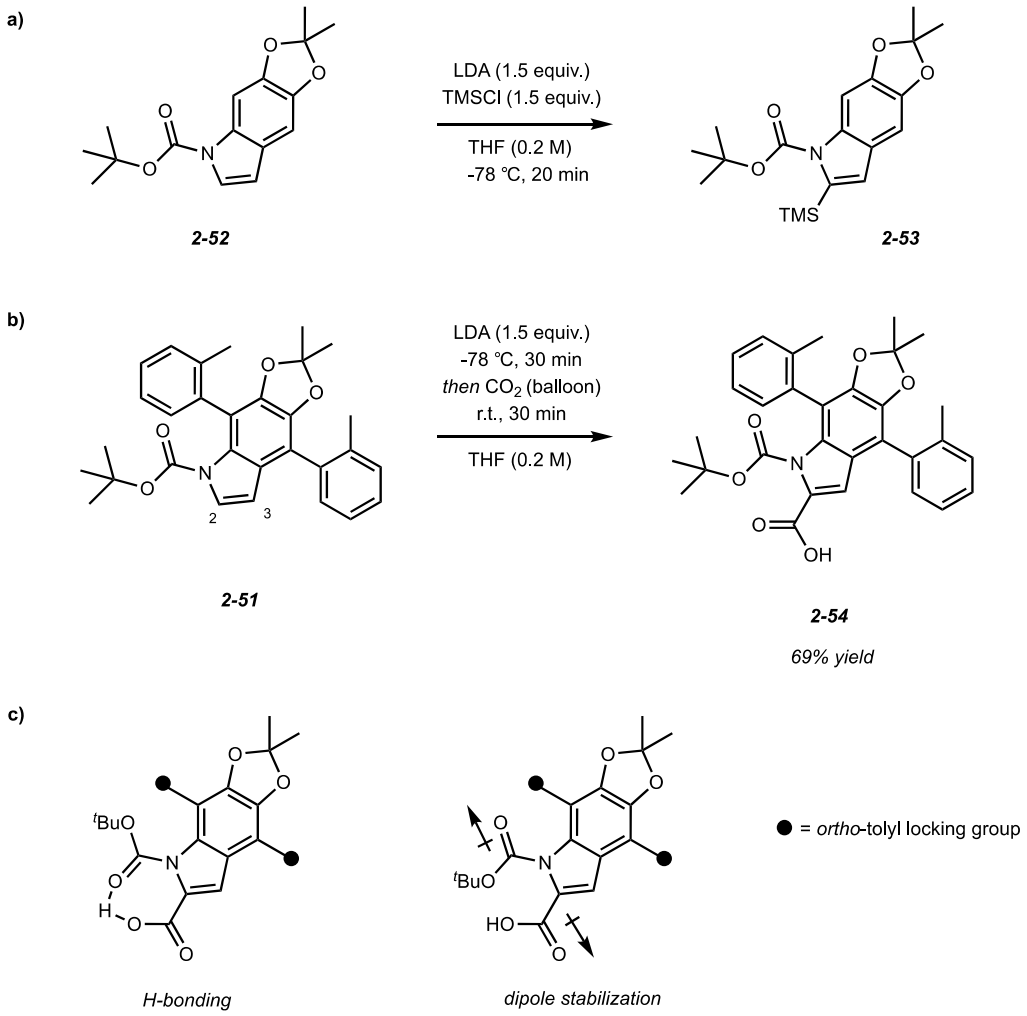

Scheme 2.13. **a)** Organolithiation conditions for C2 silylation used for Kaxiras tetramer studies (unpublished work by previous group member Dr. Haiyan Huang) and **b)** conditions as adapted for carboxylation of substrate **2-51**. **c)** Proposed H-bonding or dipole stabilization favoring a single Boc rotamer of substrate **2-54**.

3.4. Deprotection Efforts

Next in the synthesis was to remove the protecting groups from substrate **2-54** to move towards substrate **2-55**, blocked 5,6-dihydroxyindole-2-carboxylic acid (**DHICA-Me**) (Scheme 2.14a). We suspected that deprotection of a substrate with a free acid would lead to unstable materials that would be difficult to handle for reasons of solubility and purification. We thus first considered protection of the acid with an ester for ease of handling of the material moving forward

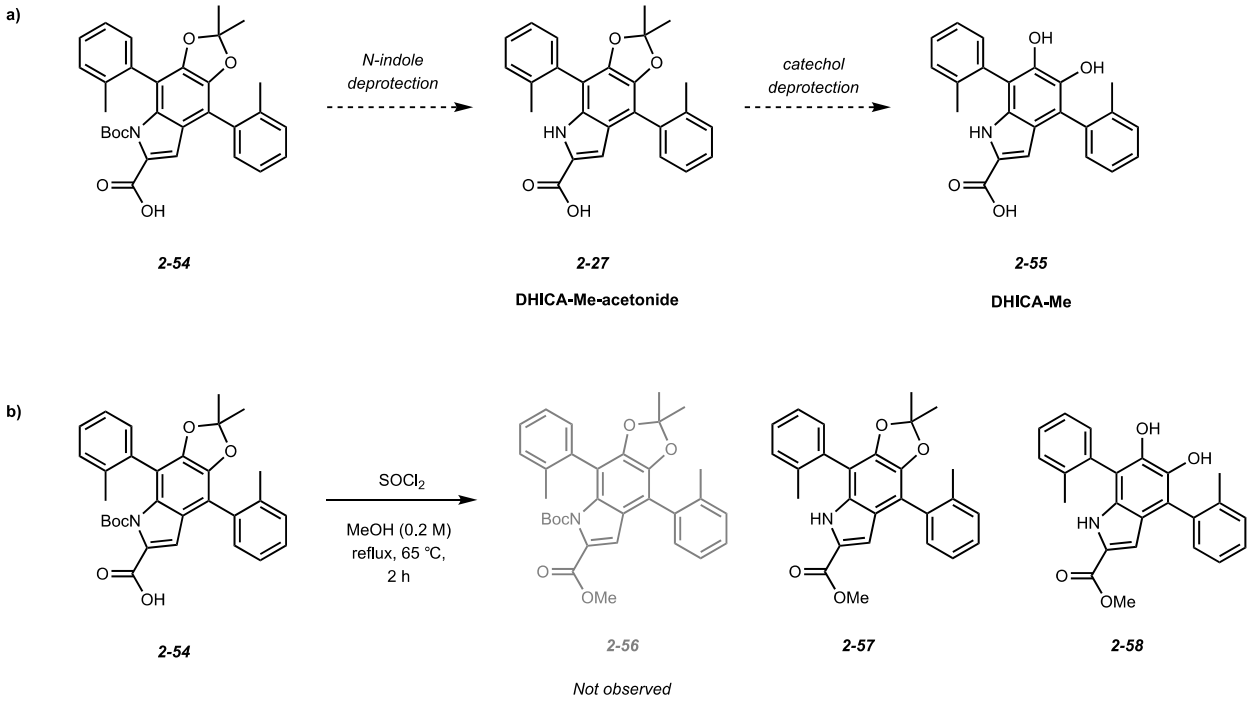

Scheme 2.14. **a)** Remaining transformations of substrate **2-54** to reach **DHICA-Me 2-55**. **b)** Substrate **2-54** was subjected to esterification conditions.

in the synthesis. Substrate **2-54** was subjected to esterification conditions using thionyl chloride and methanol under reflux. The formation of a methyl ester confirmed the presence of a carboxylic acid functional group in the starting material. However, the results were a surprise, in that the expected esterified product **2-56** was not observed; rather, a mixture of the blocked, free-NH, acetonide-protected 5,6-dihydroxyindole-2-methylester derivative **2-57** and the blocked, free-NH 5,6-dihydroxyindole-2-methylester derivative (**DHIME-Me**) **2-58** was obtained (Scheme 2.14b). This revealed that the acidic conditions employed for the esterification are in effect sufficient for removal of both the nitrogen and the hydroxyl protecting groups. As reaction time progresses, increased amounts of product **2-58** are observed. No amount of **2-56** has been observed in any trial thus far, even after shortening reaction times.

We propose a mechanism in which the initial formation of the acetyl chloride **2-59** with $SOCl_2$ generates an equivalent of hydrochloric acid (HCl); subsequent addition of methanol to form the methyl ester **2-56** also generates an equivalent of HCl (Scheme 2.15). This *in situ*

formation of HCl is what facilitates the Boc and acetonide removal. As no Boc-protected species is observed, we suggest that it is the Boc group being removed first. A C2-ester derivative at the catechol state may be expected to be much less reactive and much more stable than the theoretical

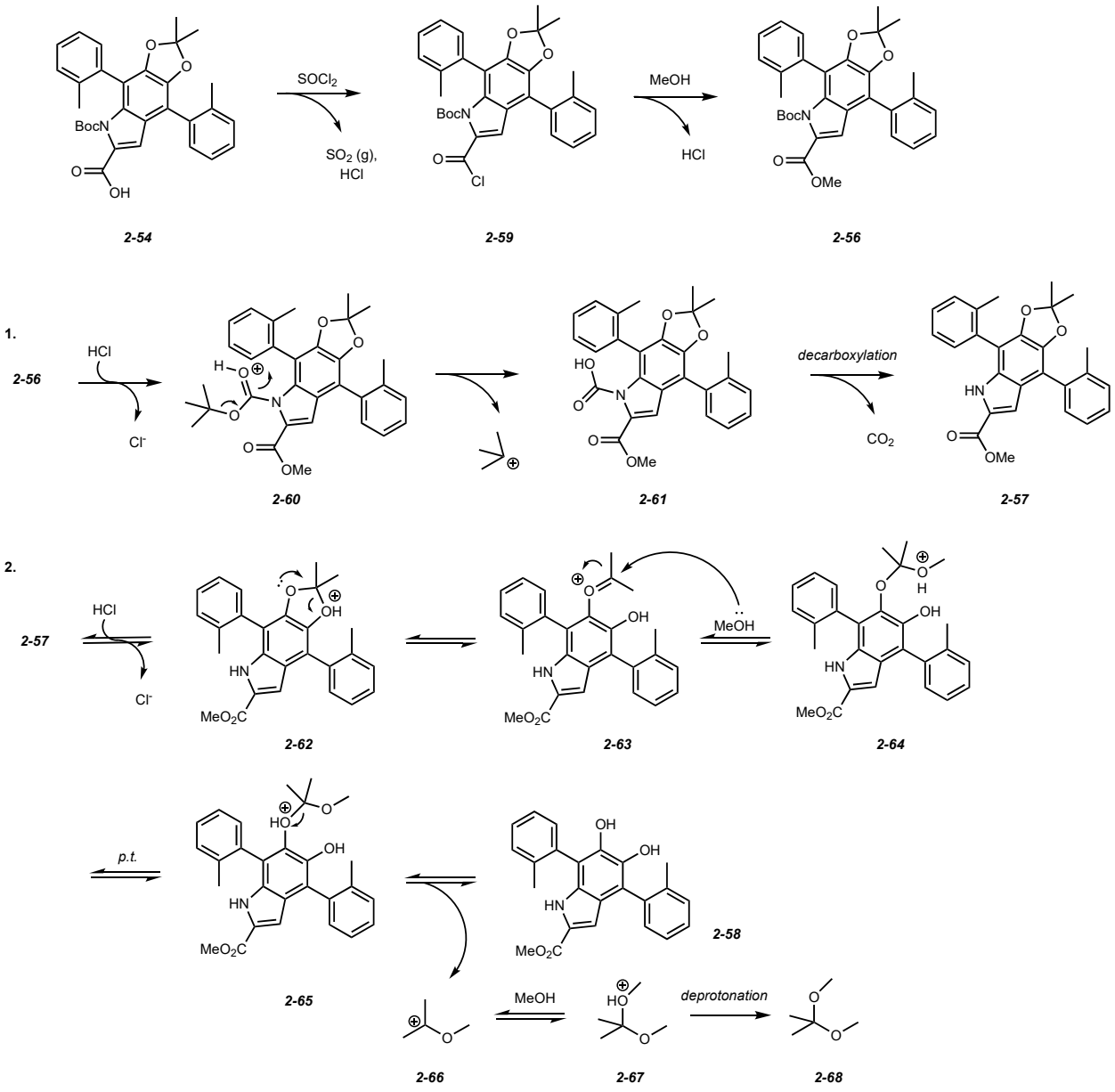

Scheme 2.15. Proposed mechanism of deprotection events occurring after esterification of substrate **2-54**.

C2-carboxyl derivative at the catechol state; luckily, these results showed that, indeed, **2-58** may be isolated as a stable compound. This result opened up an alternate route towards **2-carboxy-IQ-Me**: it offered the option to continue synthetic efforts with the methyl ester intact.

Although the attainment of **DHIME-Me 2-58** is an encouraging result, the conditions used as they stand are not ideal, as it leads to mixtures of compounds. Though these mixtures are separable by column chromatography, it is of interest to have better control over discrete transformations. Further optimization is desired to discover conditions for better-controlled synthesis. To continue the synthetic route from **2-58** would require a saponification to return the ester to a free acid, followed by an oxidation to result in the desired **2-carboxy-IQ-Me 2-1**. Studies based on **2-58** hold potential and will continue to be investigated (see future work, Chapter 3).

Synthetic efforts to deprotect the free acid derivative **2-54** also continued. We considered seeking conditions which might remove both the Boc and the acetonide protecting groups in one go to reach **2-55**; a global deprotection seemed a feasible possibility as both protecting groups may typically be removed under acidic conditions. It would eliminate one step from the forward synthesis. The conditions previously used for acetonide removal in the melanin project (work by Dr. Haiyan Huang and Ms. Xueqing Wang) using a 1:1 mixture of concentrated HCl and ethylene glycol in acetonitrile at elevated temperature were first considered. When the reaction was run at room temperature, no conversion of the starting material **2-54** was observed. Upon heating to 70 ºC, we observed formation of a white precipitate which was revealed, interestingly, to be ammonium chloride; after some speculation, we hypothesized that it was coming from the workup of the preceding carboxylation reaction in that it was actually the ammonium salt of the carboxylate, **2-54a,** that was being formed upon quenching of the reaction and washing with saturated ammonium chloride (Scheme 2.16). The pKa of the C2 carboxylic acid of **DHICA** has experimentally been established as 4.25[8]; given this, it would make sense that ammonium (pKa of 9.24) could serve as the counter cation to yield **2-54a**. NMR analysis of the remaining reaction mixture revealed small amounts of starting material, and a complex mixture overrun by a large broad signal in the aromatic region; we were unable to confirm the identity of any products.

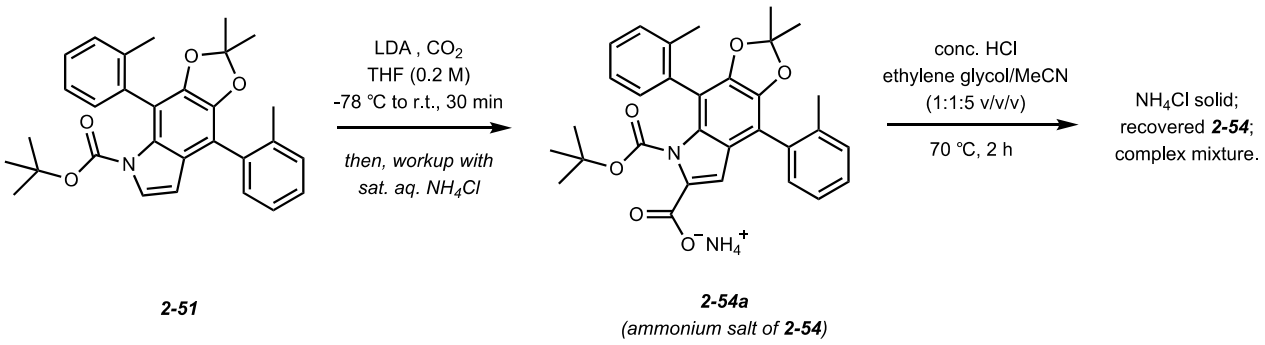

Scheme 2.16. Suspected formation of the ammonium salt **2-54a** following workup of the carboxylation reaction with saturated aqueous ammonium chloride. Advancing the latter to acidic deprotection conditions resulted in NH_4Cl salt crashing out of solution.

Going forward, carboxylation reactions were worked up with a stronger acid, 1 M aqueous HCl, to ensure that the carboxylic acid product was fully protonated. Product **2-54** obtained from carboxylation reactions following this modification to the workup procedure was again advanced to the deprotection conditions outlined in the previous paragraph (entry 1, Table 2.3). Ammonium chloride no longer crashed out of solution; unfortunately, however, neither was any of the desired **DHICA-Me 2-55** observed. The NMR spectrum of the crude reaction mixture suggested a complex mixture of species which indicated decomposition. One possibility is that product **2-55** was forming in solution, but is unstable at high temperatures and in strongly acidic environments and thus decomposes. Alternatively, we propose that decomposition could be an indication of the formation of polymeric mixtures resulting from spontaneous chain formation, chain aggregation and chain elongation that we hypothesize occurs with autoxidation once the dihydroxyindole has been deprotected. If either of these was the case, it would mean that the above conditions are effective for deprotection, but that **2-55** is susceptible to autoxidation and thus not isolable. This, however, remains speculative and further studies are necessary.

Table 2.3. Deprotection conditions applied to substrate **2-54** (obtained from reactions worked up with 1 M HCl).

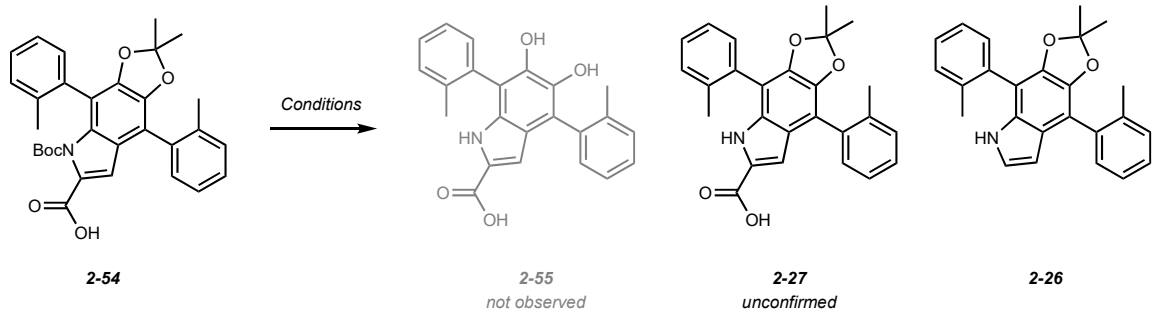

2-54 ***2-55*** *not observed* ***2-27*** *unconfirmed* ***2-26***

Entry	*Scale (mmol)*	*Result*
1	conc. HCl ethylene glycol MeCN 70 °C, 2 h	decomposition
2	aq. 1 M HCl MeCN 70 °C, 2 h	suspected **2-27**
3	aq. 1 M HCl ethylene glycol MeCN 70 °C, 2 h	**2-26;** unidentified byproducts
4	Ethane-1,2-dithiol; $AlCl_3$ $MeNO_2$ 0 °C, 1 h	No RSM by crude NMR; complex mixture
5	$InCl_3$, H_2O MeCN	RSM
6	$NaBAr^F_4$ H_2O / DCM 30 °C, overnight	RSM; unidentified byproducts
7	$NaBAr^F_4$ H_2O / THF 60 °C, overnight	RSM; unidentified byproducts; suspected **2-27**

We considered lowering the concentration of acid. Heating with 1 M HCl in acetonitrile for 2 hours yielded what appeared initially by ^{1}H NMR to be Boc-deprotected product **2-27**, as the *tert*-butyl protons were no longer apparent in the spectrum, but further attempts at purification led to decomposition and full characterization has not yet been achieved (entry 2, Table 2.3). The suspected C3 proton appears at 6.8 ppm as a doublet with a *J*-coupling constant of 2.2 Hz. This would be consistent with the presence of a $^{4}J_{N\text{-}H}$, similar to the splitting pattern previously observed for the C3 proton of substrate **2-26**. A broad singlet at 9.97 ppm is assumed to be the NH signal of the unprotected nitrogen. Signals referencing the protons of the acetonide protecting group in the starting substrate **2-54** are still present; we thus concluded that these conditions are not strong enough for removal of the acetonide.

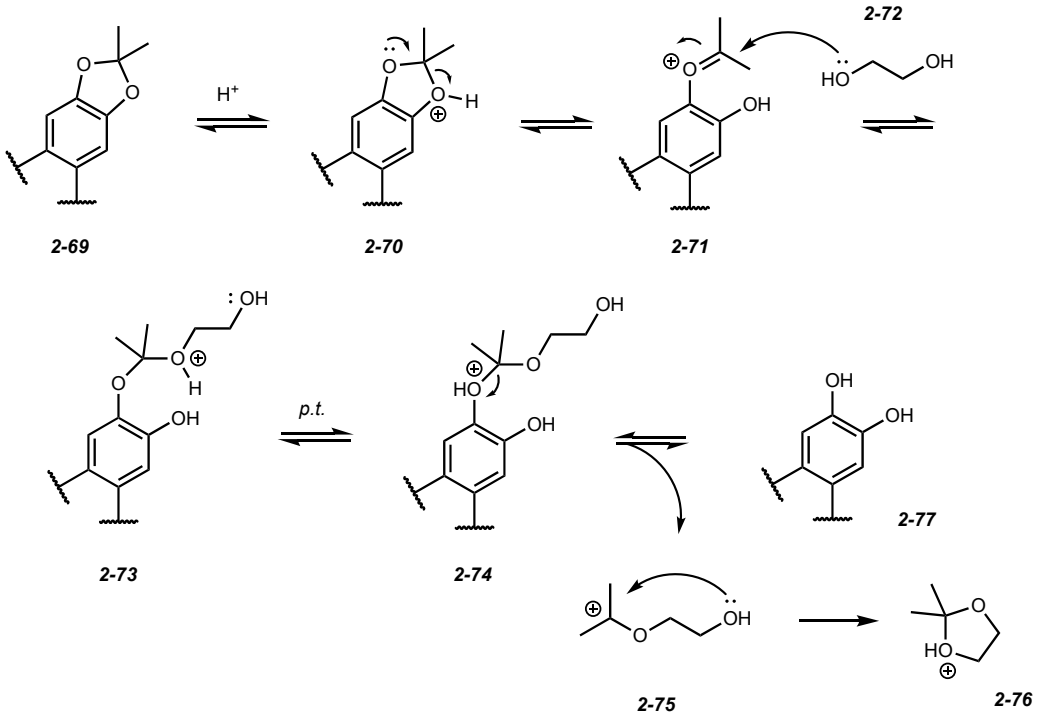

Scheme 2.17. Proposed mechanism of ethylene glycol addition to favor deprotected dihydroxyindole product.

In order to push acetonide deprotection, we considered addition of ethylene glycol for sequestration of the acetonide-removal byproduct (entry 3, Table 2.3). We hypothesized that this might counter the reversibility of the reaction and push the equilibrium further towards dihydroxyindole product (Scheme 2.17). In preliminary trials, however, we observed decarboxylation at C2 to occur before removal of the acetonide group, as substrate **2-26** was isolated from the reaction mixture (Scheme 2.18a). No species lacking the acetonide group was isolated. This result implies that these conditions are effective at removal of the Boc group. The decarboxylation is undesired but unsurprising: decarboxylation under acidic conditions on related indole substrates has been reported in the literature. It was used by Ito *et al.* in 1986 for the decarboxylative treatment of natural eumelanins, then again by Prota *et al*. in 1992 for the purpose of probing the degree of incorporation of **DHICA**-derived units in the biopolymer (see Chapter 1, Section 2).[9] In these cases melanin samples were refluxed in 6 M HCl, and the production of CO_2 was then measured as proxy for the **DHICA** units from which it originated.

Typically, decarboxylation mechanisms proceed by i) initial formation of a carboxylate, then ii) loss of CO_2, followed by iii) subsequent generation of a carbanion, and finally iv) protonation of the carbanion. Acid-catalyzed decarboxylation reactions of carboxylic-acid derivates of aromatic compounds have been well documented in the literature since the 19th century[10] and follow a slightly different mechanism; works by Kluger *et al.* suggest it to proceed via i) protonation of the indole ring, ii) reversible addition of water to the carboxylic acid to form a hydrate **2-79**, iii) C-C bond cleavage to liberate indole **2-80** and protonated carbonic acid **2-81**, and finally iv) decomposition of protonated carbonic acid to CO_2 and H_3O^+ (Scheme 2.18b).[10] As regards our substrate in the conditions discussed above, we hypothesize that the Boc group is first lost to yield compound **2-27**; then, that protonation of the indole ring forms the charged intermediate **2-82**, which undergoes C-C bond cleavage to release CO_2 and yield substrate **2-26** (Scheme 2.18c).

It is unclear why this result was only observed with 1 M HCl in the presence of ethylene glycol, and not in the absence of ethylene glycol. Further investigations would be necessary to probe this discrepancy. In addition, it is notable to find that decarboxylation of our substrate already begins to occur at an acid concentration of 1 M. In future synthetic efforts a delicate compromise will have to be struck between mild- (i.e., < 1 M) to non- acidic conditions preferrable

for avoidance of undesired C2 decarboxylation, while still able to effect removal of the acetonide protecting group.

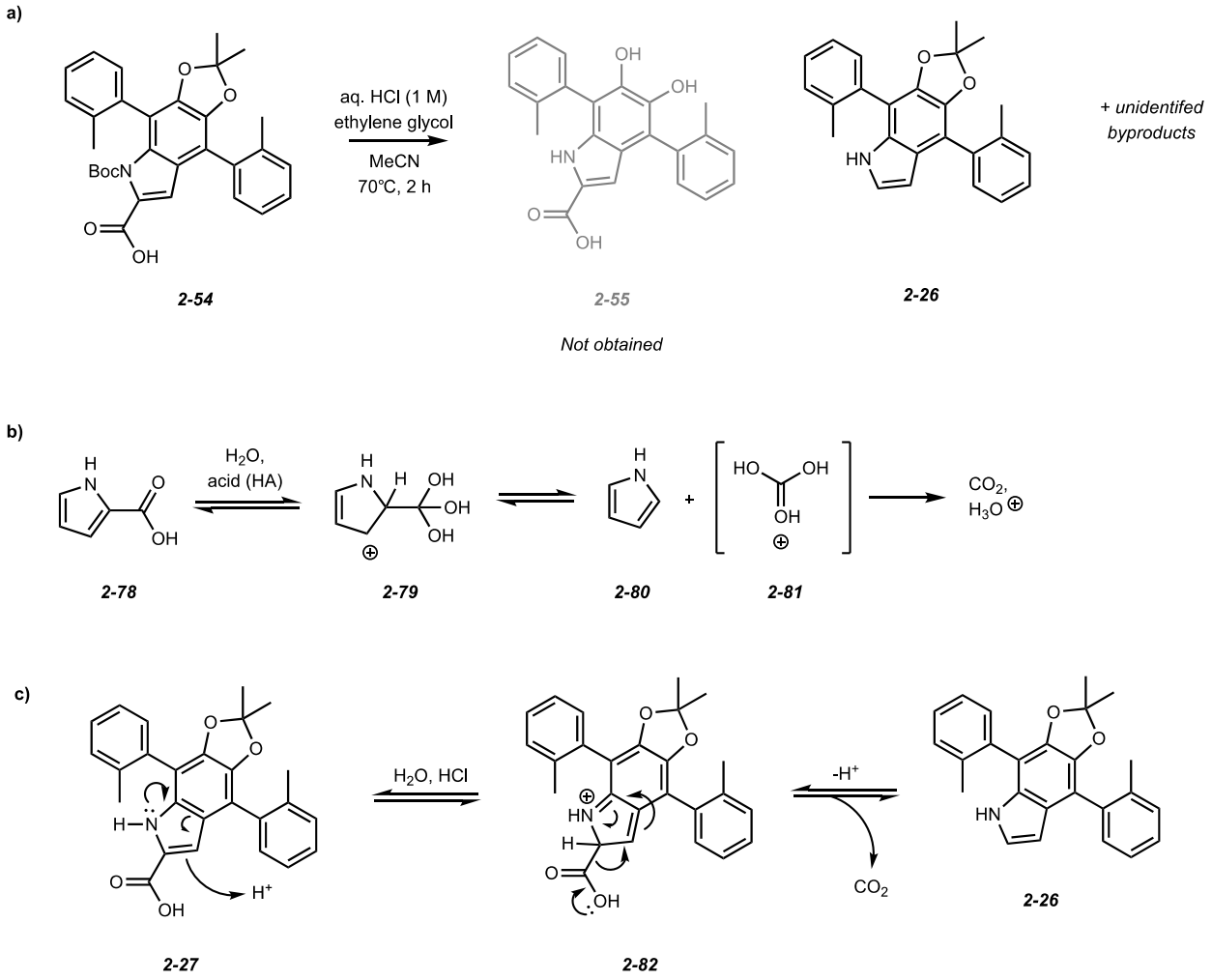

Scheme 2.18. a) Acidic conditions with ethylene glycol drove decarboxylation. **b)** Hydrolytic decarboxylation of pyrrole-2-carboxylic acid as investigated by Kluger *et al.*; **c)** The presumed mechanism of decarboxylation under acidic conditions as applies to our substrate **2-27** following Boc deprotection. We suggest that the mechanism proceeds via i) protonation of the indole ring, followed by ii) C-C bond cleavage to liberate CO_2 and the indole **2-26**.

We also investigated several non-acidic conditions. Previously in the group use of an excess of ethane-1,2-dithiol and aluminum chloride had been effective in removing the acetonide from dimer derivatives (work by Dr. Haiyan Huang). However, previous work in the group had

also shown the ensuing oxidation to be hindered by residual dithiol in the isolated dihydroxyindole product (work by Mr. Yiming Zhang). Applying these conditions to our substrate afforded a complex mixture (entry 4, Table 2.3). Isolation of the species of interest proved difficult; repeated efforts to remove excess dithiol by aqueous washes and column chromatography were insufficient. Though the presence of product **2-55** was able to be detected by mass spectrometry analysis, we were unable to confirm this result by NMR. We moved on to try alternative methods of deprotection.

Conditions adapted from Zimmer *et al*. using indium chloride and water at room temperature for acetonide removal did not achieve any conversion of starting material (entry 5, Table 2.3).[11] Conditions adapted from Liu *et al.*[12] using sodium tetrakis[3,4-bis(trifluoromethyl)phenyl]borate in catalytic amounts were next attempted: the reaction run at 30 ºC in H_2O/DCM yielded only fully recovered starting material (entry 6, Table 2.3). Upon increasing the temperature to 60 ºC in H_2O/THF, however, we began to observe conversion of the starting material; but, the product of interest did not match the signals expected for compound **2-55** (entry 7, Table 2.3). Attempts to isolate this new species only led to decomposition, precluding its characterization.

Though these studies are not yet complete, they have revealed some promising leads, and continuation of this project will include further investigation and modification of the conditions discussed above. Foreseen efforts will be discussed in Chapter 3.

4. Diversification of C2 Functionalization

During the project we considered also expanding the scope of functional groups able to be installed at C2 of a blocked **DHI** derivative. Various functional groups could act as handles for later-stage manipulations, or generate derivatives by which to study compound properties such as solubility or electronics. Resultant properties of these compounds could influence the scope of application of blocked **DHI** derivatives in medicinal or materials fields. Thus far in the project the use of organolithium reagents for nucleophilic addition at the C2 position has proven robust. It is

our hope that the same chemistry could prove to be of use for installation of alternate groups at the C2 position.

4.1 Silyl Groups

First we looked to explore C2 silylation using conditions developed by Dr. Haiyan Huang for the Kaxiras tetramer synthesis. Using 1.5 equivalents of trimethylsilyl chloride (TMSCl) and 1.5 equivalents of lithium diisopropylamide (LDA) in THF at –78ºC for 2 hours yielded **2-83** where R=R'=R"= methyl in 69% yield (entry 1, Table 2.4). We tried additional silyl groups to explore the scope of possible functionalization. Unfortunately no silylated product was observed with the use of any bulkier silyl reagents, even with lengthened reaction times and/or heating. When triisopropylsilyl chloride (TIPSCl) was used as silane reagent, 25% starting material **2-51** was recovered along with Boc-deprotected byproduct **2-26**. When the bulkier *tert*-butyldimethylsilyl chloride (TBDMSCl) was tried, 56% starting material **2-51** was recovered. We hypothesize that sterics prevent the desired addition: i.e., that bulkier substituents on the silyl electrophile impede approach of the substrate to electrophile. Ultimately only one C2-silylated compound was added to the project library. Should attainment of these substrates continue to be pursued, silylation may be reattempted using more reactive silyl reagents, such as the corresponding bromide, iodide, or triflate, instead of the chloride. In addition, the library could be expanded by diversification of the protecting group on the indole nitrogen, such as a mesylate, or tosylate.

Table 2.4. Summary of C2 silylation efforts.

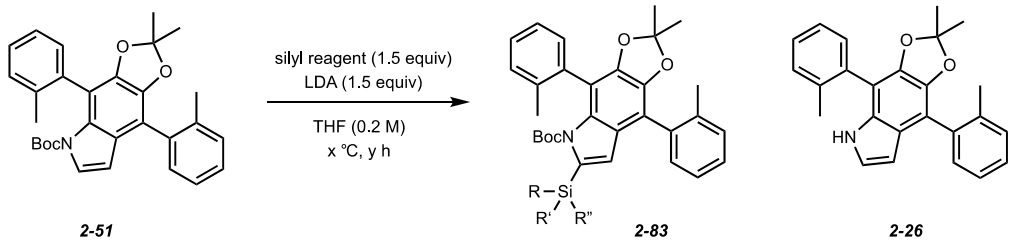

2-51 *2-83* *2-26*

Entry	*Silyl Reagent*	*x, Temperature (*ºC)	*y, Time (h)*	*Yield*
1	TMSCl	–78 ºC	2	69% **2-83** where R=R'=R"= Me
2	TIPSCl	r.t.	18	25% RSM, 26% **13**, unidentified byproducts
3	TBDMSCl	60 ºC	4	53% RSM, unidentified byproducts

5. Conclusions

This concludes the synthetic efforts made towards access of **2-carboxy-IQ-Me**. Robust conditions for a C2 carboxylation on a blocked **DHI** core have been established. Efforts have been made towards subsequent removal of the nitrogen and the dihydroxy protecting groups, but undesired decarboxylation or decomposition of products has so far precluded achievement of this goal. The possibility of alternative C2 functionalization on a blocked **DHI** core has begun to be investigated and has garnered interest as another potential extension of this project. A blocked 5,6-dihydroxyindole-2-methylester derivative has been synthesized, and presents an alternative approach towards synthesis of the desired **2-carboxy-IQ-Me** target. The installation of silyl groups at C2 has also been attempted. These and other C2-functionalized compounds could allow for the ability to tailor properties of blocked **DHI** derivatives. The next chapter will outline anticipated future work.

6. References

1. Wang, X.; Kinziabulatova, L.; Bortoli, M.; Manickoth, A.; Barilla, M. A.; Huang, H.; Blancafort, L.; Kohler, B.; Lumb, J.-P. Indole-5, 6-quinones display hallmark properties of eumelanin. *Nat. Chem.* **2023**, *15* (6), 787–793.
2. Pezzella, A.; d'Ischia, M.; Napolitano, A.; Palumbo, A.; Prota, G., An integrated approach to the structure of Sepia melanin. Evidence for a high proportion of degraded 5, 6-dihydroxyindole-2-carboxylic acid units in the pigment backbone. *Tetrahedron*, **1997**, *53* (24), 8281-8286.
3. **(a)** Batcho, A. D.; Leimgruber, W. Indoles from 2-Methylnitrobenzenes by Condensation with Formamide Acetals Followed by Reduction: 4-Benzyloxyindole. *Org. Synth.* **1985,** *63*, 214. **(b)** E. Zembower, D.; Xie, Y.; Koohang, A.; J. Kuffel, M.; M. Ames, M.; Zhou, Y.; Mishra, R.; Aye Mar, A.; T. Flavin, M.; Xu, Z.-Q., Methylenedioxy- and Ethylenedioxy-Fused Indolocarbazoles: Potent Human Topoisomerase I Inhibitors and Antitumor Agents. *Anti-Cancer Agents in Medicinal Chemistry* **2012,** *12* (9), 1117-1131. **(c)** Leibig, D.; Müller, A. H. E.; Frey, H. Anionic Polymerization of Vinylcatechol Derivatives: Reversal of the Monomer Gradient Directed by the Position of the Catechol Moiety in the Copolymerization with Styrene. *Macromolecules* **2016,** *49* (13), 4792-4801.
4. Molloy, J. J.; O'Rourke, K. M.; Frias, C. P.; Sloan, N. L.; West, M. J.; Pimlott, S. L.; Sutherland, A.; Watson, A.J. Mechanism of Cu-catalyzed aryl boronic acid halodeboronation using electrophilic halogen: development of a base-catalyzed iododeboronation for radiolabeling applications. *Org. Lett.* **2019***, 21*(7), 2488-2492.
5. Katritzky, A. R., & Akutagawa, K. Carbon dioxide: A reagent for the protection of nucleophilic centres and the simultaneous activation of alternative locations to electrophilic attack.: Part I. A new synthetic method for the 2-substitution of 1-unsubstituted indoles. *Tetrahedron Lett.* **1985**, *26*(48), 5935-5938.
6. Mikhael, M.; Alektiar, S. N.; Yeung, C. S.; Wickens, Z. K. Translating planar heterocycles into three-dimensional analogs via photoinduced hydrocarboxylation. *Angew. Chem. Int. Ed.* **2023**, *62*, e202303264.
7. Grotjahn, S., & König, B. Photosubstitution in dicyanobenzene-based photocatalysts. *Org. Lett.* **2021**, *23* (8), 3146-3150.

8. **(a)** Huijser, A.; Pezzella, A.; Hannestad, J.K.; Panzella, L.; Napolitano, A.; d'Ischia, M.; Sundström, V. UV-Dissipation Mechanisms in the Eumelanin Building Block DHICA. *Chem. Phys. Chem.* **2010**, *11* (11), 2424-2431. **(b)** Charkoudian, L.K. & Franz, K.J. Fe (III)-coordination properties of neuromelanin components: 5, 6-dihydroxyindole and 5, 6-dihydroxyindole-2-carboxylic acid. *Inorg. Chem.* **2006**, *45* (9), 3657-3664.
9. **(a)** Tsukamoto, K.; Palumbo, A.; D'Ischia, M.; Hearing, V. J.; Prota, G. 5, 6-Dihydroxyindole-2-carboxylic acid is incorporated in mammalian melanin. *Biochem. J.* **1992**, *286* (2), 491-495. **(b)** Ito, S. Reexamination of the structure of eumelanin. *Biochim. Biophys. Acta - Gen. Subj*, **1986**, *883* (1), 155-161.
10. Mundle, S. O.; Lacrampe-Couloume, G.; Lollar, B. S.; Kluger, R. Hydrolytic decarboxylation of carboxylic acids and the formation of protonated carbonic acid. *J. Am. Chem. Soc.* **2010**, *132* (7), 2430-2436.
11. Pfrengle, F.; Dekaris, V.; Schefzig, L.; Zimmer, R.; Reissig, H. U. Indium trichloride mediated cleavage of acetonides in the presence of acid-labile functional groups-enhancing the synthetic utility of 1, 3-dioxolanyl-substituted 1, 2-oxazines. *Synlett*, **2008,** *2008* (19), 2965-2968.
12. Chang, C. C.; Liao, B. S.; Liu, S. T. Deprotection of acetals and ketals in a colloidal suspension generated by sodium tetrakis (3, 5-trifluoromethylphenyl) borate in water. *Synlett*, **2007**, *2007* (02), 0283-0287.

Chapter 3: Conclusions and Future Directions

1. Introduction

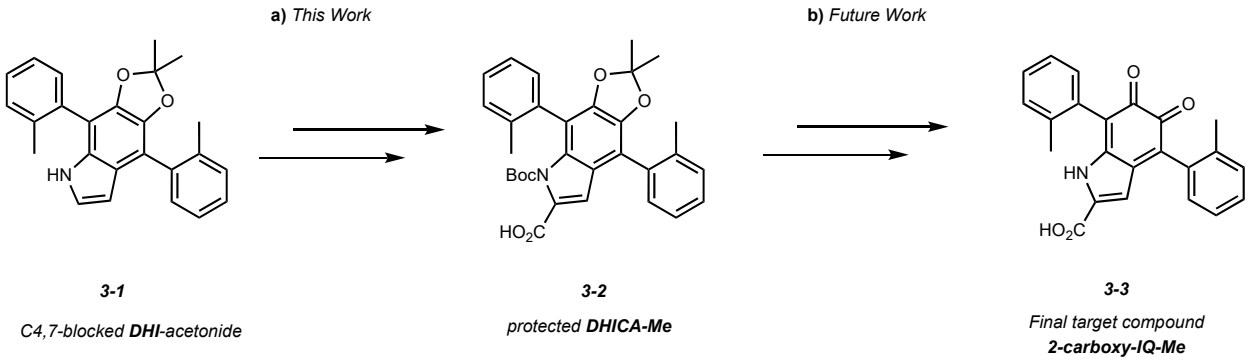

Scheme 3.1. **a)** Chemistry established in this work. **b)** Remaining transformations to effect in order to obtain the target compound **3-3**.

This M.Sc. project has established the chemistry for carboxylation at the C2 position of a C4,7-blocked **DHI** derivative. Efforts to obtain the final **2-carboxy-IQ-Me** target **3-3** will continue in the group. It remains to successfully remove the nitrogen- and alcohol- protecting groups of compound **3-2**. If this can be accomplished, then we may subsequently attempt oxidation to the final **IQ** monomer **3-3** (Scheme 3.1). While finishing the synthesis is the primary task at hand, the results achieved thus far have also paved the way for consideration of alternate C2 functionalization. Other potential directions which the project may travel are also discussed below.

2. Completing the Synthesis: Blocked 2-carboxy-IQ

Thus far, the carboxylation reaction has only been run up to a scale of 0.5 mmol. This first attempt at scale-up, however, compromised yields. The crude showed conversion of starting material; further study is needed to clarify what side reactions may be occurring. Optimization studies for scale-up are then necessary, taking into consideration the variables of time, equivalents of the organolithium reagent, concentration of the reaction mixture, and temperature.

It then remains to find suitable conditions for removal of the Boc, and finally the acetonide, protecting groups. Acidic deprotection conditions may continue to be explored. A one-step dual deprotection remains a possibility. While the use of 1 M HCl is suspected to remove only the Boc protecting group and not the acetonide, we observe decomposition and inconclusive results with the use of concentrated HCl. A study of incremental variation of the concentration of acid would be of interest.

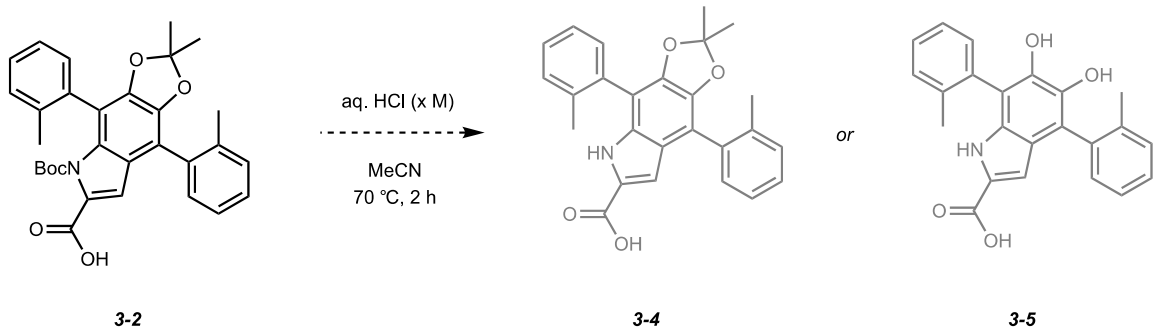

Scheme 3.2. Proposed investigation of HCl concentration in acidic deprotection conditions, where *x* molarity is varied incrementally. The final reaction concentration with respect to substrate **3-2** is 0.03 M.

The installation of a methyl ester at C2 has already been discussed under the context of deprotection efforts (Chapter 2, Section 3.4). We thus have access to a stable, C4,7-blocked dihydroxyindole-2-methylester (**DHIME-Me**) **3-6**. This result may offer an alternative synthetic route towards the target compound: a saponification, followed by an oxidation, would lead to **3-3** (Scheme 3.3).

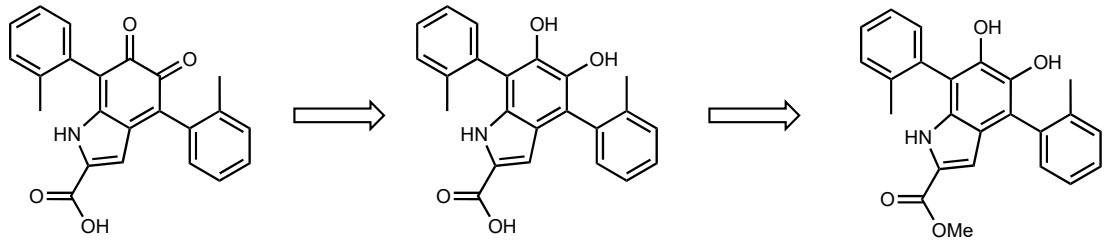

3-3 *3-5* *3-6*

Scheme 3.3. Proposed retrosynthesis of the desired compound **2-carboxy-IQ-Me 3-3** from blocked dihydroxyindole-2-methylester (**DHIME-Me**) **3-6**.

3. Oligomers of Blocked DHICA

It is known that the **DHICA** precursor is a fundamental component of the eumelanin network.[1] This work focuses on **DHICA** at a monomer level; however, oligomeric forms may also be incorporated and relevant to structure-property relationships. It is of interest to determine whether this work's method of C2-carboxylation may be applied not only to monomers, but also to dimers, even trimers, tetramers, etc. of blocked **DHI**. These may include any of C4,4', C7,7', C4,7', C2-4', or C2-7' couplings (Scheme 3.4). We expect that the presence of carboxylate groups in the natural eumelanin network substantially informs its hallmark spectroscopic features. If carboxylated **DHI** oligomers proved to be synthetically accessible, and, further, could be oxidized to the corresponding orthoquinone forms, then they could be submitted to spectroscopic studies. It would be of great interest to investigate how and to what extent such structures mimic the properties of natural eumelanin.

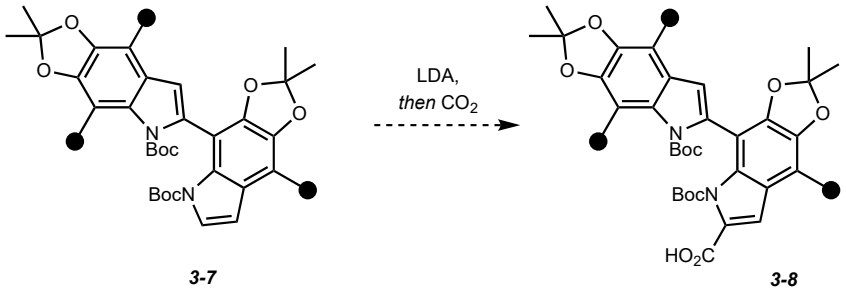

3-7

example dimer of blocked DHI

● = aryl blocking group, or other DHI[CA] unit

3-8

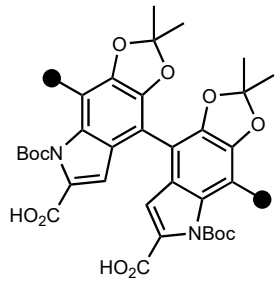

3-9
4,4' coupled

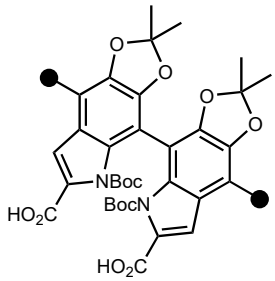

3-10
7,7' coupled

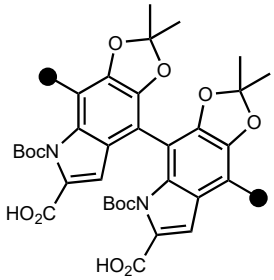

3-11
4,7' coupled

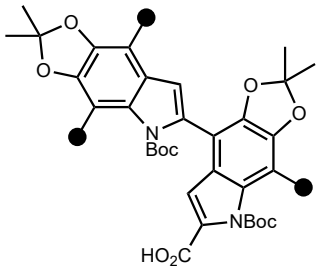

3-12
2,4' coupled

Scheme 3.4. Proposed application of the carboxylation chemistry established in this work to oligomers of blocked, protected **DHI**. Some hypothetical structures are drawn.

4. Development of a Blocked C2-ester Derivative Library

Alternatively, C2-ester derivatives themselves may prove to be compounds of interest and the development of a library of blocked C2-esterified **DHI** derivatives is an attractive extension of the project. It is possible that C2-ester derivatives – both at the catechol and orthoquinone state – would be easier to handle than the free acid derivative for reasons of stability and solubility. Further, varying the type of ester at C2 could give rise to interesting new properties. For instance, introducing an ester substitution of greater steric bulk such as a *tert*-butyl ester **3-13a** would likely impact aggregation behaviors of the compound, or adding a longer carbon chain such as an *n*-octyl ester **3-13b** would increase the lipophilicity (Scheme 3.5). We predict that altering the ester functionalization would present a manner of tailoring physical properties, while preserving photophysical properties, of these derivatives.

If we were instead interested in altering the photophysical properties of the compound, we might consider varying the carbonyl type to an amide (**3-13c**). This is now a coupling handle for late-stage manipulation. C2-amide derivatives might be of interest for application in materials chemistry, for example allowing the tethering of these compounds to amino-functionalized surfaces (**3-13d**).[2]

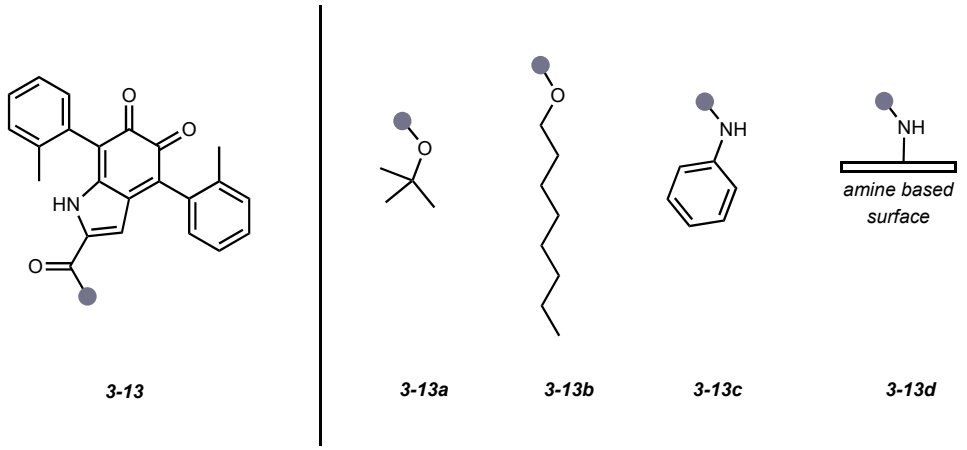

Scheme 3.5. Hypothetical C2-carbonyl-functionalized orthoquinone derivative **3-13** and some proposed diversifications.

5. Building from the C2 Position of Blocked DHI

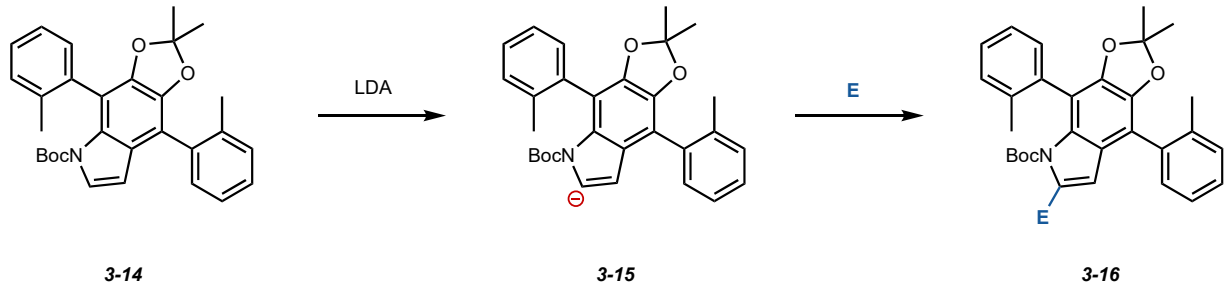

3-14 *3-15* *3-16*

Scheme 3.6. Diversification of C2-functionalized derivatives from the C2 anion **3-15**, where E = electrophile.

Knowing that the anion at C2 of a C4,7-blocked **DHI** derivative can be easily formed, we may also consider trapping it with a range of electrophiles beyond esters and amides. The carboxylation methodology which we have established here offers a great point from which to diversify to other C2-functionalized derivatives. This could allow for modification and tailoring of physiochemical properties through the C2 position, and the broadening of application of these materials.

5.1 Silyl groups

It is important to note that silyl electrophiles of large steric demand are not easily installed at the C2 position of a blocked **DHI** derivative (see Chapter 2, Section 4.1); thus far, only a trimethylsilyl (TMS) group has been successfully installed. All the same, the presence of a silicon functional group would give rise to desirable properties and it could be worth pursuing alternative methods of expanding the C2-silicon-functionalized **DHI** library. A silicon group can act as a functional handle for late-stage manipulations, and influence physical properties such as lipophilicity and crystallinity.[3] The latter may make such blocked **DHI** derivatives able to be of use in biomedicinal fields.

One potential application lies in positron emission tomography (PET) imaging. This is a non-invasive imaging technology which allows for the tracking of the path and uptake of compounds within the body. ^{18}F-labeled compounds are often used as PET radiotracers.[4a-c] In the case that an -SiR_2F functional group is able to be installed at the C2 position of our blocked derivatives to form **3-18**, the ^{19}F could be isotopically exchanged for ^{18}F to form the radiolabeled compound **3-19** (Scheme 3.7).[4d] These silicon-type **DHI** derivatives would then have the potential to reveal how such compounds get incorporated biologically.

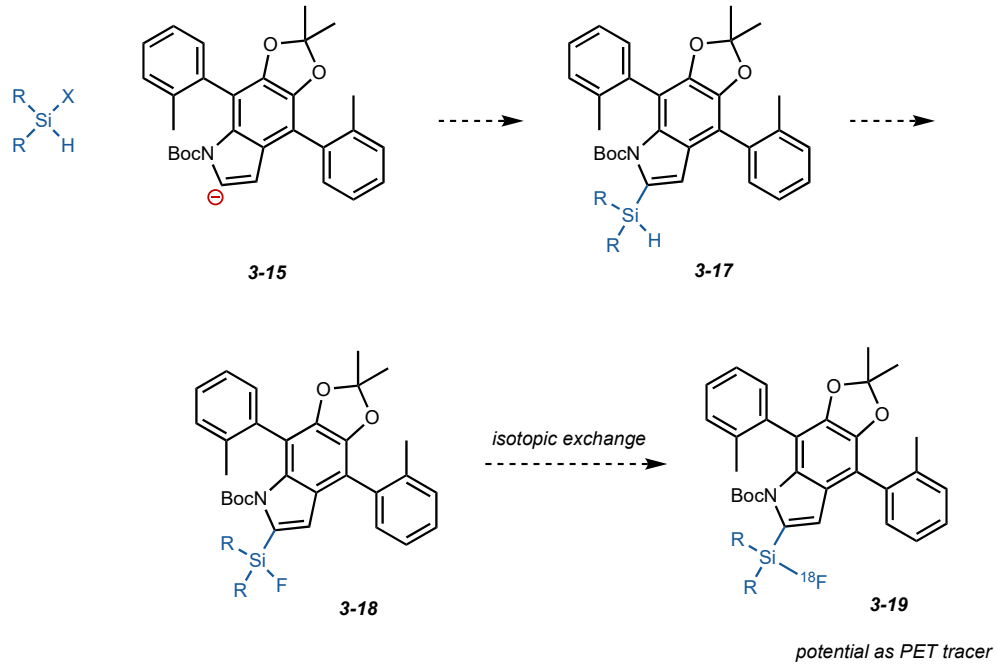

Scheme 3.7. Hypothetical synthesis of ^{18}F-labeled, C2-functionalized, blocked **DHI** derivatives.

5.2 Other Electrophiles

Other electrophiles may be attached to C2 for investigation of the extent to which they alter the electronics, physiochemical properties, redox potentials, or polarity of a blocked derivative. Electron-withdrawing functional groups that might be considered include trifluoromethyl,

phosphinic acid, cyano, alkyne, or ketone groups (Scheme 3.8). Based on work from Togni, we believe it may be possible to install a trifluoromethyl group at C2 of **3-14** using the hypervalent iodine reagent **3-20**.[5] A phosphinic acid analog **3-26** could be obtained via phosphorous-centered radical with the addition of phosphinate **3-21**.[6] The latter would present the distinct advantage of the use of ^{31}P NMR, while being similar in pKa to the original blocked **DHICA** derivative. We can also foresee the possibility of interfacing the C2 anion **3-15** with other electrophiles, including 1-cyanoimidazole **3-22**, a Weinreb amide **3-23**, or sulfonyl acetylene **3-24** for installation of a variety of electron-withdrawing functional groups.[7,8,9] Should acetonide deprotection and subsequent oxidation be possible of the resulting compounds **3-25** to **3-29** to obtain the corresponding blocked orthoquinones, it would hold interest to then study how these different functional groups affect the photophysical properties of a blocked indolequinone core.

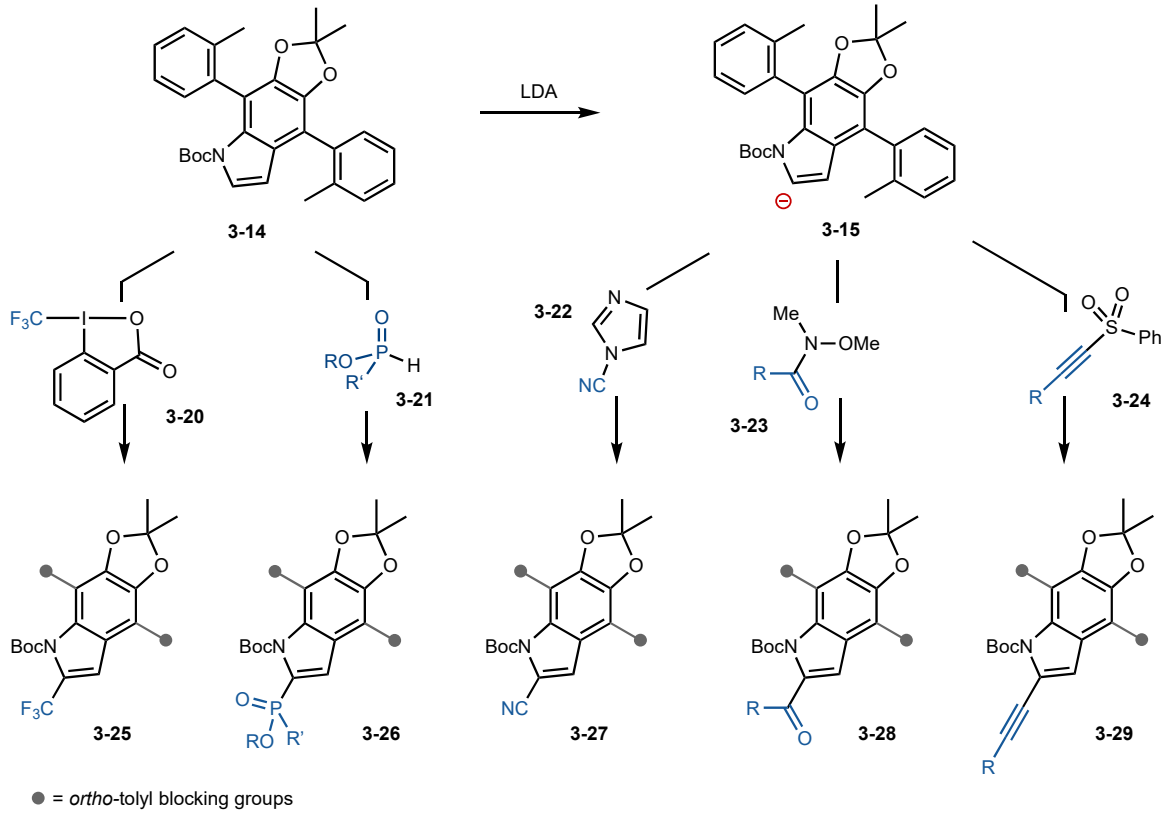

Scheme 3.8. Selection of electron-withdrawing groups proposed for diversification of C2-functionalization and study of the effect on electronic or physiochemical properties.

6. Conclusions

It is first of interest to continue synthetic efforts towards the target **2-carboxy-IQ-Me**. This M.Sc. project achieved robust conditions for carboxylation of a blocked **DHI**-acetonide. This result opens the project to expand to other types of C2-functionalization beyond the carboxylate. The ensuing acetonide deprotection is a remaining challenge for both the carboxylated- and diversified derivatives. We hope that property analysis of any new C2-functionalized compounds would help to inform on the structure-function-property relationships of the eumelanin biopolymer, or open the door for use of these blocked **DHI** compounds in materials and biomedicinal fields.

7. References

1. Pezzella, A.; d'Ischia, M.; Napolitano, A.; Palumbo, A.; Prota, G. An integrated approach to the structure of Sepia melanin. Evidence for a high proportion of degraded 5, 6-dihydroxyindole-2-carboxylic acid units in the pigment backbone. *Tetrahedron* **1997**, *53* (24), 8281-8286.
2. **(a)** Miller, T., & Teplyakov, A.V. Attachment chemistry of PCMB to a primary-amine-terminated organic monolayer on a Si (111) surface. *Langmuir* **2014**, *30* (18), 5105-5114. **(b)** Duevel, R.V., & Corn, R. M. Amide and ester surface attachment reactions for alkanethiol monolayers at gold surfaces as studied by polarization modulation Fourier transform infrared spectroscopy. *Anal. Chem.* **1992**, *64* (4), 337-342. **(c)** Lahiri, J.; Ostuni, E.; Whitesides, G. M. Patterning ligands on reactive SAMs by microcontact printing. *Langmuir* **1999**, *15* (6), 2055-2060.
3. Lee, J. Y., & Fu, G. C. Room-temperature Hiyama cross-couplings of arylsilanes with alkyl bromides and iodides. *J. Am. Chem. Soc.* **2003**, *125* (19), 5616-5617.
4. **(a)** Höhne, A.; Yu, L.; Mu, L.; Reiher, M.; Voigtmann, U.; Klar, U.; Graham, K. P.; Schubiger, A.; Ametamey, S. M. Organofluorosilanes as model compounds for 18F-labeled silicon-based

PET tracers and their hydrolytic stability: Experimental data and theoretical calculations (PET= positron emission tomography). *Chem. Eur. J.* 2009, 15 (15), 3736-3743. **(b)** Mu, L.; Höhne, A.; Schubiger, P.A.; Ametamey, S.M.; Graham, K.; Cyr, J.E.; Dinkelborg, L.; Stellfeld, T.; Srinivasan, A.; Voigtmann, U.; Klar, U. Silicon-based building blocks for one-step 18F-radiolabeling of peptides for PET imaging. *Angew. Chem. Int. Ed.* **2008**, *47* (26), 4922-4925. **(c)** Schirrmacher, E.; Wängler, B.; Cypryk, M.; Bradtmöller, G.; Schäfer, M.; Eisenhut, M.; Jurkschat, K.; Schirrmacher, R. Synthesis of p-(di-tert-butyl [18F] fluorosilyl) benzaldehyde ([18F] SiFA-A) with high specific activity by isotopic exchange: a convenient labeling synthon for the 18F-labeling of N-amino-oxy derivatized peptides. *Bioconjug. Chem.* **2007**, *18* (6), 2085-2089. **(d)** Narayanam, M. K.; Toutov, A. A.; Murphy, J. M. Rapid one-step 18F-labeling of peptides via heteroaromatic silicon-fluoride acceptors. *Org. Lett.* **2020**, *22* (3), 804-808.

5. Wiehn, M. S.; Vinogradova, E. V.; Togni, A. Electrophilic trifluoromethylation of arenes and N-heteroarenes using hypervalent iodine reagents. *J. Fluor. Chem.* **2010**, *131* (9), 951-957.
6. Montchamp, J. L. Recent advances in phosphorous-carbon bond formation: synthesis of H-phosphinic acid derivatives from hypophosphorous compounds. *J. Organomet. Chem.* **2005**, *690* (10), 2388-2406.
7. Wu, Y.Q.; Limburg, D.C.; Wilkinson, D.E.; Hamilton, G.S. 1-Cyanoimidazole as a mild and efficient electrophilic cyanating agent. *Org. Lett.* **2000**, *2* (6), 795-797.
8. Robertson, F.J.; Wu, J. Phosphorothioic Acids and Related Compounds as Surrogates for H2S Synthesis of Chiral Tetrahydrothiophenes. *J. Am. Chem. Soc.* **2012**, *134* (5), 2775-2780.
9. Marzo, L.; Pérez, I.; Yuste, F.; Alemán, J.; Ruano, J.L.G. A straightforward alkylnylation of Li and Mg metalated heterocycles with sulfonylacetylenes. *Chem. Commun.* **2015**, *51* (2), 346-349.

Appendix A: Experimental Data

1. General Considerations

Unless otherwise specified, all reactions are conducted under inert atmosphere employing standard Schlenck technique. All glassware was flame-dried prior to use. Unless otherwise noted, all reagents were obtained from commercial sources (Sigma Aldrich, Alfa Aesar, Oakwood, or CombiBlock) and used as supplied without further purification.

NMR (Nuclear Magnetic Resonance), IR (Infrared) and HRMS (High-Resolution Mass spectrometry) data were all acquired through McGill Chemistry Characterization Facility (MC2). Proton nuclear magnetic resonance (^{1}H NMR) spectra were acquired using Varian Mercury 400 MHz, Varian Inova QANUC 500 MHz, Varian VNMRS 500 MHz, Bruker AVIIIHD 500 MHz, or Bruker AVIIIHD 400 MHz spectrometers. Chemical shifts (δ) are reported in parts per million (ppm) and are calibrated to the residual solvent peak. Coupling constants (*J*) are reported in Hz. Multiplicities are reported using the following abbreviations: *s* = singlet; *brs*=broad singlet; *d* = doublet; *t* = triplet; *q* = quartet; *m* = multiplet (range of multiplet is given). Carbon nuclear magnetic resonance (^{13}C NMR) spectra were acquired using Varian VNMRS 125 MHz, Bruker AVIIIHD 125 MHz, or Bruker AVIIIHD 101 MHz spectrometers. Chemical shifts (δ) are reported in parts per million (ppm) and are calibrated to the residual solvent peak. High resolution mass spectra (HRMS) were recorded using a Bruker maXis Impact TOF mass spectrometer. Fourier-transform infrared (FT-IR) spectra were recorded on an alpha Bruker FT-IR spectrometer. Analytical thin-layer chromatography was performed on pre-coated 250 mm layer thickness silica gel 60 F254 plates (EMD Chemicals Inc.). Visualization was performed by ultraviolet light and/or by staining with potassium permanganate. Purifications by column chromatography were performed using either a Biotage Isolera^{TM} One or standard column chromatography using silica gel (40-63 μm, 230-400 mesh).

2. Procedures and Characterization Data

*2.1 Compound **2-6** (200.0 mmol scale)*

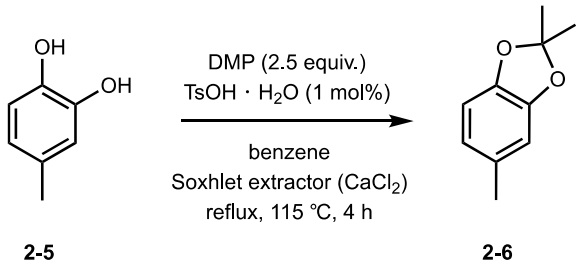

The synthesis of **2-*6*** was performed by making slight modification to the method of Frey *et al*.[1] A flame-dried, 500 mL round-bottom flask, equipped with a Teflon-coated stir bar, a Soxhlet extractor, and a rubber septum was charged with ***2-5*** (24.8 g, 200.0 mmol, 1 equiv.), p-toluenesulfonic acid monohydrate (380.4 mg, 2.0 mmol, 1 mol% equiv.) followed by benzene (100.0 mL, 2.0 M). To this solution was added 2, 2-dimethoxypropane (61.5 mL, 500.0 mmol, 2.5 equiv.) then purged with a steady stream of N_2 for 5 min prior to reflux for 4 hours with Soxhelt ($CaCl_2$, 58.0 g). The reaction mixture was then filtered on a pad of silica, washing with EtOAc. Upon concentrating the filtrate in vacuo, the resulting crude residue **2-*6*** (21.1 g, 128.4 mmol, 64 %) was obtained as a brown oil and was advanced without further purification.

Characterization: $\mathbf{R_f}$ = (hexanes) 0.5; **^{1}H-NMR** (400 MHz, $CDCl_3$): δ 6.56–6.64 (m, 3H), 2.27 (s, 3 H), 1.67 (s, 6H). The analytical data was consistent with the literature.[1]

*2.2 Compound **2-7** (128.4 mmol scale)*

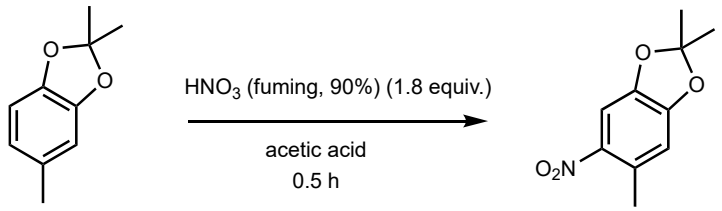

2-6 **2-7**

The synthesis of **2-7** was performed by making modification to the method of Xu *et al.* [2] A 1L round-bottom flask, equipped with a Teflon-coated stir bar was charged with **2-6** (32.8 g, 200.0 mmol, 1.0 equiv.) and acetic acid (225.0 mL). To this solution was added fuming HNO_3 (17.5 mL) in acetic acid (50.0 mL) dropwise over 30 minutes at 0 °C. The resulting mixture was stirred at ambient temperature for 30 minutes before pouring into a beaker containing ice to afford precipitate, which was collected by vacuum filtration and washed with water. The yellow crude solid was purified using silica gel column chromatography (EtOAc: hexanes, 1:9) to afford **2-7** as a bright yellow solid (28.9 g, 138.0 mmol) in 69 % yield.

Characterization: $\mathbf{R_f}$ = (DCM/hexanes, 1:9) 0.48; $^{\mathbf{1}}$**H NMR** (400MHz, $CDCl_3$): δ 7.47 (s, 1 H), 6.62 (s, 1 H), 2.56 (s, 3 H), 1.71 (s, 6 H). The analytical data was consistent with the literature.[2]

*2.3 Compound **2-8** (80 mmol scale)*

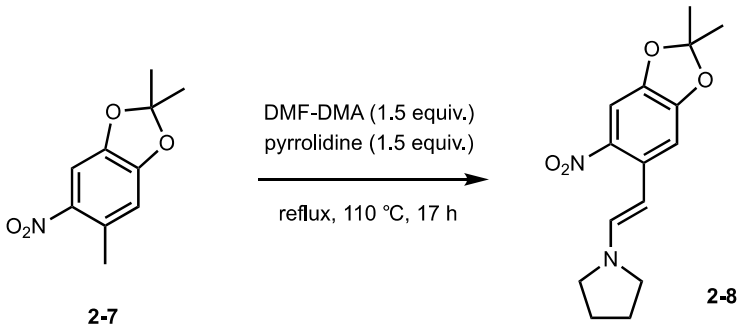

2-7 **2-8**

The synthesis of **2-8** was performed by making modifications to the method of Leimgruber *et al.*[3] A flame-dried, 250 mL round-bottom flask equipped with a Teflon-coated stir bar was charged

with **2-7** (16.7 g, 80 mmol, 1.0 equiv), pyrrolidine (10.0 mL, 120 mmol, 1.5 equiv.), and *N,N*'-dimethylformamide dimethyl acetal (16.0 mL, 120 mmol, 1.5 equiv). The resulting homogenous solution was heated at reflux (110 °C) for 17 hours under a positive pressure of N_2 and then allowed to cool to room temperature. The resulting mixture was then diluted and extracted with EtOAc (150 mL x 3) and washed with water (150 mL x 3). The phases were separated, and the organic layer was washed with brine (100 mL x 3), dried over Na_2SO_4 and concentrated *in vacuo*. In Method A, the resulting blood red crude residue was advanced without further purification. Alternatively, in Method B, the residue was dissolved in CH_2Cl_2 (15 mL) and MeOH (70 mL) and cooled to −20 °C. Filtration of the resulting mixture afforded **2-8** (18.8 g, 64.9 mmol) as a red needle crystal. Upon concentrating the filtrate *in vacuo*, the resulting residue was recrystallized from MeOH (50 mL) at −20 °C to afford **2-8** (1.6 g, 5.5 mmol) as a red solid. In total, this afforded **2-8** (20.4 g, 70.4 mmol) in 88 % yield.

Characterization: $\mathbf{R_f}$ = (EtOAc/hexanes, 1:4) 0.60; **^{1}H NMR** (400 MHz, $CDCl_3$) δ 7.41 (s, 1H), 7.10 (d, *J* = 13.4 Hz, 1H), 6.74 (s, 1H), 6.14 (d, *J* = 13.4 Hz, 1H), 3.32 (t, *J* = 6.6 Hz, 4H), 1.97 – 1.92 (m, 4H), 1.68 (s, 6H). The analytical data was consistent with the literature.[2]

*2.4 Compound **2-9** (37.1 mmol scale)*

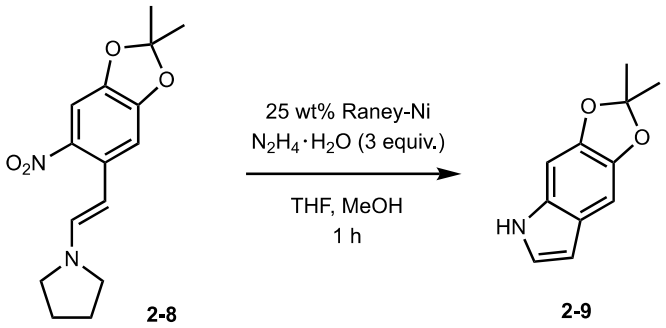

2-8 **2-9**

The synthesis of **2-9** was performed by making modifications to the method of Leimgruber *et al*.[3] A 3-neck round-bottom flask equipped with a Teflon-coated stir bar, a reflux condenser was charged with Raney-Nickel (2.7 g), THF (74.2 mL, 0.5 M), MeOH (74.2 mL, 0.5 M), and **2-8**

(10.8 g, 37.1 mmol, 1.0 equiv.). To the resulting solution was added $N_2H_4 \cdot H_2O$ (2.7 mL, 1.5 equiv.) dropwise over the course of 5 min. Additional $N_2H_4 \cdot H_2O$ (2.7 mL, 1.5 equiv.) was added after 30 min. The resulting mixture was stirred at room temperature for 2 hr prior to the filtration on a pad of Celite. Upon concentrating the filtrate *in vacuo*, the resulting residue was purified using silica gel column chromatography (EtOAc: hexanes, 1:9) to afford **2-9** as an off-white solid (5.5 g, 29 mmol) in 79 % yield.

Characterization: $\mathbf{R_f}$ = (EtOAc/hexanes, 1:9) 0.37; ^{1}**H NMR** (500 MHz, $CDCl_3$): δ 7.97 (brs, 1H), 7.05 (dd, *J* = 3.2, 2.4 Hz, 1H), 6.91 (t, *J* = 0.6 Hz, 1H), 6.76 (t, *J* = 0.7 Hz, 1H), 6.41 (ddd, *J* = 3.1, 2.1, 0.9 Hz, 1H), 1.69 (s, 7H). The analytical data was consistent with the literature.[2]

*2.5 Compound **2-4** (128.4 mmol scale)*

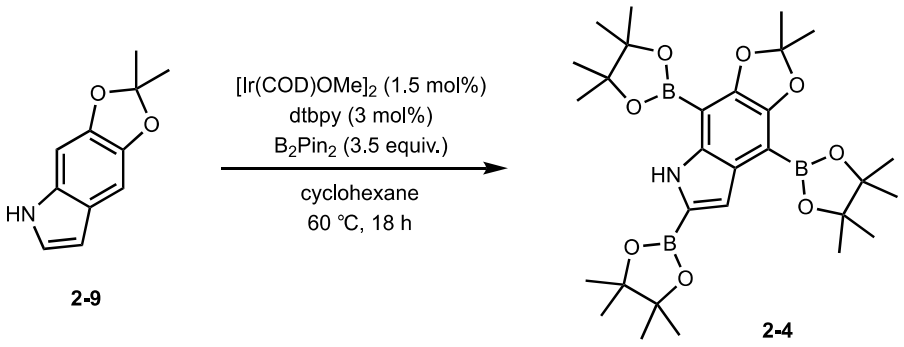

A flame-dried Schlenk flask equipped with a Teflon-coated stir bar, was charged with **2-9** (5.0 g, 26.4 mmol, 1.0 equiv), B_2pin_2 (21.5 g, 85.0 mmol, 3.5 equiv), 4,4'-di-tert-butyl-2,2'-bipyridyl (212.7 mg, 0.8 mmol, 3 mol%), and $[Ir(COD)(OMe)]_2$ (262.7 mg, 0.4 mmol, 1.5 mol%). The Schlenk flask was evacuated and backfilled with N_2 (3x), and then cyclohexane (52.8 mL, 0.5 M) was added under a positive pressure of N_2. The reaction mixture was stirred at 60 °C for 18 h, and then transferred to a round-bottom flask and concentrated *in vacuo*. The reaction mixture was then purified by silica gel column chromatography (EtOAc/hexanes 2:8). After concentration of the collected fractions, the resulting white solid was triturated with hexanes to remove residual B_2pin_2.

The resulting solid was then filtered and dried under vacuum to afford **2-4** as a white solid. **Characterization: R_f** = (EtOAc/hexanes, 3:7) 0.45; **^{1}H NMR** (400 MHz, d_6-acetone) δ 9.38 (brs, 1H), 7.34 (d, J = 2.4 Hz, 1H), 1.66 (s, 6H), 1.41 (s, 12H), 1.38 (s, 12H), 1.35 (s, 12H). The analytical data was consistent with the literature.[4]

*2.6 Compound **2-18** (8.8 mmol scale)*

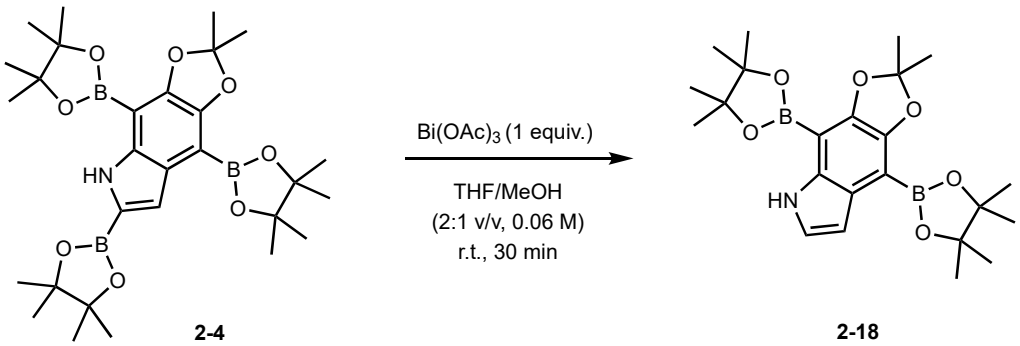

2-4 **2-18**

A round bottom flask equipped with a Teflon-coated stir bar was charged with **2-4** (5.0 g, 8.8 mmol, 1.0 equiv) and $Bi(OAc)_3$ (3.4 g, 8.8 mmol, 1.0 equiv), dissolved in a 1:2 v/v mixture of MeOH/THF (0.06 M), then stirred at room temperature for 30 min under nitrogen. Upon completion the reaction mixture was filtered through a pad of Celite® and the filtrate concentrated *in vacuo*. This crude reaction mixture was purified by silica gel column chromatography (EtOAc/hexanes 2:8). The resulting material was filtered and dried under vacuum to afford **2-18** as a white solid (3.3 g, 7.6 mmol, 86%).

Characterization: R_f = (3:7 EtOAc/hexanes) 0.7; **^{1}H NMR** (500 MHz, d_6-acetone): δ 9.69 (s, 1H), 7.07 (dd, J = 3.1, 2.5 Hz, 1H), 6.76 (dd, J = 3.1, 2.3 Hz, 1H), 1.64 (s, 6H), 1.39 (s, 12H), 1.36 (s, 12H); **^{13}C NMR** (126 MHz, d_6-acetone): δ 149.98, 148.58, 134.07, 124.40, 122.04, 116.22, 83.54, 82.95, 29.41, 29.26, 29.10, 28.95, 28.79, 28.64, 28.49, 25.37, 24.41, 24.31; **HRMS** (ESI) for $C_{23}H_{33}B_2NO_6$: Calculated [M+H$^+$]: 442.2567; Found [M+H$^+$]: 442.2569.

*2.7 Compound **2-26** (1.20 mmol scale)*

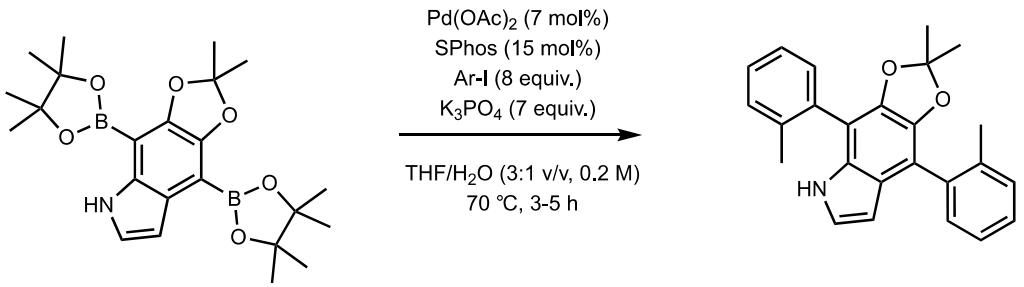

2-18 **2-26**

A round bottom flask equipped with a Teflon-coated stir bar and a rubber septum was charged with **2-18** (529.5 mg, 1.20 mmol, 1.0 equiv), $Pd(OAc)_2$ (18.9 mg, 0.08 mmol, 7 mol%) and SPhos (73.9mg, 0.18 mmol, 15 mol%). The reaction vessel was then evacuated and backfilled with N_2 (3x), followed by the addition of THF (4.5 mL) to dissolve the solids. The aryl iodide 2-iodotoluene (1.2 mL, 9.6 mmol, 8 equiv) was then added to the reaction mixture, followed by the addition of a degassed aqueous solution of K_3PO_4 (1.5 mL, 5.6 M, 7 equiv). The reaction mixture was then warmed to 70 °C, and the reaction monitored by TLC for completion over the course of 3–5 hours. Upon complete consumption of **2-18**, the reaction mixture was cooled to room temperature, diluted with EtOAc (10 mL/mmol of **2-18**), transferred to a separatory funnel, and washed with H_2O (2 x 5 mL/mmol of **2-18**). The organic layer was then collected, dried over sodium sulfate, filtered, and concentrated in vacuo. The reaction mixture was then purified by silica gel column chromatography (EtOAc/hexanes 1:9) and triturated in hexanes to yield **2-26** as a white solid (274.7 mg, 0.74 mmol, 62%).

Characterization: $\mathbf{R_f}$ = (1:9 EtOAc/hexanes) 0.44; **IR** (cm^{-1}): 3340, 2985, 2919, 1431, 1402, 1310, 1210, 1066, 1006, 874, 756, 737, 660, 447; **^{1}H NMR** (800 MHz, d_6-acetone, mixture of atropisomers): δ 9.71 (s, 1H), 7.43 – 7.41 (m, 2H), 7.38 – 7.36 (two overlapping d, J = 12.0 Hz, 2H), 7.33 (app td, J = 7.5, 1.5 Hz, 1H), 7.32 - 7.28 (m, 3H), 7.08 (app dd, J = 2.8, 1.8 Hz, 1H), 6.11 – 6.09 (two overlapping t, J = 2.8, 1.8 Hz, 1H), 2.29 – 2.26 (four overlapping s, 6H), 1.67 – 1.60 (four overlapping s, 6H); **^{13}C NMR** (201 MHz, d_6-acetone, mixture of atropisomers): δ 142.39, 142.35, 140.50, 140.45, 138.32, 138.30, 137.83, 137.81, 136.39, 133.98, 131.37, 131.36,

131.26, 131.23, 131.21, 130.96, 130.93, 130.61, 130.55, 128.80, 128.23, 126.76, 126.73, 126.24, 126.22, 123.85, 123.69, 122.56, 122.48, 117.55, 117.53, 113.22, 113.13, 113.07, 106.93, 106.87, 102.15, 102.13, 102.09, 102.07, 26.04, 26.01, 25.93, 20.35, 20.27, 20.17, 20.11; **HRMS** (ESI) for $C_{25}H_{23}NO_2$: Calculated [M+Na$^+$]: 392.1621; Found [M+Na$^+$]: 392.1611.

*2.8 Compound **2-51** (0.45 mmol scale)*

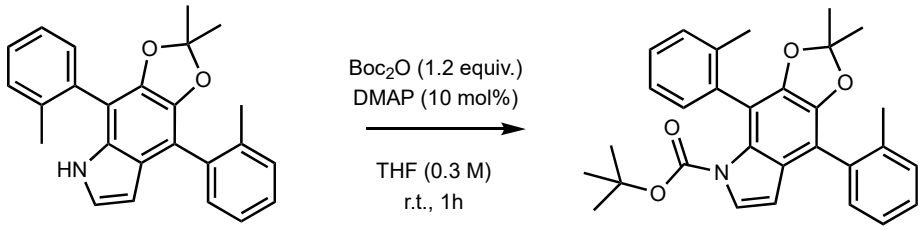

2-26 **2-51**

A round-bottom flask equipped with a Teflon-coated stir bar and rubber septum was charged with **2-26** (165 mg, 0.45 mmol, 1 equiv.), DMAP (5.5 mg, 0.045 mmol, 0.1 equiv) and Boc_2O (0.12 g, 0.54 mmol, 1.2 equiv.) followed by THF (1.5 mL, 0.3 M). The resulting homogeneous reaction mixture was stirred at room temperature for 1 h and then concentrated *in vacuo*. This afforded a crude reaction mixture that was purified by column chromatography (EtOAc/hexanes, 1:9) to afford **2-51** as a white solid (198.6 mg, 0.42 mmol, 94% yield).

Characterization: $\mathbf{R_f}$ = (1:9 EtOAc/hexanes) 0.66; **IR** (cm^{-1}): 2980, 1750, 1730, 1370, 1296, 1205, 1136, 1113, 984, 883, 829, 752, 753, 665, 449; **^{1}H NMR** (500 MHz, d_6-acetone, mixture of atropisomers): δ 7.40 – 7.39 (two overlapping d, J = 2.0 Hz, 1H), 7.38 – 7.29 (m, 5H), 7.25 – 7.09 (m, 3H), 6.19 – 6.16 (two overlapping d, J = 3.7 Hz, 1H), 2.35 – 2.24 (four overlapping s, 6H), 1.69 – 1.60 (four overlapping s, 6H), 1.30 (two overlapping s, 9H); **^{13}C NMR** (126 MHz, d_6-acetone, mixture of atropisomers) δ 170.81, 149.38, 144.56, 144.50, 142.25, 142.16, 137.85, 137.78, 137.54, 136.40, 136.37, 135.08, 135.05, 131.36, 131.08, 131.02, 131.00, 130.80, 130.75, 129.78, 129.55, 129.19, 129.11, 128.68, 128.64, 127.85, 127.25, 127.22, 126.39, 126.38, 126.21, 126.10, 126.01, 125.98, 118.42, 118.34, 113.88, 113.83, 111.55, 111.51, 106.42, 83.51, 83.50,

60.48, 27.66, 26.00, 25.94, 25.92, 25.83, 20.79, 20.61, 20.16, 14.47; **HRMS** (ESI) for $C_{30}H_{31}NO_4$: Calculated [M+Na$^+$]: 492.2151; Found [M+Na$^+$]: 492.2144.

*2.9 Compound **2-83** (0.11 mmol scale)*

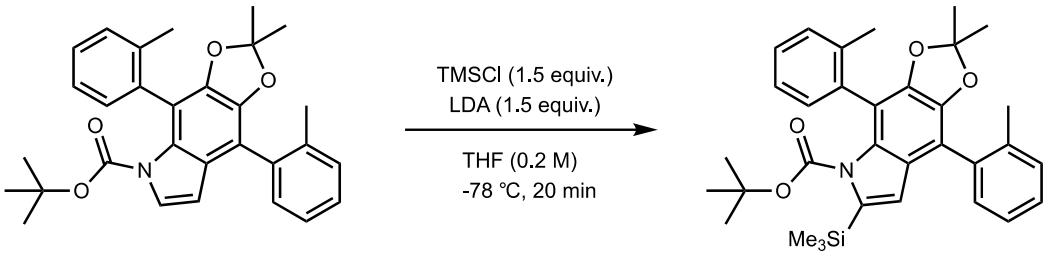

2-51 **2-83**

A flame-dried Schlenk flask, equipped with a Teflon-coated stir bar and rubber septum, was charged with **2-51** (50 mg, 0.11 mmol, 1 equiv.) followed by THF (0.53 mL, 0.2 M). To the resulting homogeneous reaction solution was added TMSCl (0.03 mL, 0.16 mmol, 1.5 equiv.), and LDA (0.16 mL, 0.16 mmol, 1.5 equiv., 1.0 M in THF/hexanes) dropwise at -78 °C. The resulting solution was stirred at -78 °C for 20 min prior to quenching by saturated aqueous NH_4Cl solution. The resulting mixture was then extracted three times with EtOAc. The combined organic fractions were washed with brine and dried over $MgSO_4$, filtered and concentrated *in vacuo*. The resulting crude was purified by column chromatography (EtOAc/hexanes, 1:9) to yield **2-83** as a white solid (39.6 mg, 0.073 mmol, 69% yield).

Characterization: $\mathbf{R_f}$ = (1:9 EtOAc/hexanes) 0.72; **^{1}H NMR** (500 MHz, d_6-acetone, mixture of atropisomers): δ 7.41 – 7.28 (m, 6H), 7.28 – 7.22 (m, 2H), 6.48 – 6.44 (two overlapping s, 1H), 2.39 – 2.24 (four overlapping s, 6H), 1.70 – 1.58 (four overlapping s, 6H), 1.12 (s, 9H), 0.26 (two overlapping s, 9H); **^{13}C NMR** (126 MHz, d_6-acetone) δ 152.89, 145.21, 145.11, 142.30, 142.16, 142.06, 137.93, 137.86, 137.71, 136.45, 136.41, 135.00, 134.96, 132.32, 131.72, 131.48, 131.18, 131.12, 130.18, 129.99, 128.78, 128.74, 128.45, 126.79, 126.74, 126.45, 126.44, 126.42, 118.61, 118.53, 118.15, 118.09, 113.54, 113.50, 111.09, 111.06, 84.99, 84.96, 27.55, 26.09, 26.02, 25.88,

20.97, 20.25, 0.31; **HRMS** (ESI) for $C_{33}H_{39}NO_4Si$: Calculated [M+Na^+]: 564.2546; Found [M+Na^+]: 564.2553.

*2.10 Compound **2-54** (0.064 mmol scale)*

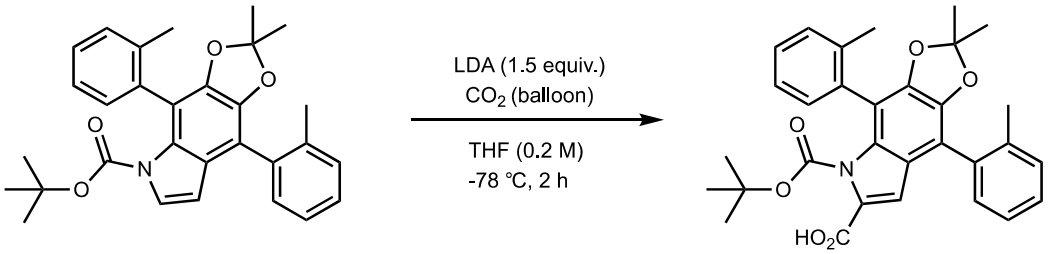

2-51 **2-54**

A 10mL flame-dried Schlenk tube, equipped with a Teflon-coated stir bar and rubber septum, was charged with **2-51** (30 mg, 0.064 mmol, 1 equiv.) followed by THF (0.32 mL, 0.2 M). The resulting homogeneous reaction solution was allowed to equilibrate to -78 °C before the addition of LDA (0.1 mL, 0.1 mmol, 1.5 equiv., 1.0 M in THF/hexanes) dropwise. Upon completion of the addition, the reaction mixture was stirred at -78 °C for 30 minutes. It was then sparged vigorously with dry CO_2 (g) which was passed from a balloon to the reaction mixture via a long needle (20 gauge, 6-inch) through the rubber septum with a vent needle for an additional 30 minutes while being allowed to warm to room temperature. The reaction was then quenched with 1 M aqueous HCl. The resultant mixture was extracted with EtOAc x 3, then washed with 1 M aqueous HCl x 3. The combined organic fractions were dried over Na_2SO_4, filtered and concentrated *in vacuo.* The resulting white solid was triturated out of hexanes and purified by column chromatography (EtOAc:hexanes 2:8) to afford **2-54** as a white solid (22.6 mg, 0.044 mmol) in 69 % yield.

Characterization: $\mathbf{R_f}$ = (EtOAc) 0.18; **IR** (cm^{-1}): 2978, 2931, 1760, 1680, 1541, 1419, 1371, 1138, 1024, 885, 837, 752, 665; **^{1}H NMR** (500 MHz, d_6-acetone): δ 11.13 (brs, 1H), 7.43 – 7.29 (m, 6H), 7.25 (app t, J = 7.5 Hz, 1H), 7.21 – 7.18 (app dd, J = 3.2 Hz, 7.5 Hz, 1H), 6.84 (s, 1H), 2.28 – 2.25 (four overlapping s, 6H), 1.66 – 1.60 (four overlapping s, 6H), 1.21 (s, 9H); **^{13}C NMR**

(126 MHz, d_6-acetone) δ 161.73, 149.92, 147.04, 141.99, 138.72, 138.68, 137.94, 134.58, 133.32, 131.64, 131.47, 131.36, 131.33, 131.18, 131.16, 130.90, 129.04, 128.98, 126.71, 126.69, 126.57, 122.31, 122.22, 119.08, 119.03, 114.07, 112.04, 112.02, 108.53, 85.36, 27.32, 26.04, 25.97, 25.94, 25.79, 20.43, 20.35, 20.17, 20.13; **HRMS** (ESI) for $C_{31}H_{31}NO_6$: Calculated [M+Na$^+$]: 536.2049; Found [M+Na$^+$]: 536.2054.

*2.11 Compounds **2-57**, **2-58** (0.043 mmol scale)*

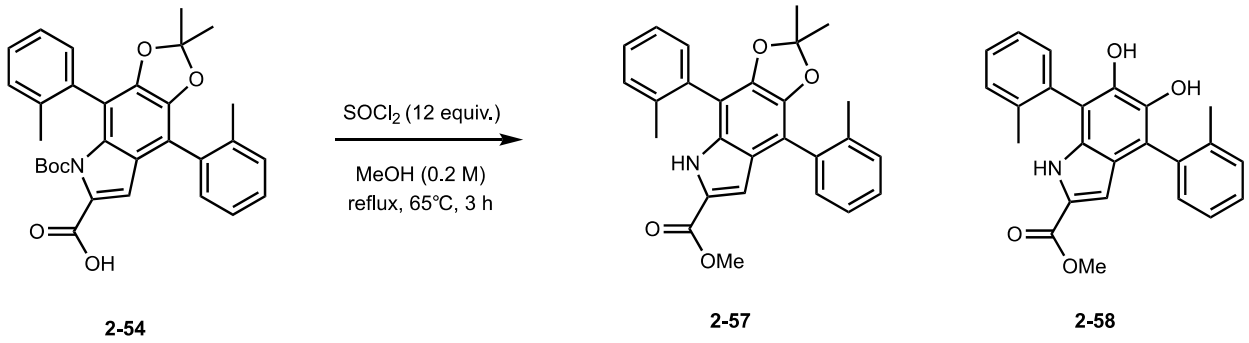

2-54 **2-57** **2-58**

A flame-dried round-bottom flask was equipped with a Teflon-coated stir bar, rubber septum, and **2-54** (22.2 mg, 0.043 mmol, 1 equiv.), followed by MeOH (0.22 mL, 0.2 M). To the resulting homogeneous solution was added thionyl chloride (0.038 mL, 0.52 mmol, 12 equiv.) dropwise at 0 °C. Upon completion of addition, the solution was heated to reflux (65 °C) for 3 hours, then cooled to room temperature and concentrated *in vacuo*. The resulting crude reaction mixture was purified by column chromatography (EtOAc/hexanes, 1:9) to separate **2-57** (8.4 mg, 0.0196 mmol, 46% yield) as a an off-white residue and **2-58** (6 mg, 0.0155 mmol, 36% yield) as yellowish solid.

Characterization: 2-57 R$_f$ = (2:8 EtOAc/hexanes) 0.59; **IR** (cm^{-1})**:** 2920, 2852, 1687, 1438, 1261, 1205, 1012, 752; **^{1}H NMR** (800 MHz, d_6-acetone): δ 10.17 (brs, 1H), 7.43 – 7.37 (m, 5H), 7.37 – 7.33 (m, 3H), 7.33 – 7.29 (m, 1H), 6.79 – 6.78 (two overlapping s, 1H), 3.73 (s, 3H), 2.29-2.26 (four overlapping s, 6H), 1.70 – 1.63 (four overlapping s, 6H); **^{13}C NMR** (201 MHz, d_6-acetone) δ 162.11, 145.46, 141.66, 138.44, 138.42, 137.86, 137.84, 135.25, 132.95, 131.38, 131.26, 131.25, 131.22, 131.15, 131.13, 131.10, 129.17, 128.71, 127.02, 126.89, 126.86, 126.47, 126.44, 122.61,

118.65, 118.63, 113.60, 109.13, 107.10, 51.57, 32.64, 26.16, 26.06, 26.04, 25.91, 23.33, 20.26, 20.19, 20.15, 20.07, 14.35; **HRMS** (ESI) for $C_{27}H_{25}NO_4$: Calculated [M+Na$^+$]: 450.1681; Found [M+Na$^+$]: 450.1679.

2-58 R_f = (2:8 EtOAc/hexanes) 0.28; **IR** (cm^{-1}): 3508, 2920, 1678, 1438, 1213, 748; **^{1}H NMR** (800 MHz, *d*$_6$-acetone): δ 9.72 (brs, 1H), 7.65 (brs, 1H), 7.41 (brs, 1H), 7.37 – 7.27 (m, 9H), 6.61 (app t, *J* = 2.0 Hz, 1H), 3.71 (s, 1H), 2.21 – 2.20 (four overlapping s, 6H); **^{13}C NMR** (201 MHz, *d*$_6$-acetone) δ 162.26, 143.91, 139.08, 138.91, 138.88, 138.29, 138.27, 136.59, 136.57, 134.26, 132.47, 131.80, 131.71, 131.62, 131.52, 131.13, 131.11, 130.93, 130.90, 128.92, 128.51, 126.85, 126.82, 126.69, 126.45, 121.44, 121.42, 119.24, 119.18, 111.35, 111.28, 108.93, 108.92, 108.87, 51.50, 20.16, 20.08, 20.05, 19.97; **HRMS** (ESI) for $C_{24}H_{21}NO_4$: Calculated [M+Na$^+$]: 410.1368; Found [M+Na$^+$]: 410.1377.

*2.12 Compound **2-10** (1.2 mmol scale)*

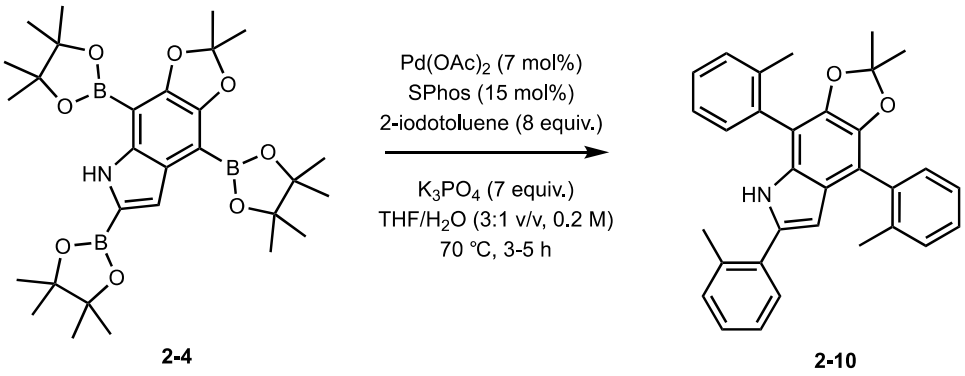

A round bottom flask equipped with a Teflon-coated stir bar and a rubber septum was charged with **2-4** (681 mg, 1.20 mmol, 1.0 equiv), $Pd(OAc)_2$ (18.9 mg, 0.08 mmol, 7 mol%) and SPhos (73.9mg, 0.18 mmol, 15 mol%). The reaction vessel was then evacuated and backfilled with N_2 (3x), followed by the addition of THF (4.5 mL) to dissolve the solids. The aryl iodide 2-iodotoluene (1.2 mL, 9.6 mmol, 8 equiv.) was then added to the reaction mixture, followed by the addition of a degassed aqueous solution of K_3PO_4 (1.5 mL, 5.6 M, 7 equiv.). The reaction mixture

was then warmed to 70 °C, and the reaction monitored by TLC for completion over the course of 3–5 hours. Upon complete consumption of **2-4**, the reaction mixture was cooled to room temperature, diluted with EtOAc (10 mL/mmol of **2-4**), transferred to a separatory funnel, and washed with H_2O (2 x 5 mL/mmol of **2-4**). The organic layer was then collected, dried over sodium sulfate, filtered, and concentrated in vacuo. The reaction mixture was then purified by silica gel column chromatography (EtOAc/hexanes 1:9) to yield **2-10** as a white solid (336 mg, 0.73 mmol, 61% yield).

Characterization: R_f = (EtOAc/hexanes, 1:9) 0.48; **^{1}H NMR** (500 MHz, d_6-acetone, mixture of atropisomers) δ 9.78 (s, 1H), 7.52 – 7.44 (m, 2H), 7.42 – 7.35 (m, 3H), 7.34 – 7.26 (m, 4H), 7.22 – 7.19 (m, 1H), 7.16 – 7.17 (m, 2H), 6.22 (app dd, J = 2.9, 2.3 Hz, 1H), 2.40 (app d, J = 2.9 Hz, 3H), 2.35 (s, 3H), 2.32 (s, 3H), 1.69 (s, 1.5H), 1.65 (app d, J = 7.3 Hz, 3H), 1.62 (s, 1.5H). The analytical data was consistent with the literature.[4]

*2.13 Compound **2-11** (0.73 mmol scale)*

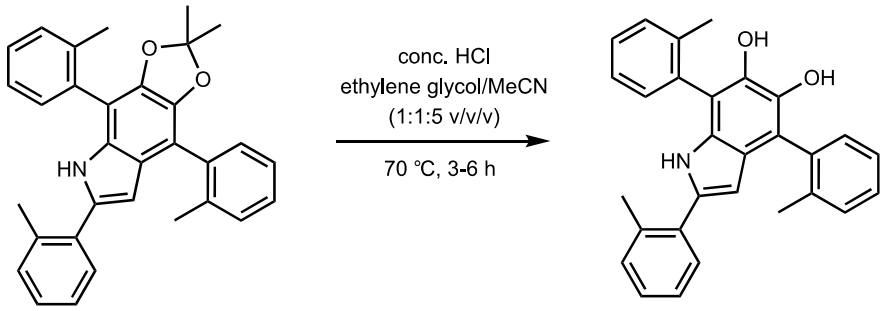

2-10 **2-11**

A round bottom flask, equipped with a Teflon-coated stir bar and a rubber septum was charged with **2-10** (335.5 mg, 0.73 mmol, 1 equiv. by weight). The reaction vessel was evacuated and backfilled with N_2 (x3) before the addition of acetonitrile (0.04 M, 5 volumes). The resulting solution was then degassed by sparging with N_2 for 15 minutes before the addition of HCl (1 volume) and ethylene glycol (1 volume) to afford a final concentration of 0.03 M with respect to **2-10**. The reaction mixture was warmed to 70 °C for 3 – 6 h, until TLC analysis revealed complete

consumption of starting material. The reaction was then cooled to room temperature, diluted with EtOAc (10 mL/mmol of **2-10**) and washed with water (3 x 5 mL/mmol of **2-10**). The organic layer was then collected, dried over sodium sulfate, filtered and concentrated in vacuo. The crude reaction mixture was purified by silica gel column chromatography and triturated with hexanes to yield **2-11** as an off-white solid (236 mg, 0.56 mmol, 77% yield).

Characterization: R_f = (EtOAc/hexanes, 3:7) 0.46; **^{1}H NMR** (800 MHz, d_6-acetone, mixture of atropisomers): δ 9.43 (two overlapping brs, 1H), 7.40 – 7.37 (m, 2H), 7.36 – 7.32 (m, 3H), 7.30 – 7.24 (m, 4H), 7.19 – 7.17 (m, 1H), 7.17 – 7.15 (m, 1H), 7.14 – 7.09 (m, 2 H), 7.03 – 7.01 (m, 1H), 6.03 (app dd, J = 2.2, 1.1 Hz, 1H), 2.37 (s, 3H), 2.26 (app t, J = 7.0 Hz, 6H). The analytical data was consistent with the literature.[4]

*2.14 Compound **2-12** (0.56 mmol scale)*

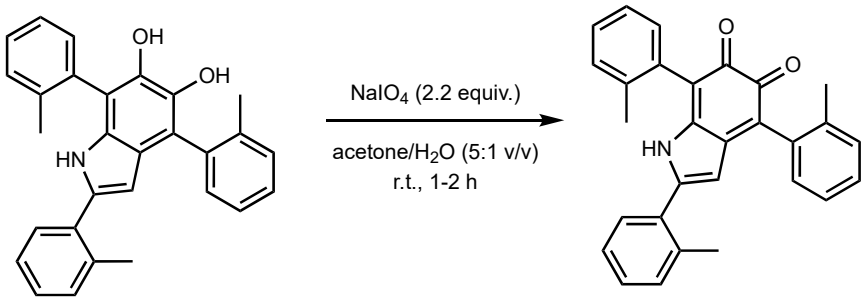

2-11 **2-12**

A round bottom flask equipped with a Teflon-coated stir bar was charged with **2-11** (235 mg, 0.56 mmol, 1.0 equiv.), $NaIO_4$ (263 mg, 1.23 mmol, 2.2 equiv.) and a 5:1 volume to volume mixture of acetone and H_2O (0.05 M). The reaction mixture was stirred at room temperature for 1 – 2 hours until **2-11** was fully consumed as observed by TLC. Upon completion, the reaction was diluted with EtOAc (10 mL/mmol of **2-11**) and washed with water (5 mL/mmol of **2-11**). The organic layer was then collected, dried over sodium sulfate, filtered, and concentrated *in vacuo.* The crude product was purified by silica gel column chromatography (EtOAc/hexanes, 1:9) and

recrystallized from acetone/hexanes to afford the blocked-IQ **2-12** as a green solid (128.6 mg, 0.31 mmol, 55% yield).

Characterization: R_f = (EtOAc/hexanes, 1:1) 0.60; **^{1}H NMR** (800 MHz, d_6-acetone, mixture of atropisomers): δ 8.82 (s, 1H), 7.44 (app dd, J = 7.8, 1.4 Hz, 1H), 7.32 – 7.22 (m, 9H), 7.19 (s, 2H), 5.41 – 5.38 (m, 1H), 2.42 (app s, 3H), 2.30 (app s, 3H), 2.27 (app s, 3H). The analytical data was consistent with the literature.[4]

3. References

1. Leibig, D.; Müller, A. H. E.; Frey, H., Anionic Polymerization of Vinylcatechol Derivatives: Reversal of the Monomer Gradient Directed by the Position of the Catechol Moiety in the Copolymerization with Styrene. *Macromolecules* **2016,** *49* (13), 4792-4801.
2. E. Zembower, D.; Xie, Y.; Koohang, A.; J. Kuffel, M.; M. Ames, M.; Zhou, Y.; Mishra, R.; Aye Mar, A.; T. Flavin, M.; Xu, Z.-Q., Methylenedioxy- and Ethylenedioxy-Fused Indolocarbazoles: Potent Human Topoisomerase I Inhibitors and Antitumor Agents. *Anti-Cancer Agents in Medicinal Chemistry* **2012,** *12* (9), 1117-1131.
3. Batcho, A. D.; Leimgruber, W., Indoles from 2-Methylnitrobenzenes by Condensation with Formamide Acetals Followed by Reduction: 4-Benzyloxyindole. *Org. Synth.* **1985,** *63*, 214.
4. Wang, X.; Kinziabulatova, L.; Bortoli, M.; Manickoth, A.; Barilla, M. A.; Huang, H.; Blancafort, L.; Kohler, B.; Lumb, J.-P. Indole-5, 6-quinones display hallmark properties of eumelanin. *Nat. Chem.* **2023**, *15* (6), 787–793.

Appendix B: NMR Spectroscopic Data

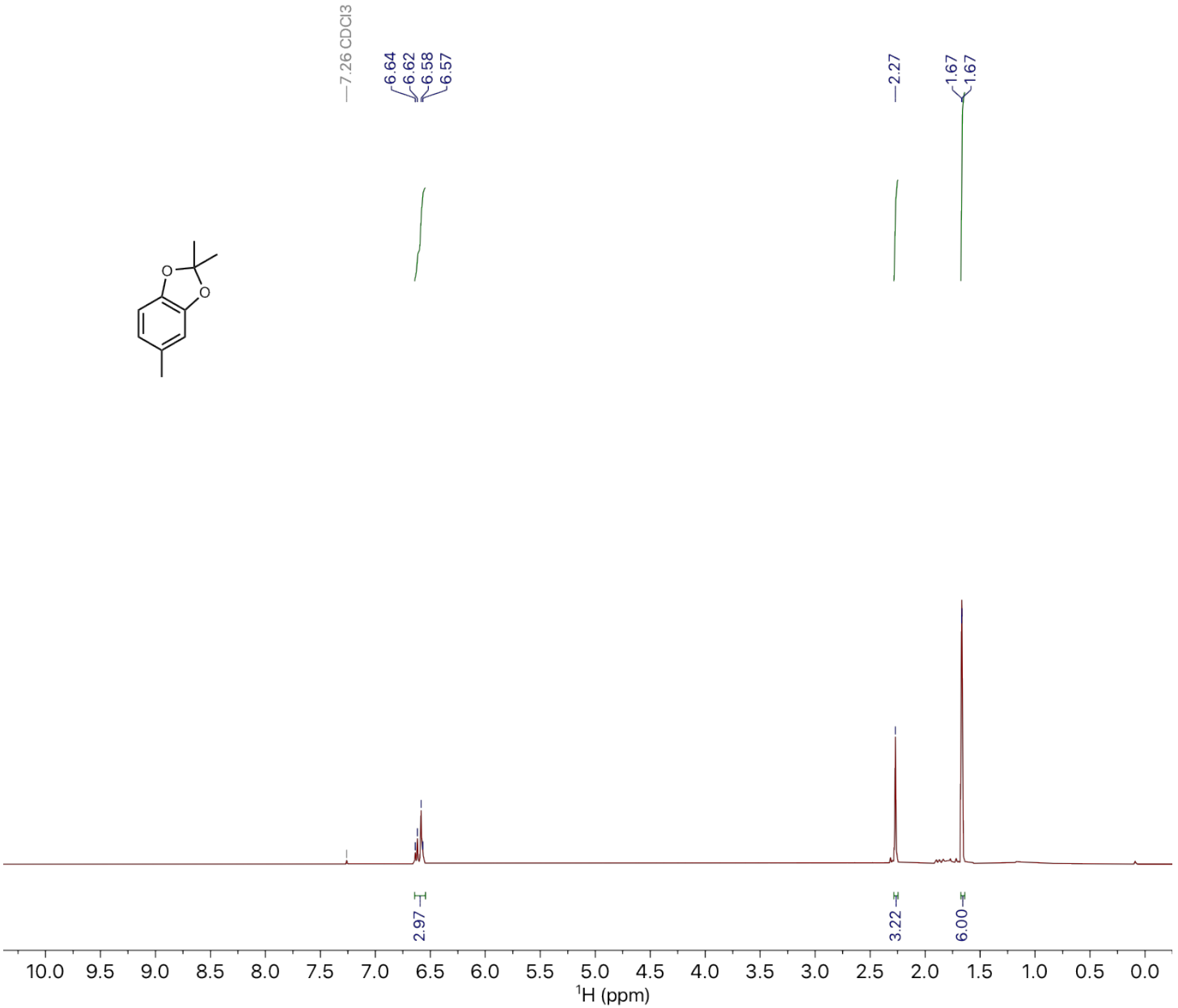
7.26 CDCl3
6.64
6.62
6.58
6.57
2.27
1.67
1.67
2.97
3.22
6.00
10.0 9.5 9.0 8.5 8.0 7.5 7.0 6.5 6.0 5.5 5.0 4.5 4.0 3.5 3.0 2.5 2.0 1.5 1.0 0.5 0.0
¹H (ppm)

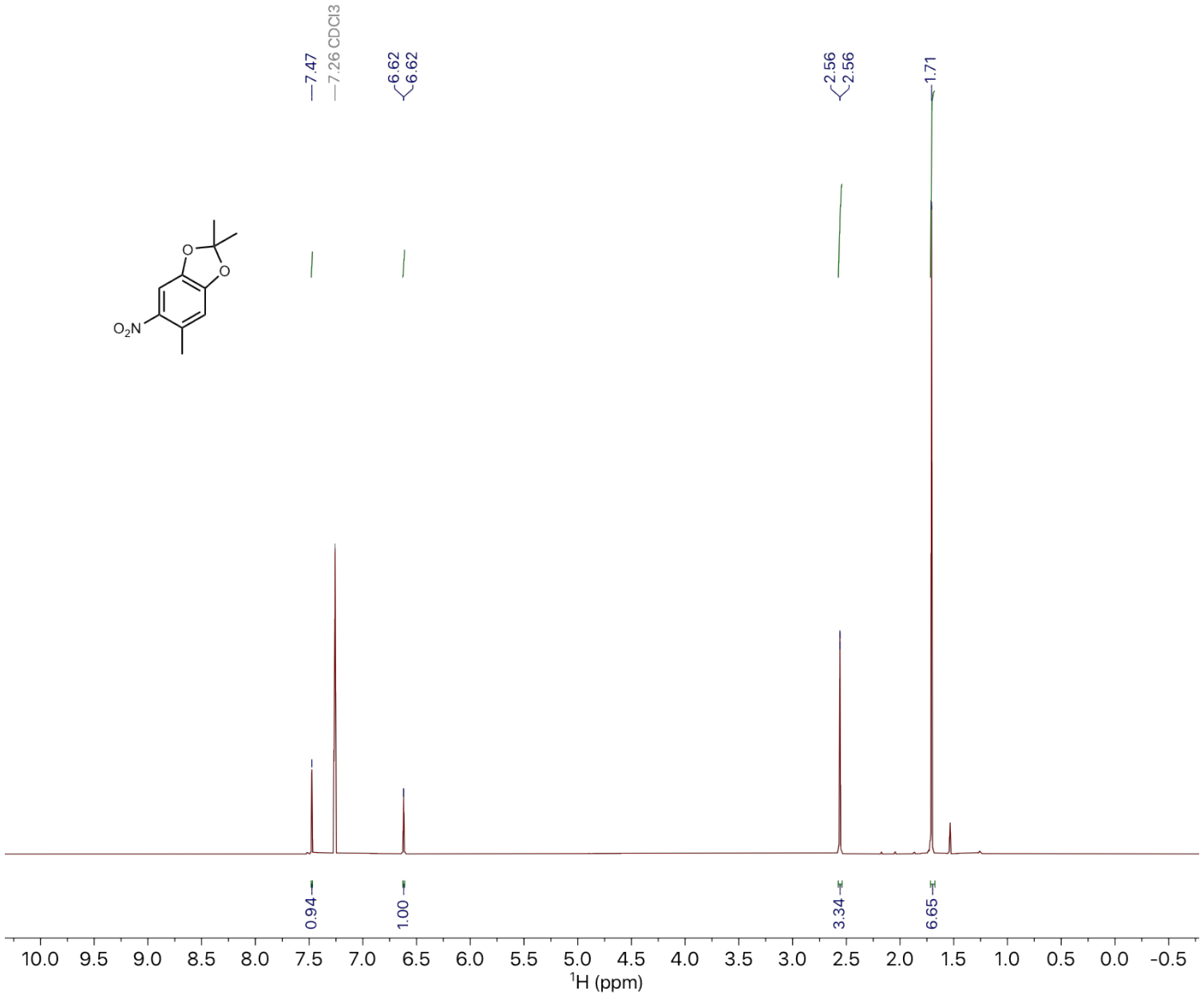
7.47
7.26 CDCl3
6.62
6.62
2.56
2.56
1.71
O2N
0.94
1.00
3.34
6.65
10.0 9.5 9.0 8.5 8.0 7.5 7.0 6.5 6.0 5.5 5.0 4.5 4.0 3.5 3.0 2.5 2.0 1.5 1.0 0.5 0.0 -0.5
1H (ppm)

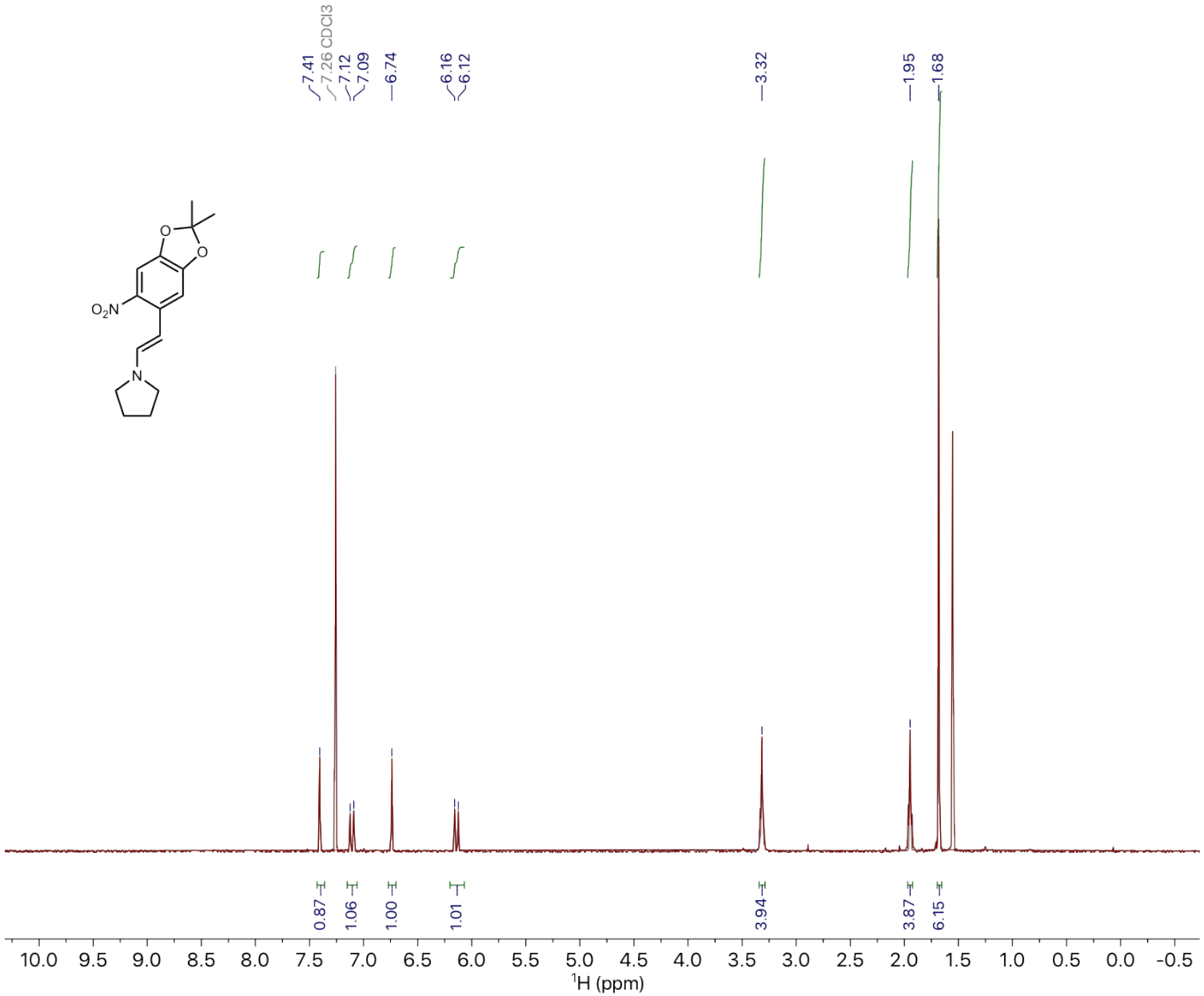
7.41
7.26 CDCl3
7.12
7.09
6.74
6.16
6.12
3.32
1.95
1.68
O2N
0.87
1.06
1.00
1.01
3.94
3.87
6.15
10.0 9.5 9.0 8.5 8.0 7.5 7.0 6.5 6.0 5.5 5.0 4.5 4.0 3.5 3.0 2.5 2.0 1.5 1.0 0.5 0.0 -0.5
1H (ppm)

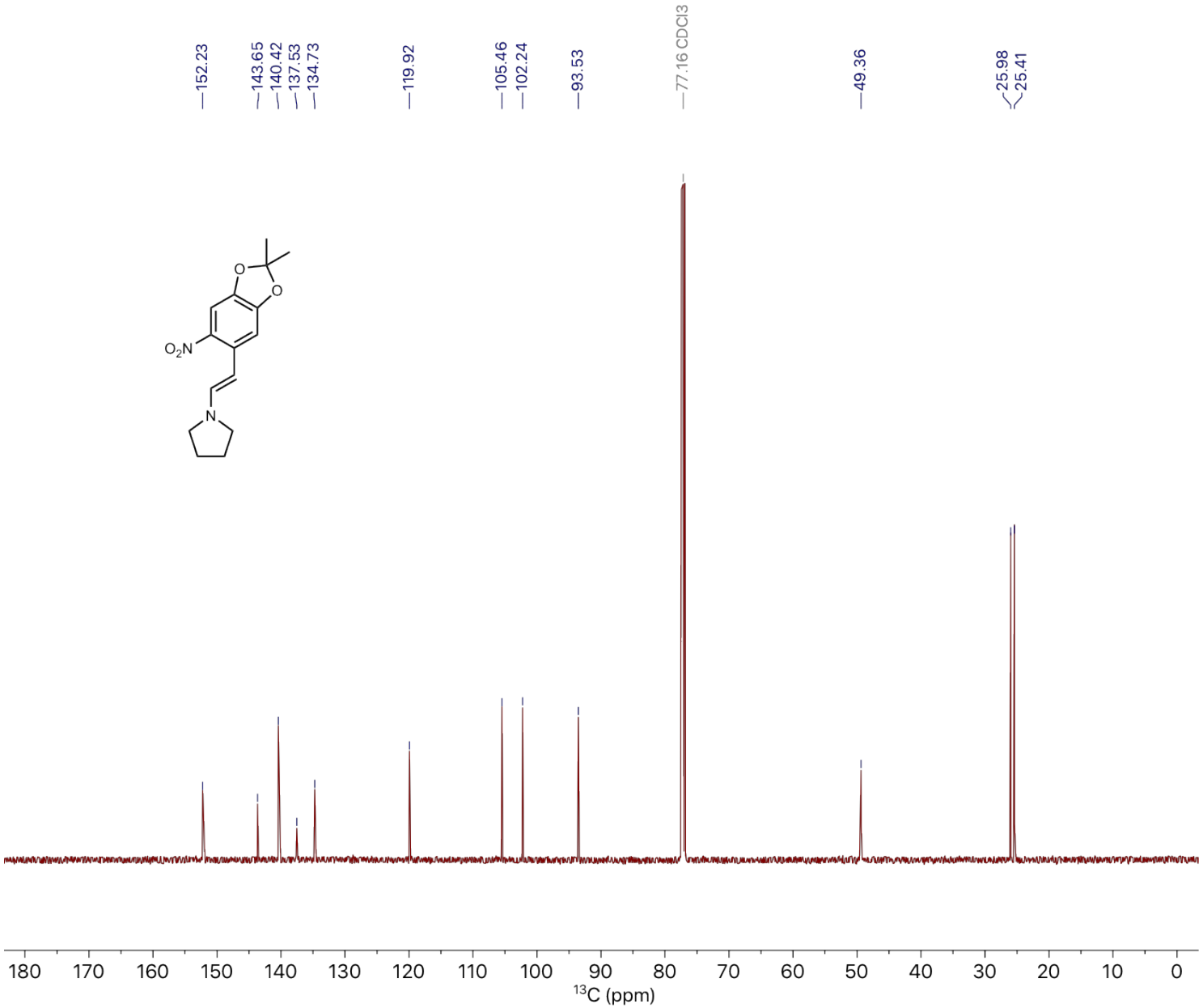
152.23
143.65
140.42
137.53
134.73
119.92
105.46
102.24
93.53
77.16 CDCl3
49.36
25.98
25.41
O
O
O2N
N
180
170
160
150
140
130
120
110
100
90
80
70
60
50
40
30
20
10
0
13C (ppm)

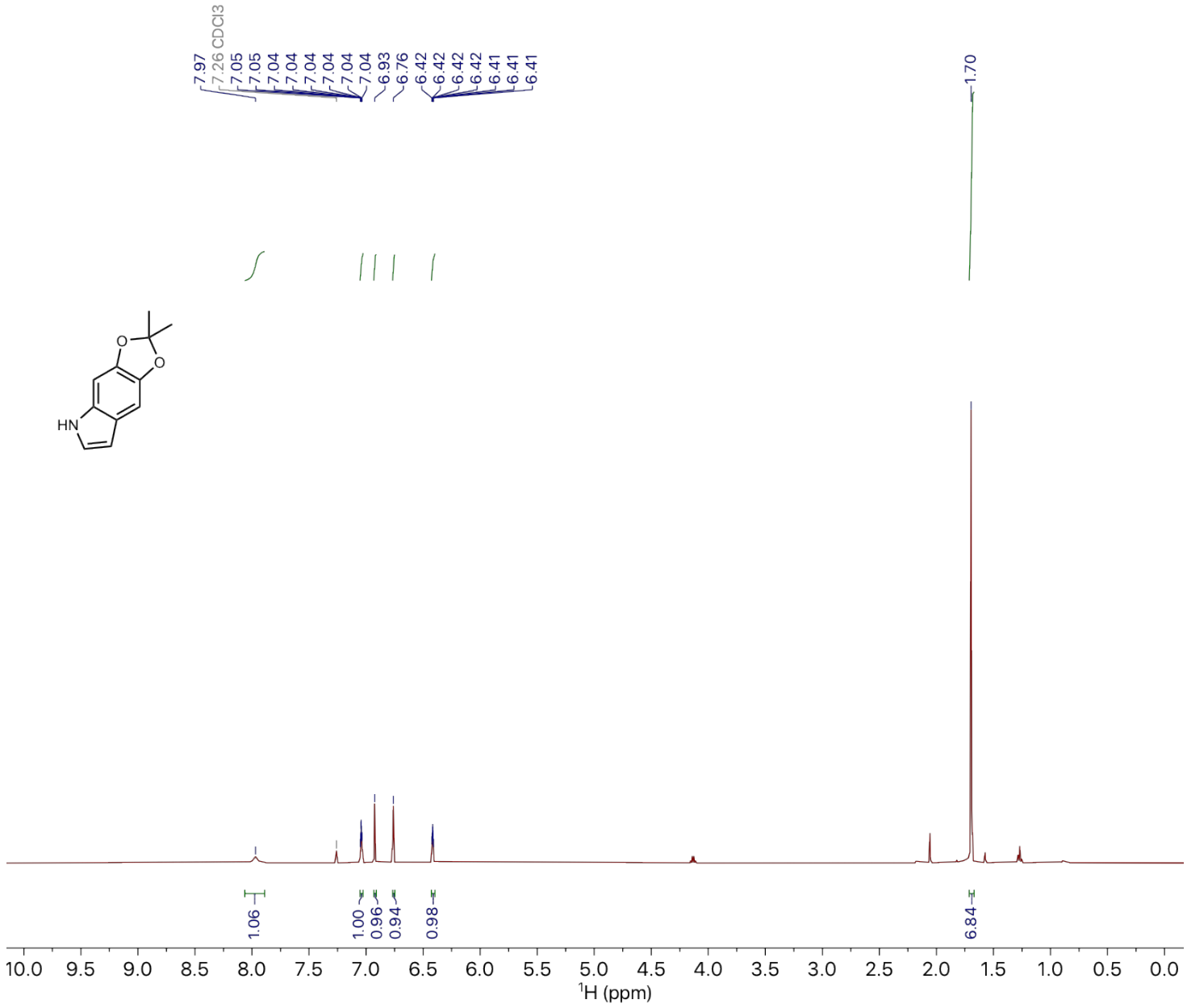
7.97
7.26 CDCl3
7.05
7.05
7.04
7.04
7.04
7.04
7.04
7.04
6.93
6.76
6.42
6.42
6.42
6.42
6.41
6.41
6.41
1.70
HN
O
O
1.06
1.00
0.96
0.94
0.98
6.84
10.0 9.5 9.0 8.5 8.0 7.5 7.0 6.5 6.0 5.5 5.0 4.5 4.0 3.5 3.0 2.5 2.0 1.5 1.0 0.5 0.0
¹H (ppm)

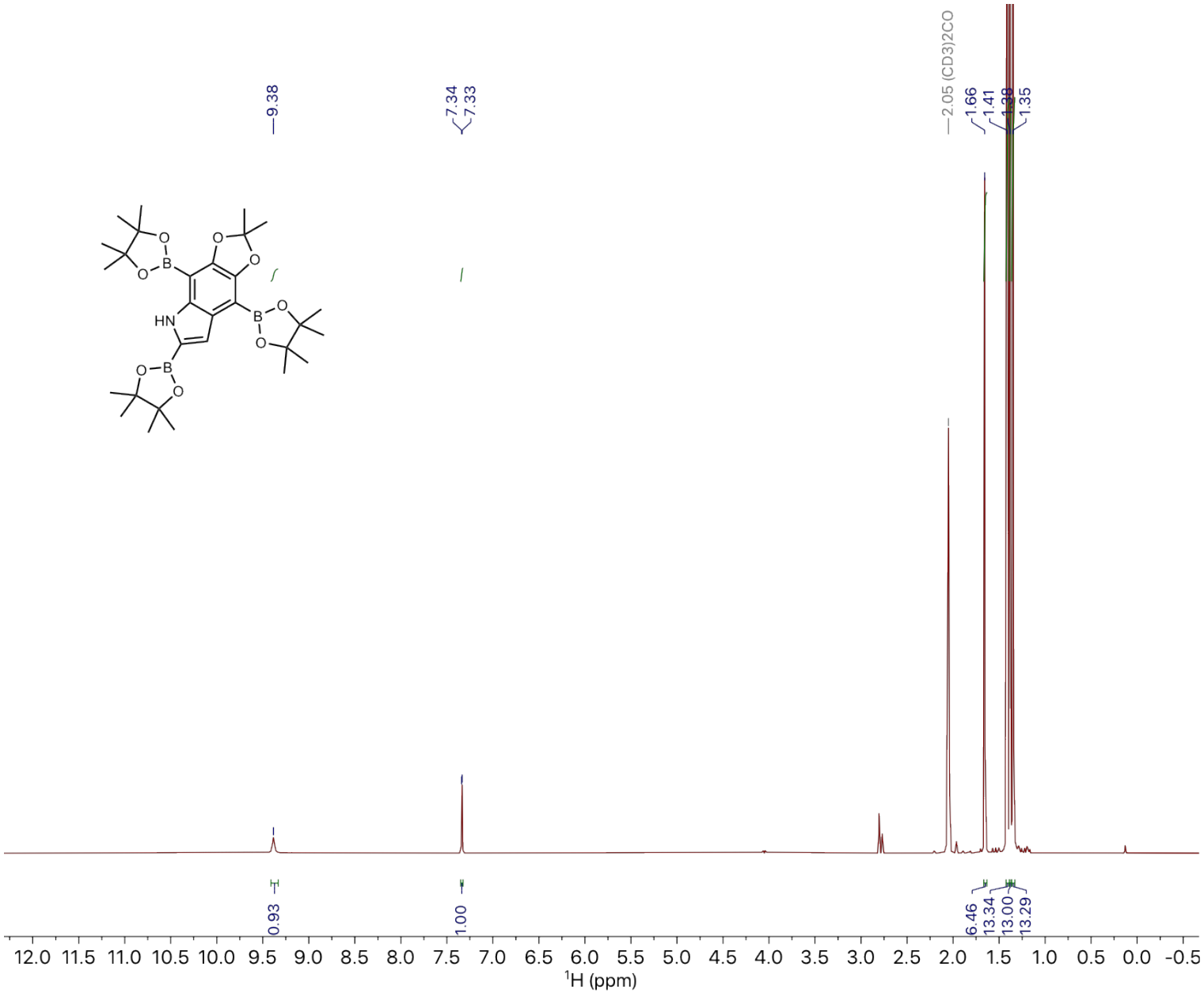
9.38
7.34
7.33
2.05 (CD3)2CO
1.66
1.41
1.39
1.35
HN
B
O
0.93
1.00
6.46
13.34
13.00
13.29
12.0 11.5 11.0 10.5 10.0 9.5 9.0 8.5 8.0 7.5 7.0 6.5 6.0 5.5 5.0 4.5 4.0 3.5 3.0 2.5 2.0 1.5 1.0 0.5 0.0 -0.5
¹H (ppm)

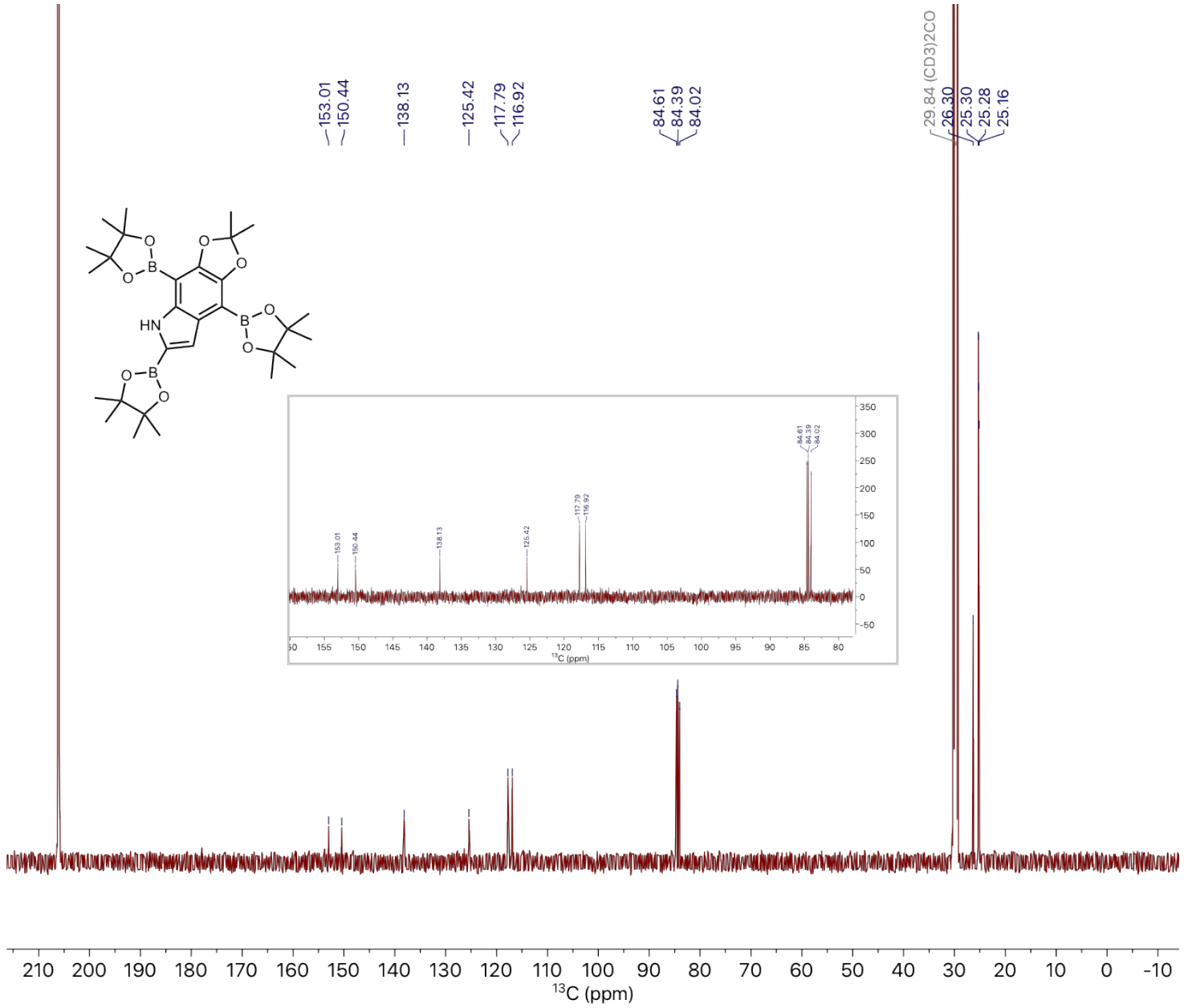
153.01
150.44
138.13
125.42
117.79
116.92
84.61
84.39
84.02
29.84 (CD3)2CO
26.30
25.30
25.28
25.16
HN
B
O
210 200 190 180 170 160 150 140 130 120 110 100 90 80 70 60 50 40 30 20 10 0 -10
13C (ppm)

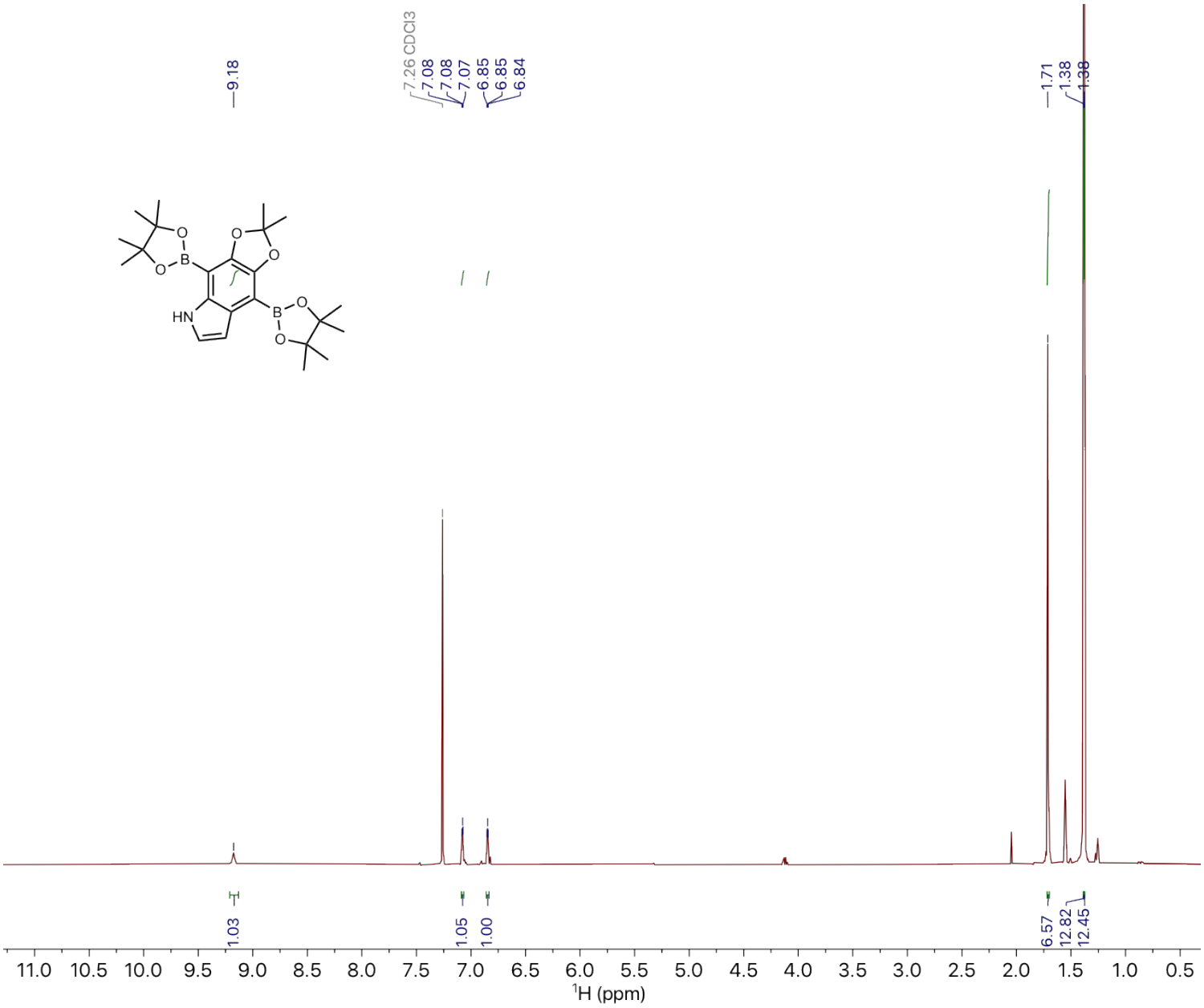
9.18
7.26 CDCl3
7.08
7.08
7.07
6.85
6.85
6.84
1.71
1.38
1.38
HN
1.03
1.05
1.00
6.57
12.82
12.45
11.0 10.5 10.0 9.5 9.0 8.5 8.0 7.5 7.0 6.5 6.0 5.5 5.0 4.5 4.0 3.5 3.0 2.5 2.0 1.5 1.0 0.5
¹H (ppm)

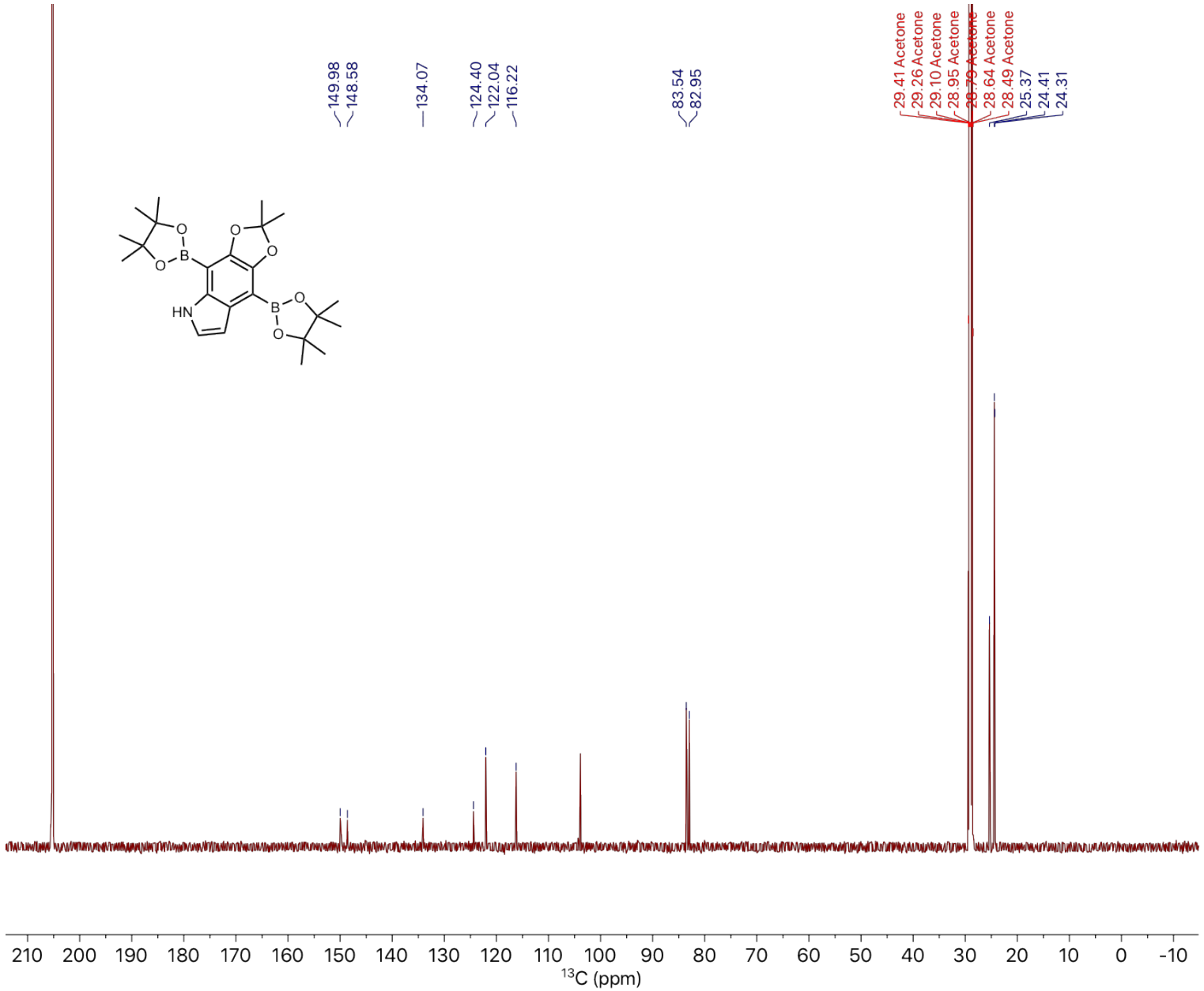
149.98
148.58
134.07
124.40
122.04
116.22
83.54
82.95
29.41 Acetone
29.26 Acetone
29.10 Acetone
28.95 Acetone
28.64 Acetone
28.49 Acetone
25.37
24.41
24.31
HN
B
O
210 200 190 180 170 160 150 140 130 120 110 100 90 80 70 60 50 40 30 20 10 0 -10
13C (ppm)

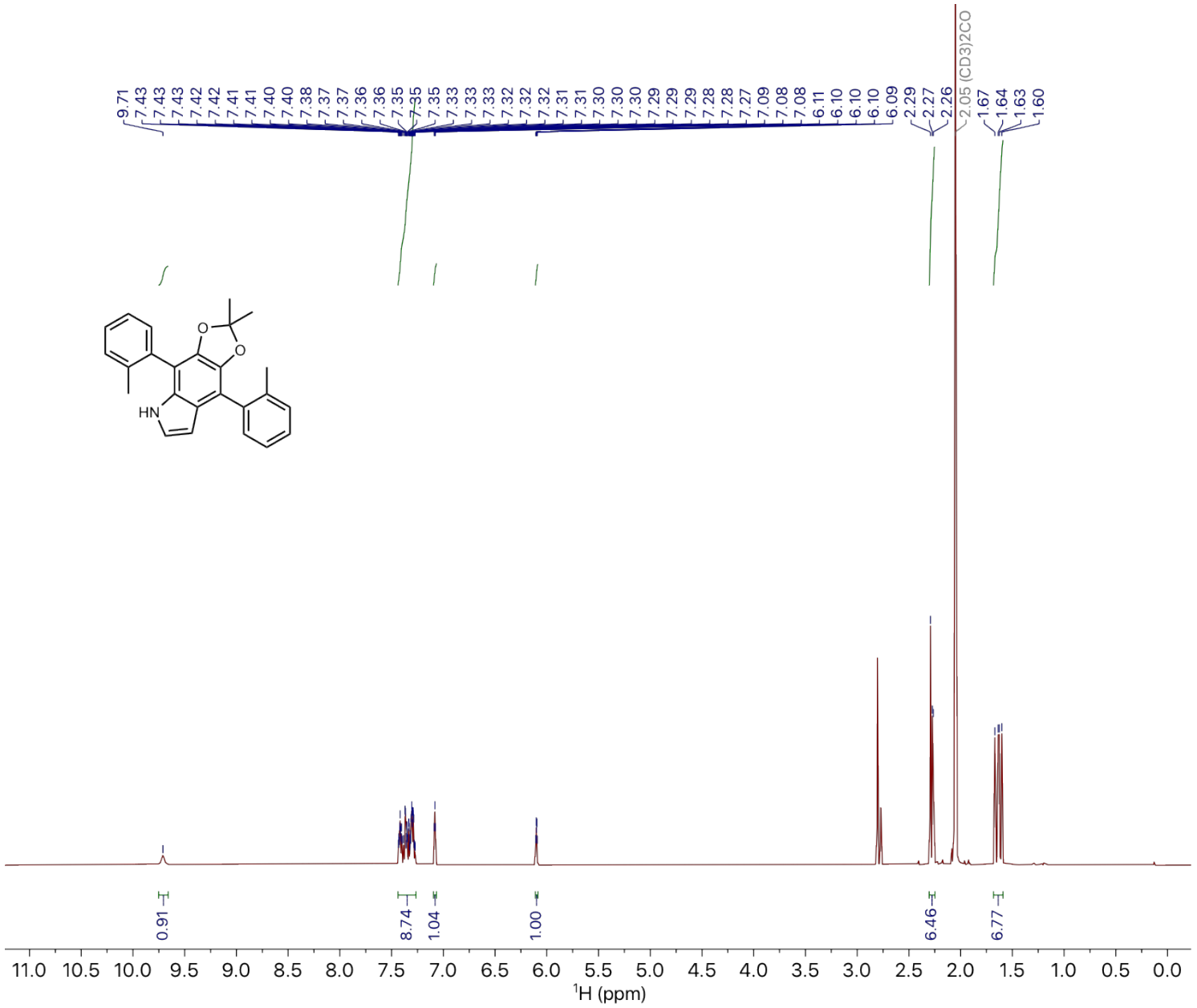
9.71
7.43
7.43
7.43
7.42
7.42
7.41
7.41
7.40
7.40
7.38
7.37
7.37
7.36
7.36
7.35
7.35
7.35
7.33
7.33
7.32
7.32
7.31
7.31
7.30
7.30
7.30
7.29
7.29
7.28
7.28
7.27
7.09
7.08
7.08
6.11
6.10
6.10
6.09
2.29
2.27
2.26
2.05 (CD3)2CO
1.67
1.64
1.63
1.60
O
O
HN
0.91
8.74
1.04
1.00
6.46
6.77
11.0 10.5 10.0 9.5 9.0 8.5 8.0 7.5 7.0 6.5 6.0 5.5 5.0 4.5 4.0 3.5 3.0 2.5 2.0 1.5 1.0 0.5 0.0
¹H (ppm)

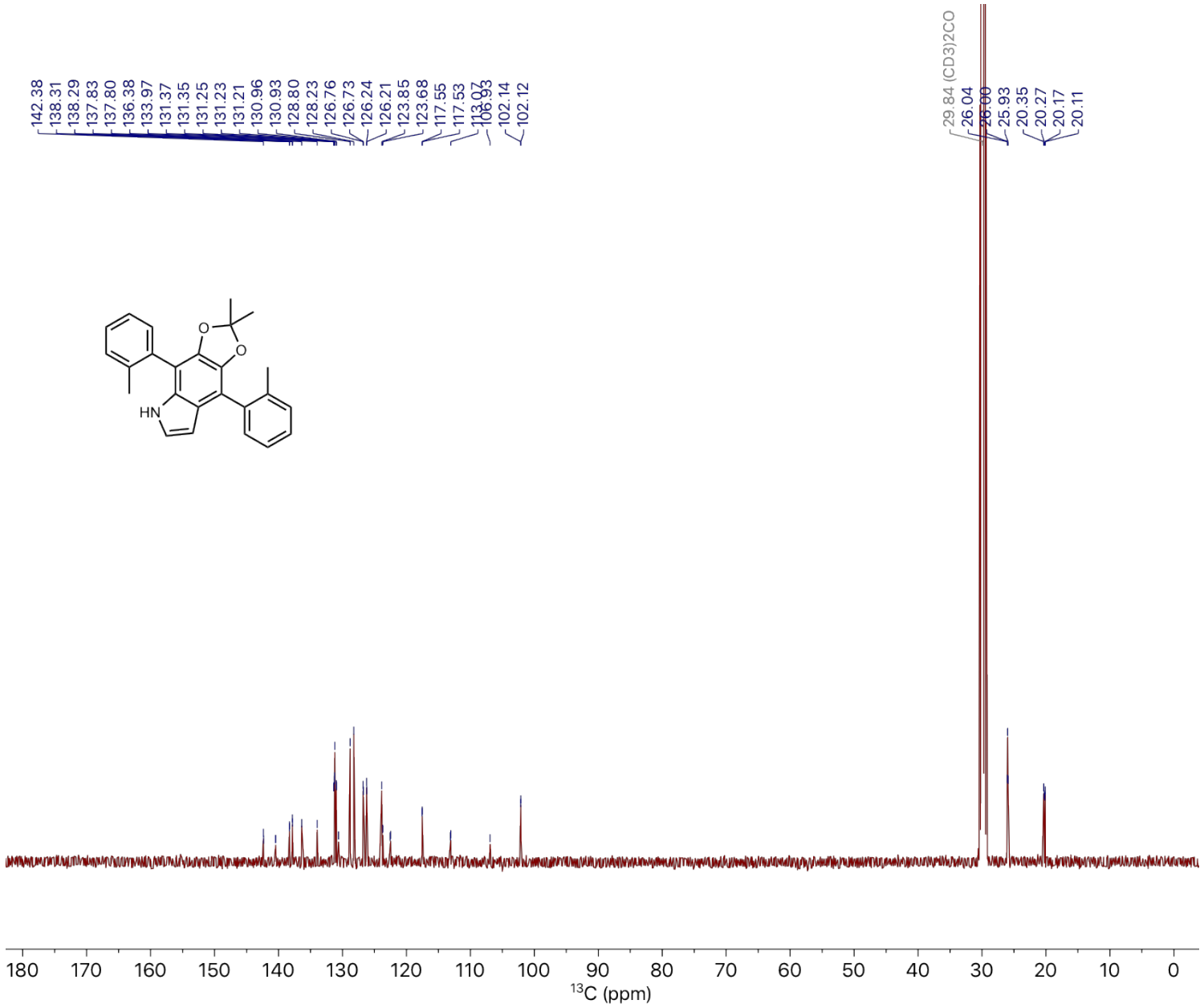
142.38
138.31
138.29
137.83
137.80
136.38
133.97
131.37
131.35
131.25
131.23
131.21
130.96
130.93
128.80
128.23
126.76
126.73
126.24
126.21
123.85
123.68
117.55
117.53
106.93
102.14
102.12
29.84 (CD3)2CO
26.04
26.00
25.93
20.35
20.27
20.17
20.11
O
O
HN
180
170
160
150
140
130
120
110
100
90
80
70
60
50
40
30
20
10
0
13C (ppm)

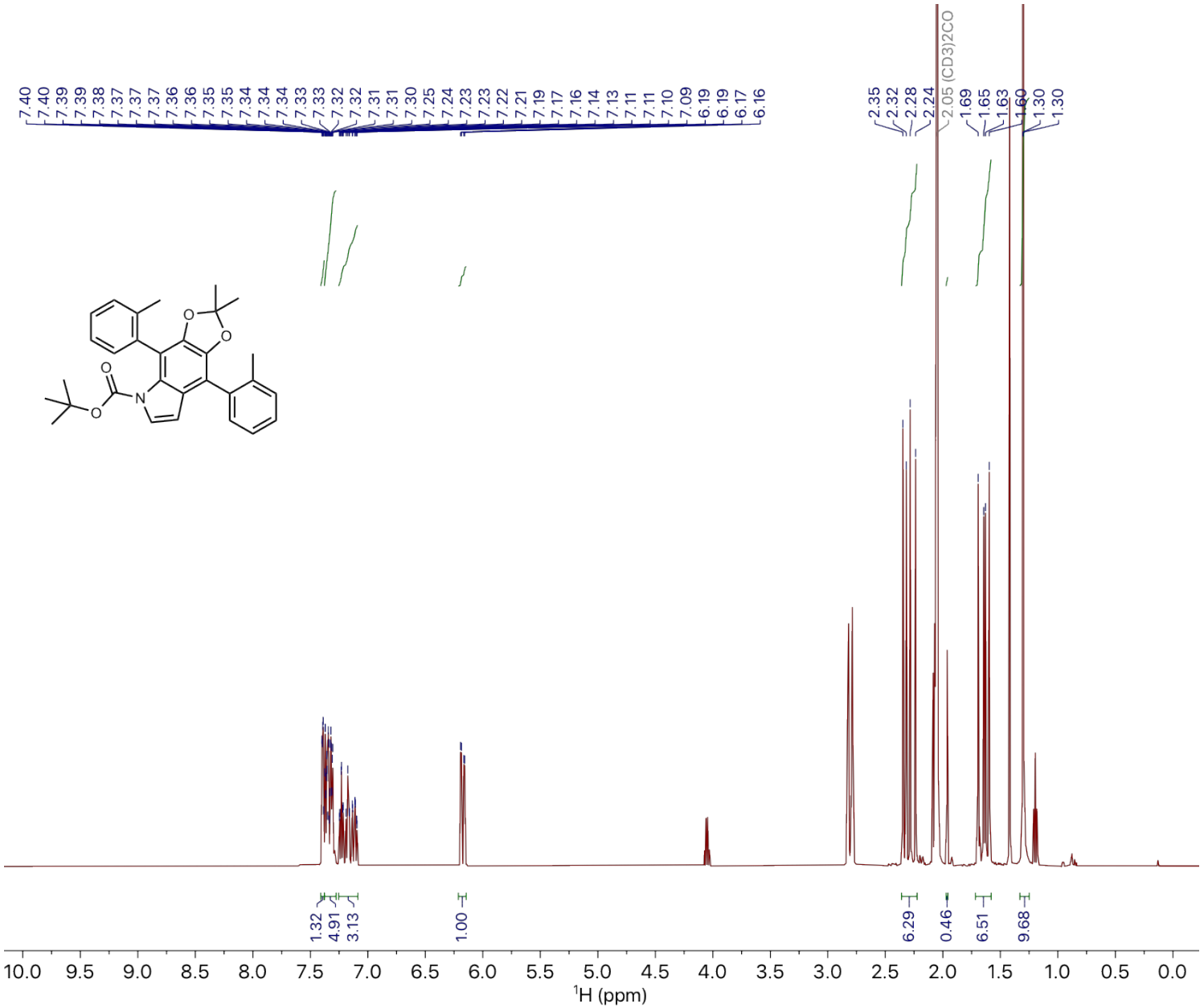
7.40
7.40
7.39
7.39
7.38
7.37
7.37
7.37
7.36
7.36
7.35
7.35
7.34
7.34
7.34
7.33
7.33
7.32
7.32
7.31
7.31
7.30
7.25
7.24
7.23
7.23
7.22
7.21
7.19
7.17
7.16
7.14
7.13
7.11
7.11
7.10
7.09
6.19
6.19
6.17
6.16
2.35
2.32
2.28
2.24
2.05 (CD3)2CO
1.69
1.65
1.63
1.60
1.30
1.30
1.32
4.91
3.13
1.00
6.29
0.46
6.51
9.68
10.0
9.5
9.0
8.5
8.0
7.5
7.0
6.5
6.0
5.5
5.0
4.5
4.0
3.5
3.0
2.5
2.0
1.5
1.0
0.5
0.0
¹H (ppm)

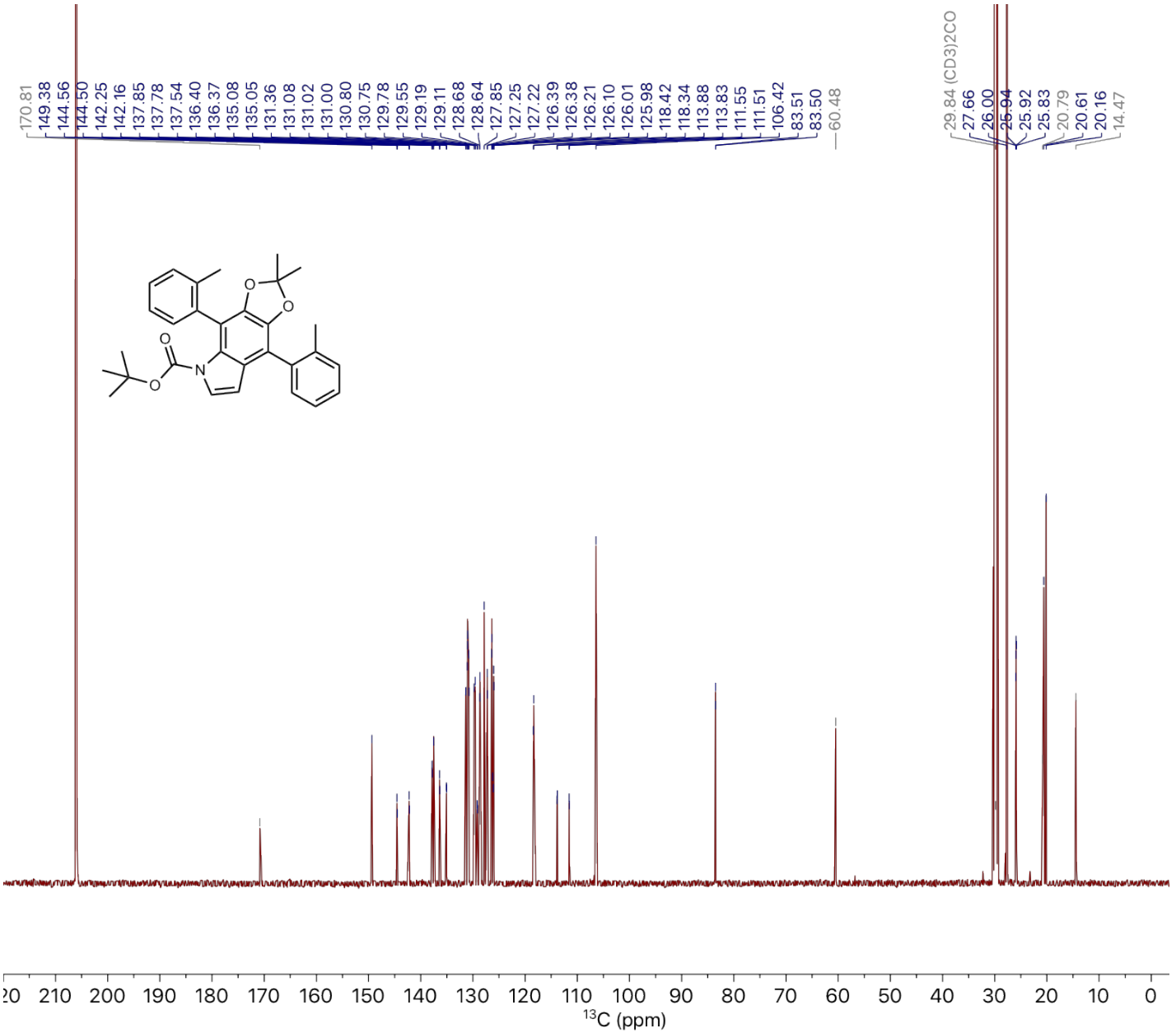
170.81
149.38
144.56
144.50
142.25
142.16
137.85
137.78
137.54
136.40
136.37
135.08
135.05
131.36
131.08
131.02
131.00
130.80
130.75
129.78
129.55
129.19
129.11
128.68
128.64
127.85
127.25
127.22
126.39
126.38
126.21
126.10
126.01
125.98
118.42
118.34
113.88
113.83
111.55
111.51
106.42
83.51
83.50
60.48
29.84 (CD3)2CO
27.66
26.00
25.94
25.92
25.83
20.79
20.61
20.16
14.47
O
O
O
O
N
220 210 200 190 180 170 160 150 140 130 120 110 100 90 80 70 60 50 40 30 20 10 0
13C (ppm)

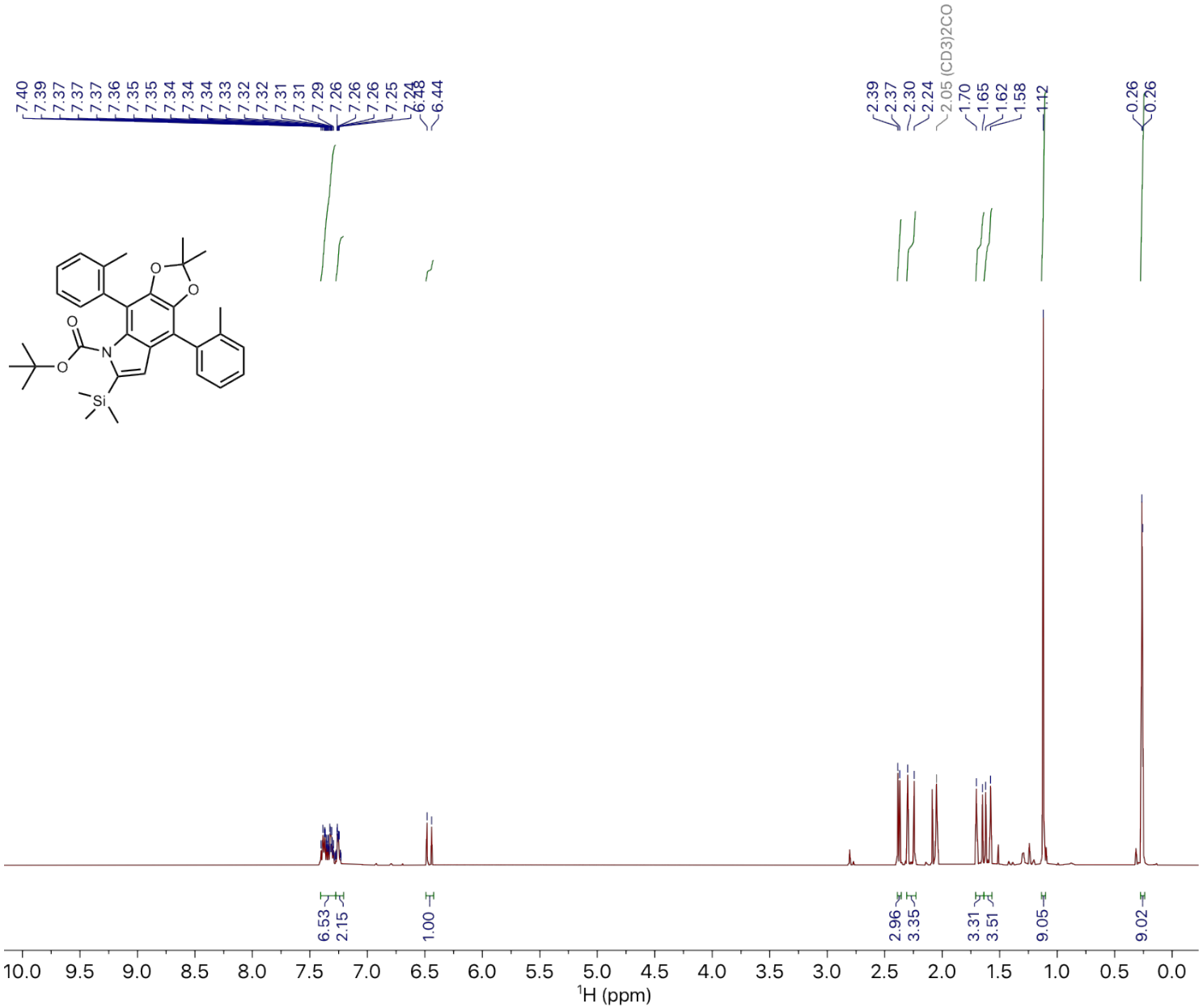
7.40
7.39
7.37
7.37
7.37
7.36
7.35
7.35
7.34
7.34
7.34
7.33
7.32
7.32
7.31
7.31
7.29
7.26
7.26
7.26
7.25
6.48
6.44
2.39
2.37
2.30
2.24
2.05 (CD3)2CO
1.70
1.65
1.62
1.58
1.12
0.26
0.26
O
O
O
O
N
Si
6.53
2.15
1.00
2.96
3.35
3.31
3.51
9.05
9.02
10.0 9.5 9.0 8.5 8.0 7.5 7.0 6.5 6.0 5.5 5.0 4.5 4.0 3.5 3.0 2.5 2.0 1.5 1.0 0.5 0.0
1H (ppm)

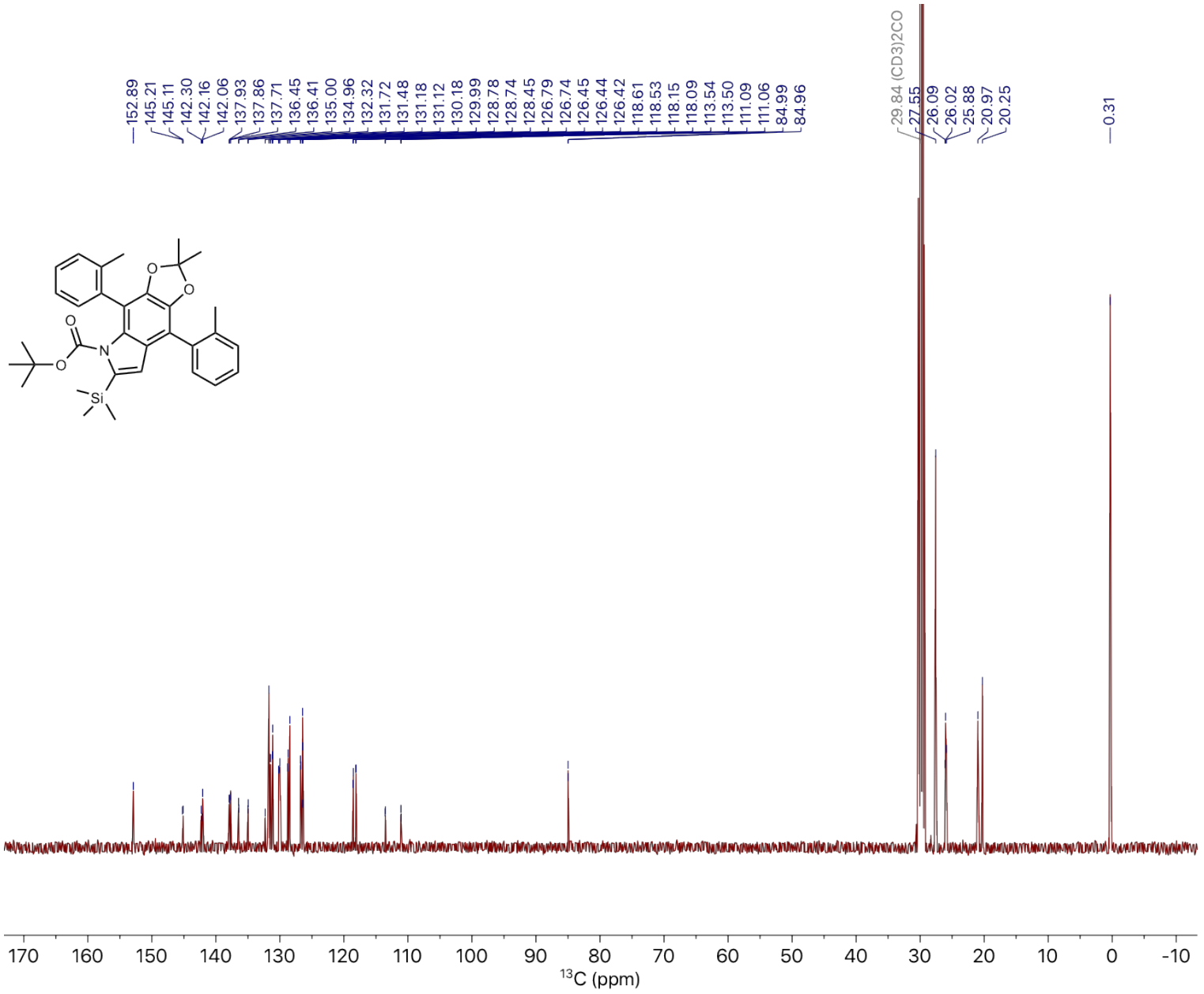
152.89
145.21
145.11
142.30
142.16
142.06
137.93
137.86
137.71
136.45
136.41
135.00
134.96
132.32
131.72
131.48
131.18
131.12
130.18
129.99
128.78
128.74
128.45
126.79
126.74
126.45
126.44
126.42
118.61
118.53
118.15
118.09
113.54
113.50
111.09
111.06
84.99
84.96
29.84 (CD3)2CO
27.55
26.09
26.02
25.88
20.97
20.25
0.31
O
O
O
O
N
Si
170
160
150
140
130
120
110
100
90
80
70
60
50
40
30
20
10
0
-10
13C (ppm)

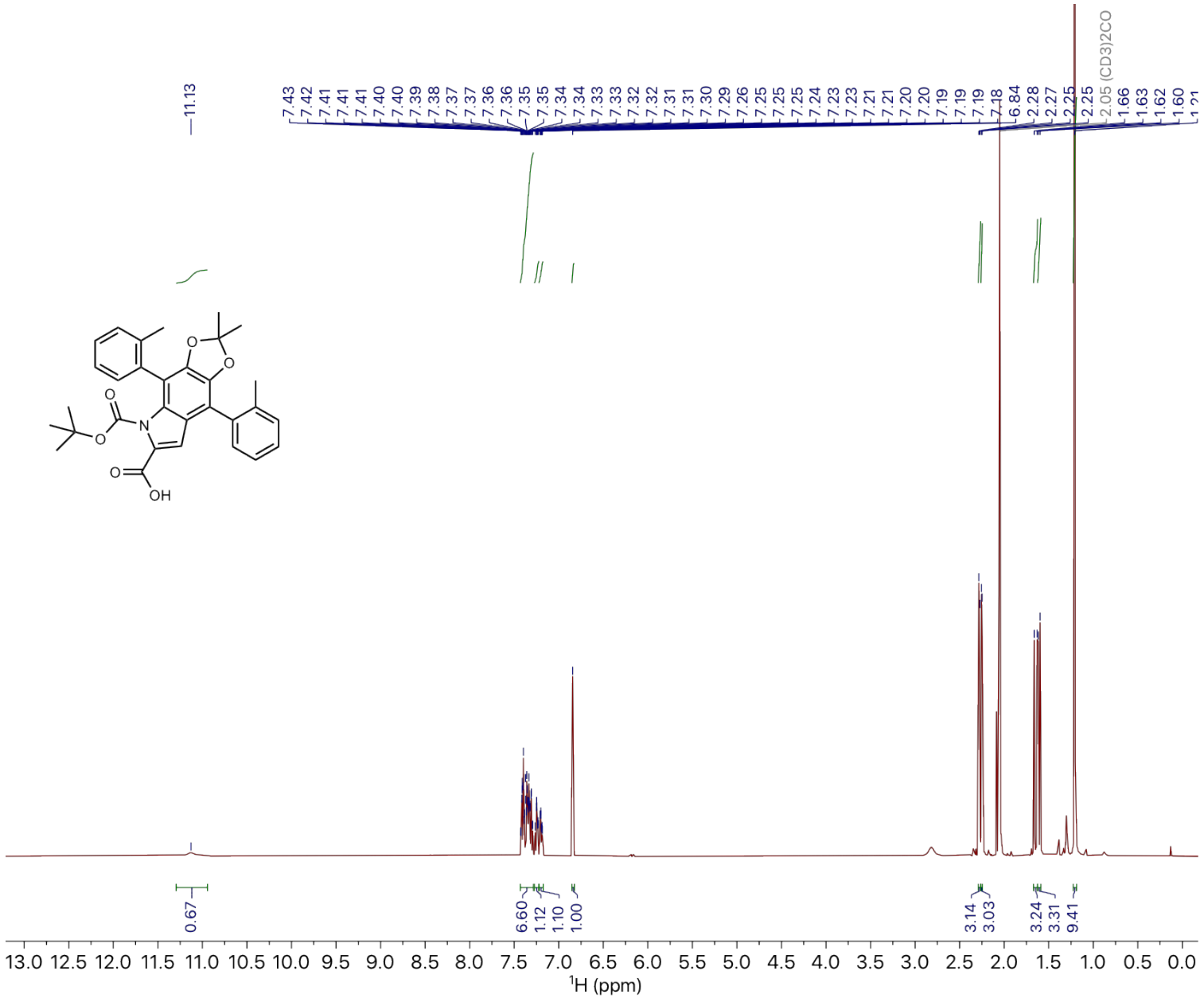
11.13
7.43
7.42
7.41
7.41
7.41
7.40
7.40
7.39
7.38
7.37
7.37
7.36
7.36
7.35
7.35
7.34
7.34
7.33
7.33
7.32
7.32
7.31
7.31
7.30
7.29
7.26
7.25
7.25
7.25
7.24
7.23
7.23
7.21
7.21
7.20
7.20
7.19
7.19
7.19
7.18
6.84
2.28
2.27
2.25
2.25
2.05 (CD3)2CO
1.66
1.63
1.62
1.60
O
O
O
O
N
O
O
OH
0.67
6.60
1.12
1.10
1.00
3.14
3.03
3.24
3.31
9.41
13.0 12.5 12.0 11.5 11.0 10.5 10.0 9.5 9.0 8.5 8.0 7.5 7.0 6.5 6.0 5.5 5.0 4.5 4.0 3.5 3.0 2.5 2.0 1.5 1.0 0.5 0.0
¹H (ppm)

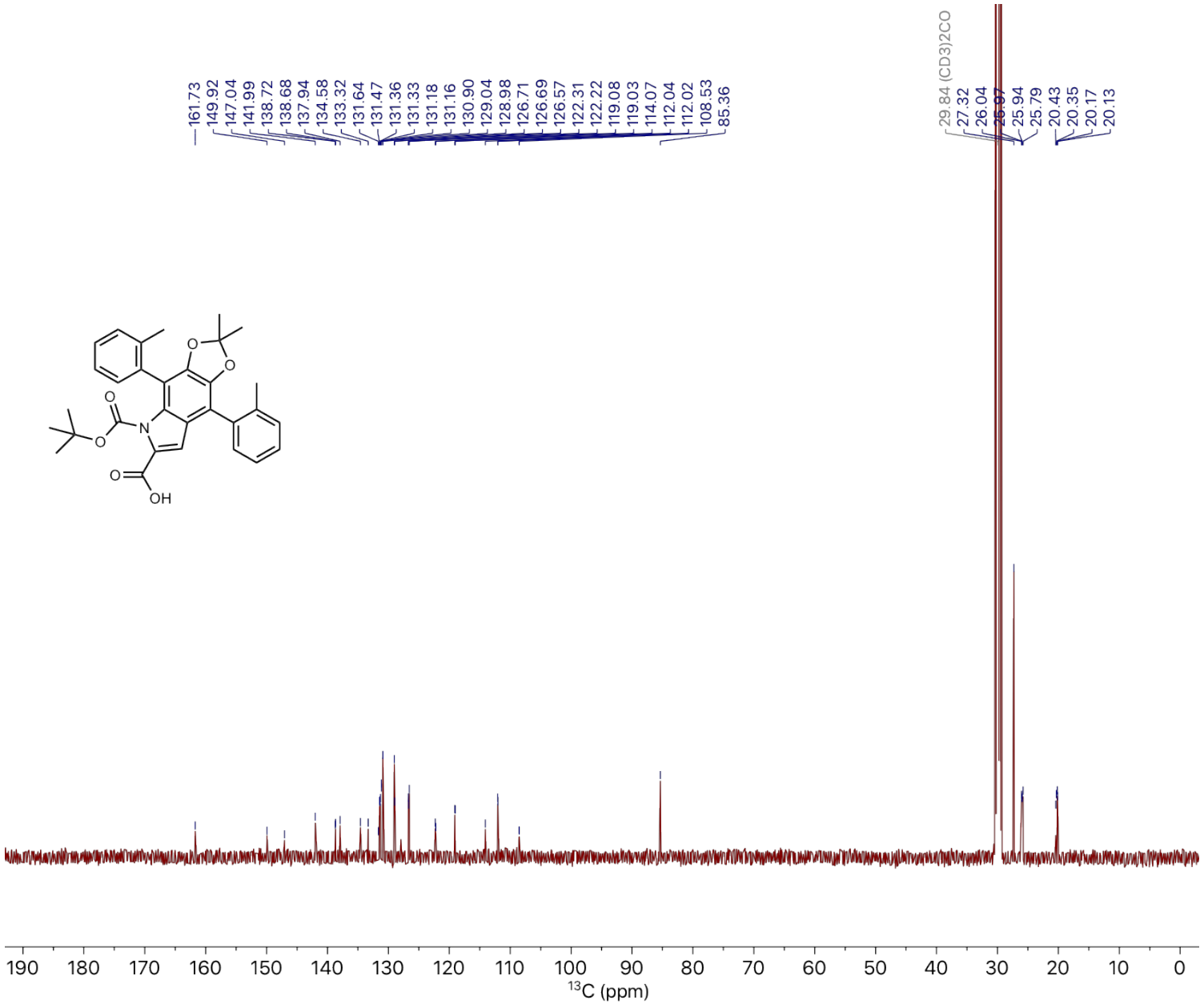
161.73
149.92
147.04
141.99
138.72
138.68
137.94
134.58
133.32
131.64
131.47
131.36
131.33
131.18
131.16
130.90
129.04
128.98
126.71
126.69
126.57
122.31
122.22
119.08
119.03
114.07
112.04
112.02
108.53
85.36
29.84 (CD3)2CO
27.32
26.04
25.97
25.94
25.79
20.43
20.35
20.17
20.13
O
O
O
O
N
O
O
OH
190
180
170
160
150
140
130
120
110
100
90
80
70
60
50
40
30
20
10
0
13C (ppm)

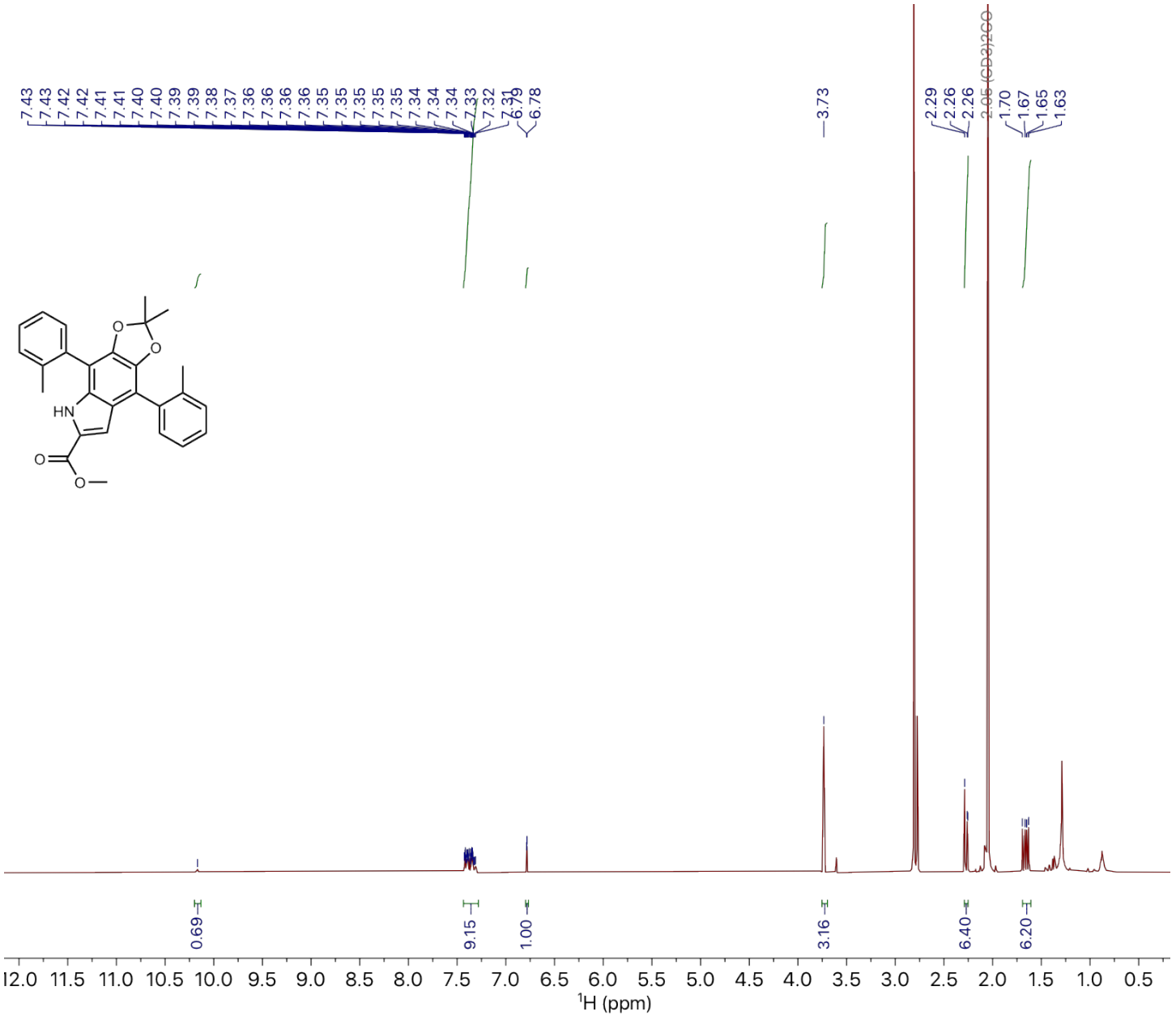
7.43
7.43
7.42
7.42
7.41
7.41
7.40
7.40
7.39
7.39
7.38
7.37
7.36
7.36
7.36
7.36
7.35
7.35
7.35
7.35
7.35
7.34
7.34
7.34
7.33
7.32
7.31
6.79
6.78
3.73
2.29
2.26
2.26
2.05 (CD3)2CO
1.70
1.67
1.65
1.63
HN
O
O
O
O
0.69
9.15
1.00
3.16
6.40
6.20
12.0 11.5 11.0 10.5 10.0 9.5 9.0 8.5 8.0 7.5 7.0 6.5 6.0 5.5 5.0 4.5 4.0 3.5 3.0 2.5 2.0 1.5 1.0 0.5
¹H (ppm)

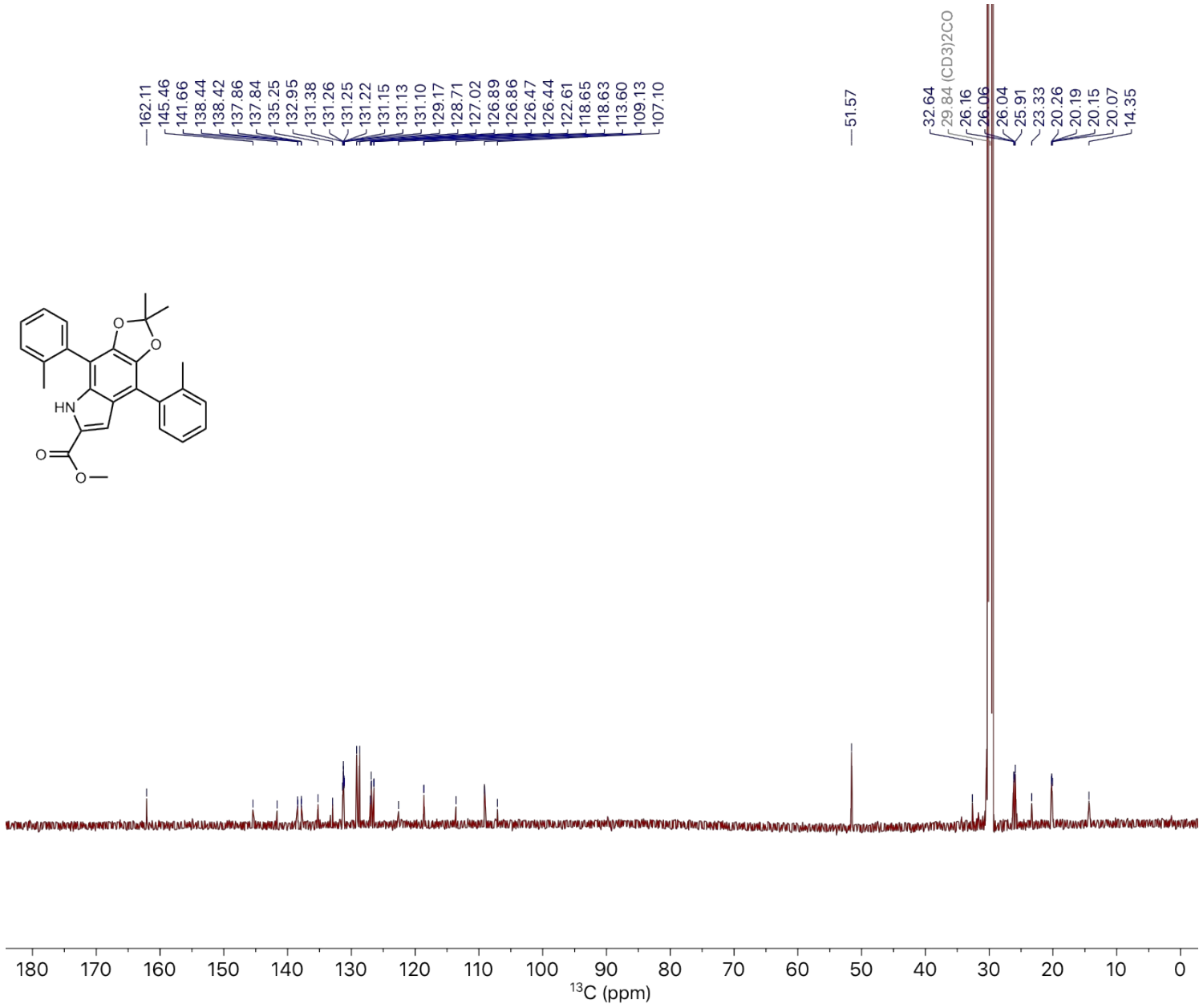
162.11
145.46
141.66
138.44
138.42
137.86
137.84
135.25
132.95
131.38
131.26
131.25
131.22
131.15
131.13
131.10
129.17
128.71
127.02
126.89
126.86
126.47
126.44
122.61
118.65
118.63
113.60
109.13
107.10
51.57
32.64
29.84 (CD3)2CO
26.16
26.06
26.04
25.91
23.33
20.26
20.19
20.15
20.07
14.35
HN
O
O
O
O
180
170
160
150
140
130
120
110
100
90
80
70
60
50
40
30
20
10
0
13C (ppm)

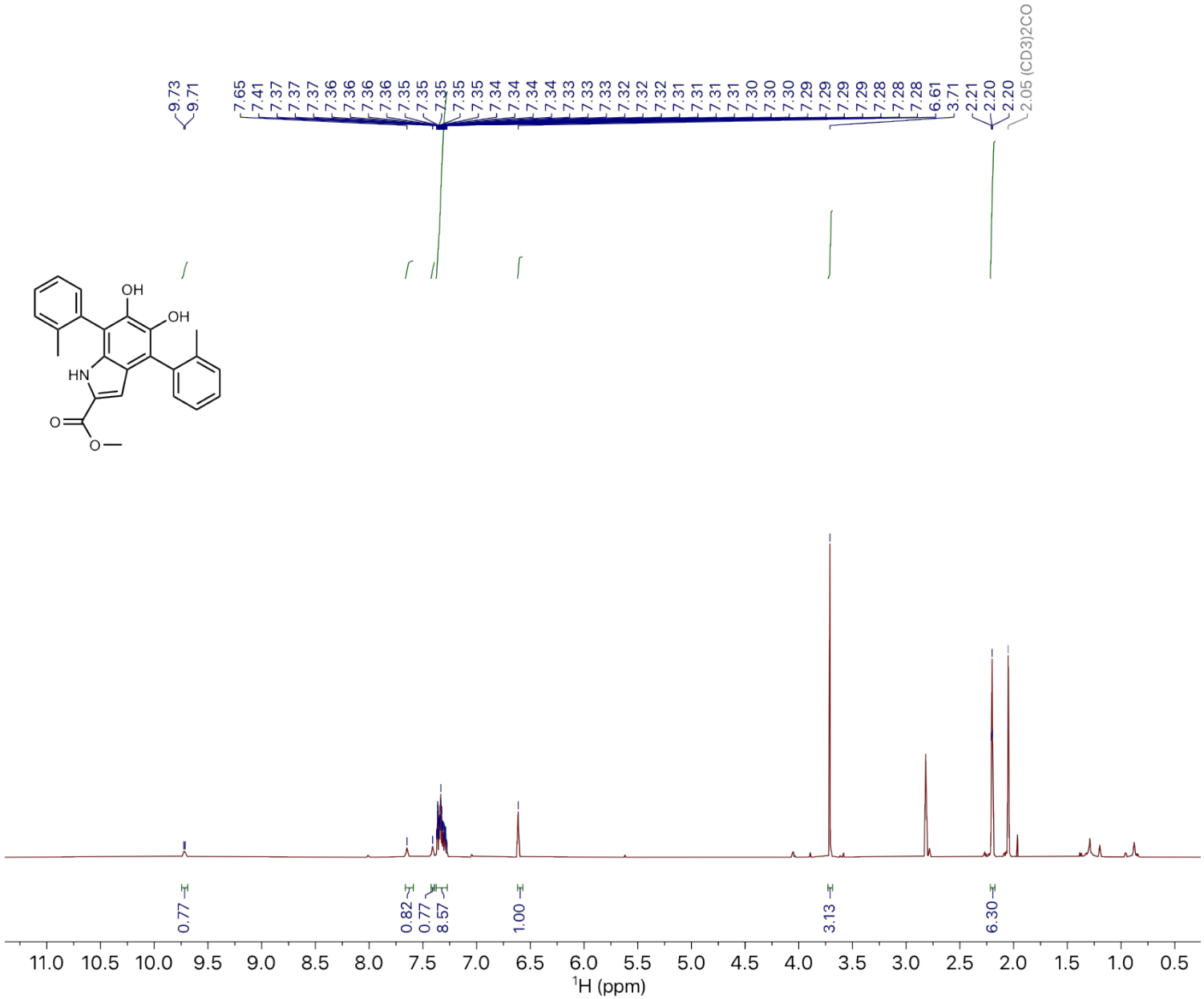
9.73
9.71
7.65
7.41
7.37
7.37
7.37
7.36
7.36
7.36
7.35
7.35
7.35
7.35
7.34
7.34
7.34
7.34
7.33
7.33
7.32
7.32
7.31
7.31
7.31
7.31
7.30
7.30
7.29
7.29
7.29
7.28
7.28
7.28
6.61
3.71
2.21
2.20
2.20
2.05 (CD3)2CO
OH
OH
HN
O
O
0.77
0.82
0.77
8.57
1.00
3.13
6.30
11.0 10.5 10.0 9.5 9.0 8.5 8.0 7.5 7.0 6.5 6.0 5.5 5.0 4.5 4.0 3.5 3.0 2.5 2.0 1.5 1.0 0.5
^{1}H (ppm)

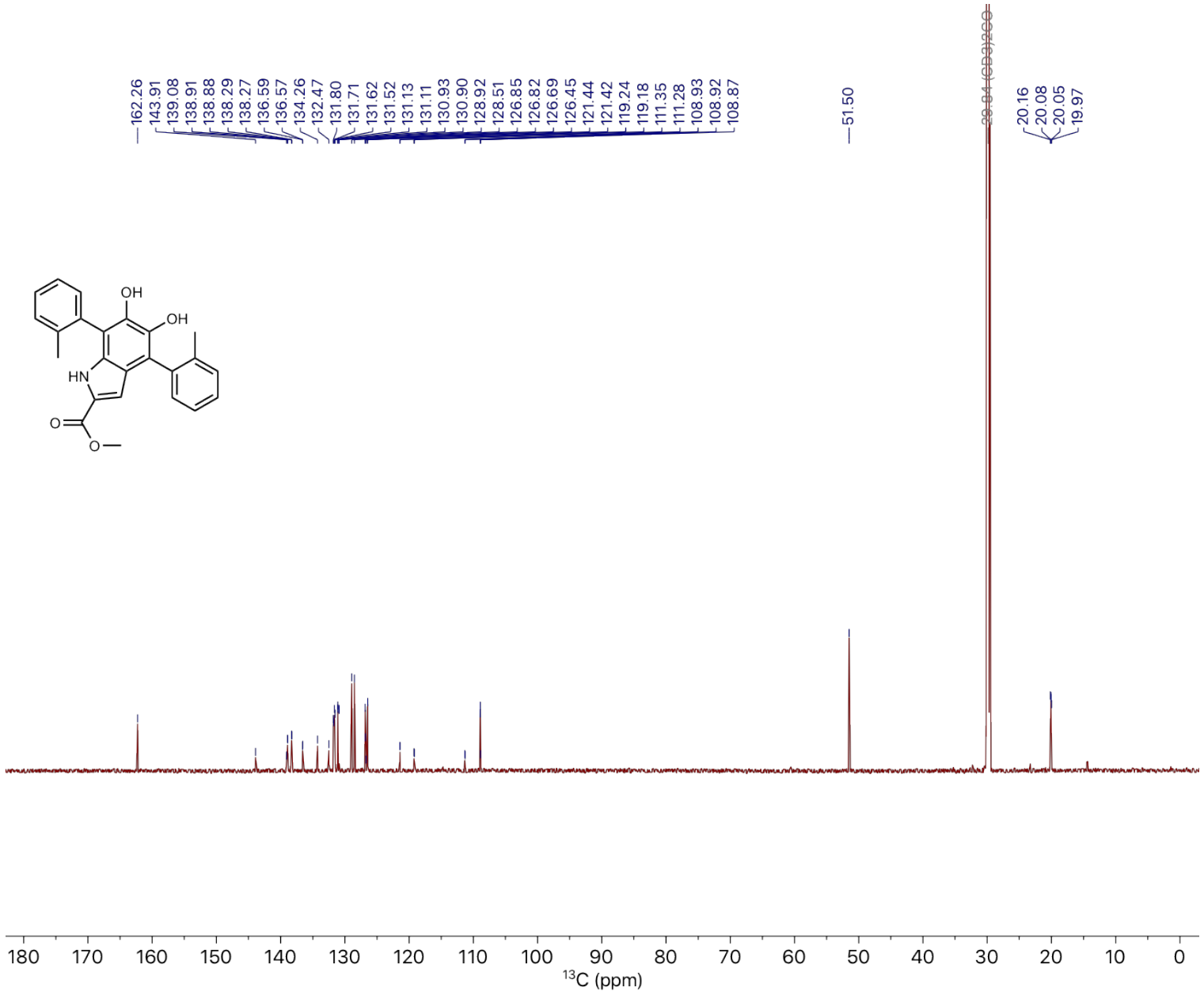
162.26
143.91
139.08
138.91
138.88
138.29
138.27
136.59
136.57
134.26
132.47
131.80
131.71
131.62
131.52
131.13
131.11
130.93
130.90
128.92
128.51
126.85
126.82
126.69
126.45
121.44
121.42
119.24
119.18
111.35
111.28
108.93
108.92
108.87
51.50
20.16
20.08
20.05
19.97
OH
OH
HN
O
O
180
170
160
150
140
130
120
110
100
90
80
70
60
50
40
30
20
10
0
13C (ppm)

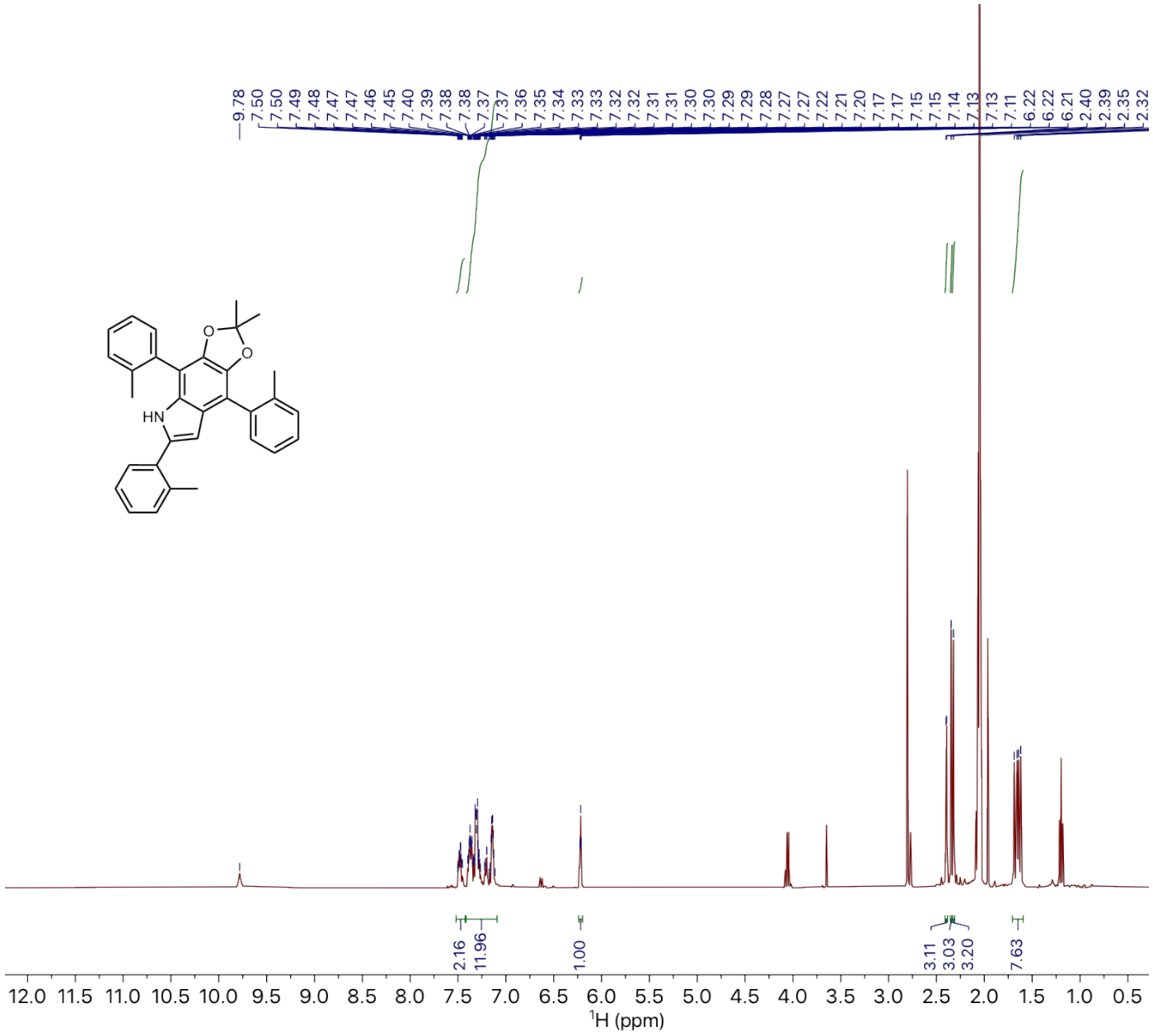
9.78
7.50
7.50
7.49
7.48
7.47
7.47
7.46
7.45
7.40
7.39
7.38
7.38
7.37
7.37
7.36
7.35
7.34
7.33
7.33
7.32
7.32
7.31
7.31
7.30
7.30
7.29
7.29
7.28
7.27
7.27
7.22
7.21
7.20
7.17
7.17
7.15
7.15
7.14
7.13
7.13
7.11
6.22
6.21
2.40
2.39
2.35
2.32
O
O
HN
2.16
11.96
1.00
3.11
3.03
3.20
7.63
12.0 11.5 11.0 10.5 10.0 9.5 9.0 8.5 8.0 7.5 7.0 6.5 6.0 5.5 5.0 4.5 4.0 3.5 3.0 2.5 2.0 1.5 1.0 0.5
^{1}H (ppm)

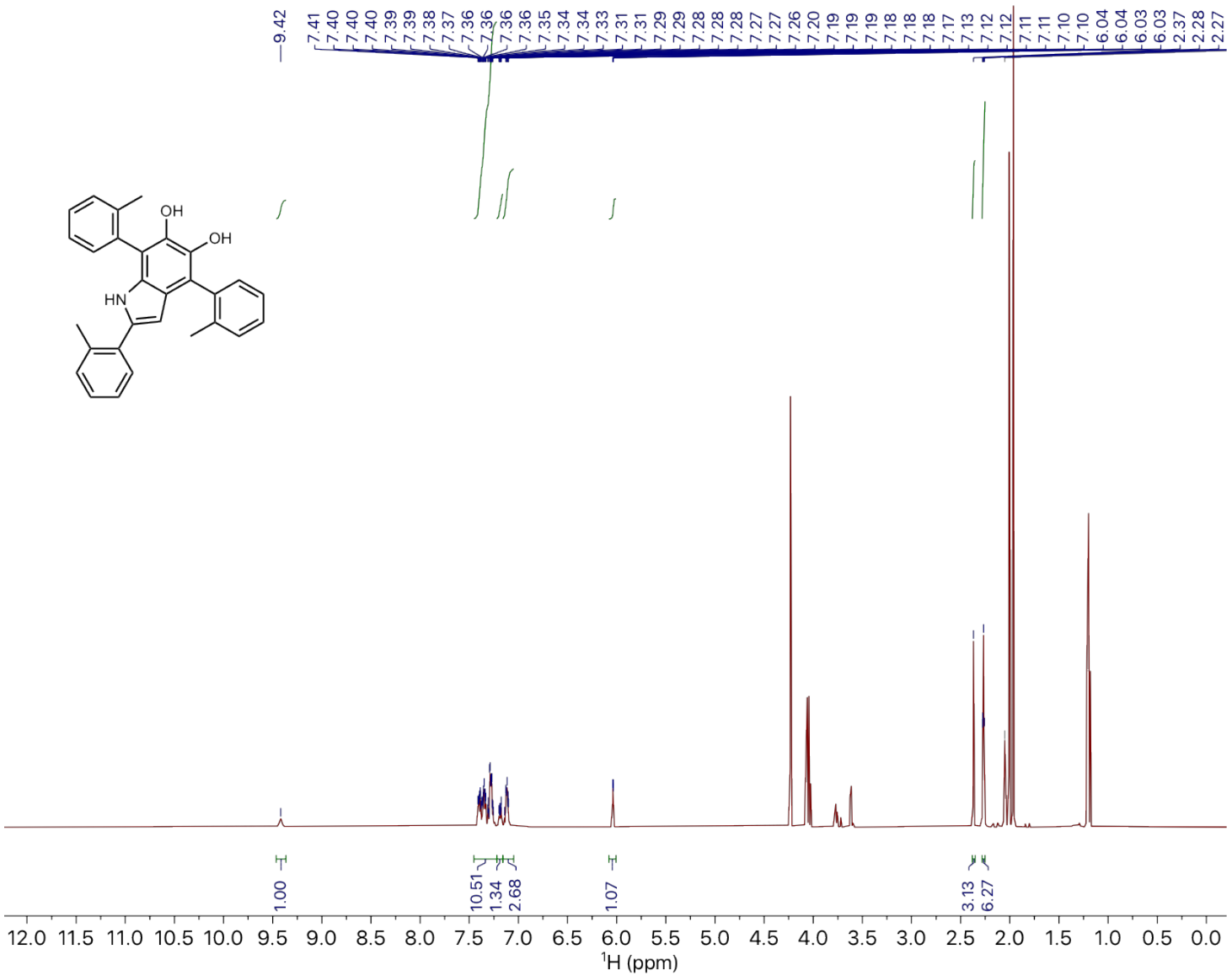
OH
OH
HN
9.42
7.41
7.40
7.40
7.40
7.39
7.39
7.38
7.37
7.36
7.36
7.36
7.35
7.34
7.34
7.33
7.31
7.31
7.29
7.29
7.28
7.28
7.28
7.27
7.27
7.26
7.20
7.19
7.19
7.19
7.18
7.18
7.18
7.17
7.13
7.12
7.12
7.11
7.11
7.10
7.10
6.04
6.04
6.03
6.03
2.37
2.28
2.27
1.00
10.51
1.34
2.68
1.07
3.13
6.27
12.0 11.5 11.0 10.5 10.0 9.5 9.0 8.5 8.0 7.5 7.0 6.5 6.0 5.5 5.0 4.5 4.0 3.5 3.0 2.5 2.0 1.5 1.0 0.5 0.0
¹H (ppm)

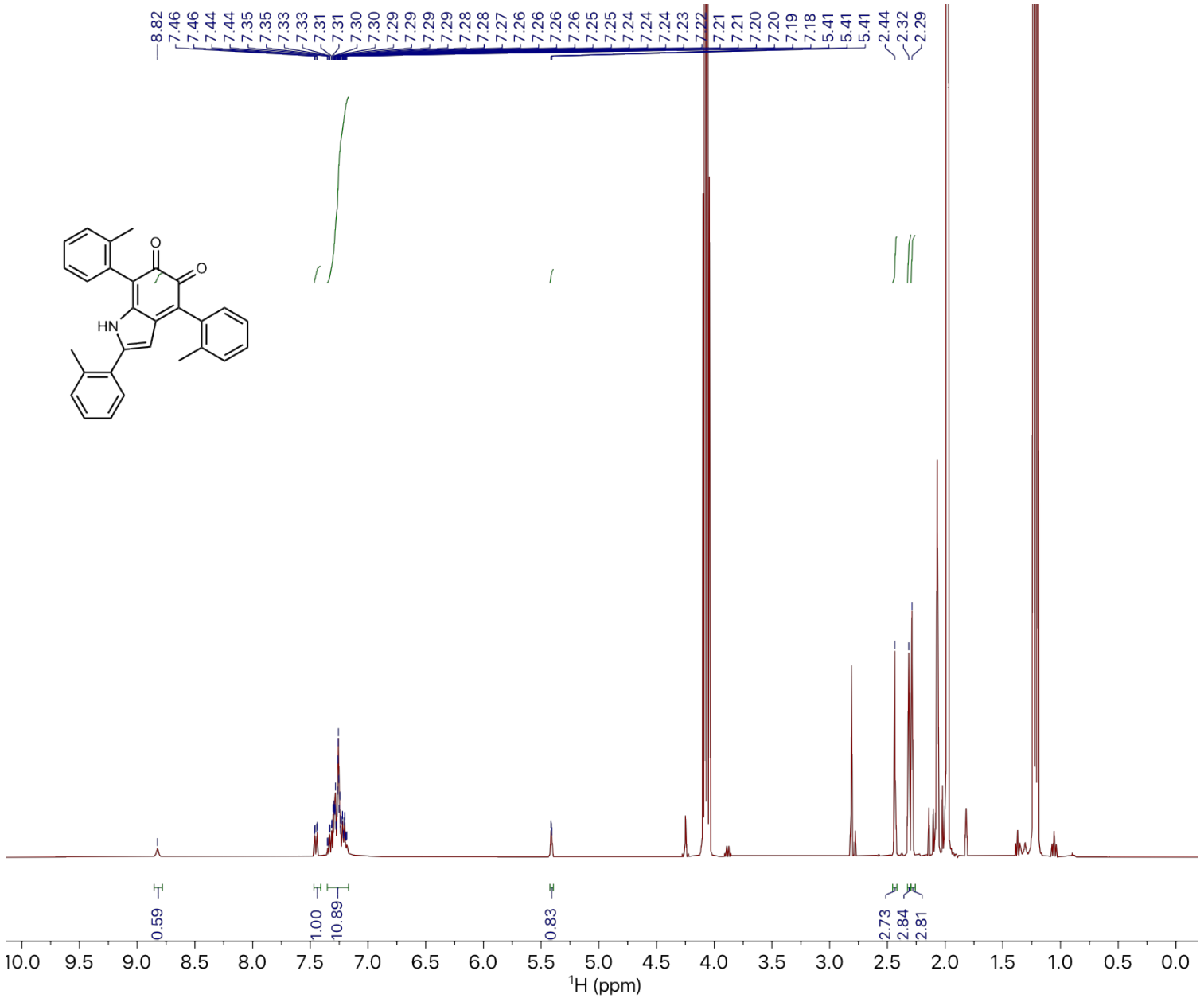
8.82
7.46
7.46
7.44
7.44
7.35
7.35
7.33
7.33
7.31
7.31
7.30
7.30
7.29
7.29
7.29
7.29
7.28
7.28
7.27
7.26
7.26
7.26
7.26
7.25
7.25
7.24
7.24
7.24
7.23
7.22
7.21
7.21
7.20
7.20
7.19
7.18
5.41
5.41
5.41
2.44
2.32
2.29
O
O
HN
0.59
1.00
10.89
0.83
2.73
2.84
2.81
10.0
9.5
9.0
8.5
8.0
7.5
7.0
6.5
6.0
5.5
5.0
4.5
4.0
3.5
3.0
2.5
2.0
1.5
1.0
0.5
0.0
^{1}H (ppm)